Characterization of metal particles by single particle analysis in urban environment

Adachi, Kouji

(Degree)
博士（理学）

(Date of Degree)
2005-03-25

(Date of Publication)
2009-04-28

(Resource Type)
doctoral thesis

(Report Number)
甲3253

(URL)
https://hdl.handle.net/20.500.14094/D1003253

DOCTORAL THESIS

Characterization of Metal Particles by Single Particle Analysis in Urban Environment

Kouji Adachi

Graduate School of Science and Technology
Kobe University
January 2005

DOCTORAL THESIS

Characterization of Metal Particles by Single Particle Analysis in Urban Environment

都市環境における個別粒子分析法を用いた金属粒子のキャラクタリゼーション

Kouji Adachi

Graduate School of Science and Technology
Kobe University
January 2005

Abstract

This doctoral thesis describes metal contaminations caused by particulate matter in urban environment (Kobe, Japan). The analytical method used in this study were single particle analysis, which could show the contribution of individual pollutant source in multi-polluted urban area. The materials investigated in this study were mainly street dust, soil, tire dust, and atmospheric depositions. The sources of pollution investigated in this study were automobile, traffic materials, mineral materials, steel plant, atmospheric depositions from long-range and local transportation. This thesis can be devided into seven sections and their brief summaries are described below.

Iron particles emitted from steel plant. Steel plant is one of the largest pollutant sources in urban environment for gaseous, particulate, and heat pollutant. In this study area, we have a steel plant with large smelting furnace. The company or administrative agency has carried out several monitoring for the gaseous or particulate matters emissions. However the study focused on characterized particulate matter by single particle analysis from a steel plant has not been carried out in this area and any other regions. This study investigated the spherical iron particles discharged from the steel plant and determined the distribution in the urban environment. The results showed that the detailed morphology of the spherical iron particles and the distribution patterns in soils and street dust suggesting the emission pathway and impacts for the urban environment.

Morphological characterization and chemical contribution of tire dust in street dust. Tire dust is a source of Zn for street dust, and causes heavy metal pollution in urban environment. Nevertheless, their morphology and chemical characteristics are not well known. Therefore, we analyzed the morphology of tire dusts collected from street dust and evaluated their chemical contribution to street dust. The tire dust particles were spindly, with a length of a few hundred μm, and had Al, Si, Fe, S,

Ca, and Zn particles attached to their surface. Mg, S, Ca, Cu, and Zn in the street dust correlated closely to their darkness intencities. These results suggest that the tire dust was generated from friction between tire treads and asphalt pavement, and that the tire dust particles became larger by accumulating together. At the same time, the tire dust took in asphalt pavement, minerals, brake linings, and many other materials that were present on the road. Additionally, the black materials such as tire dust and asphalt contribute to the chemical compositions like Mg,Ca, S, Cu, and Zn in street dust.

Characterization of heavy metal particles embedded in tire dust. This study characterizes the morphology and chemical composition of heavy metal particles embedded in tire dust and traffic-related materials (brake dust, yellow paint, and tire tread) as measured by a field emission scanning electron microscope equipped with an energy dispersive X-ray spectrometer (FESEM-EDS). In 60 samples of tire dust, we detected 2288 heavy metal particles, which we classified into 4 groups using cluster analysis according to the following typical elements: cluster 1: Fe, cluster 2: Cr/Pb, cluster 3: multiple elements (Ti, Cr, Fe, Cu, Zn, Sr, Y, Zr, Sn, Sb, Ba, La, Ce, Pb), cluster 4: ZnO. According to their morphologies and chemical compositions, the possible sources of each cluster were as follows: 1: brake dust (particles rich in Fe and with trace Cu, Sb, and Ba), 2: yellow paint ($CrPbO_4$ particles), 3: brake dust (particulate Ti, Fe, Cu, Sb, Zr, and Ba) and heavy minerals (Y, Zr, La, and Ce), 4: tire tread (zinc oxide). When the chemical composition of tire dust was compared to that of tire tread, the tire dust was found to have greater concentrations of heavy metal elements as well as mineral or asphalt pavement material characterized by Al, Si, and Ca. We conclude that tire dust consists not only of the debris from tire wear but also of assimilated heavy metal particles emitted from road traffic materials such as brake lining and road paint.

Single particle characterization of size-fractionated street dust. The relationship between particle distributions and chemical compositions of street dust were investigated in Kobe, Japan. Street dust are significant pollutants in urban areas, and

their toxicity differs according to the particle size. In the present study, we analyzed the distributions of particle size, chemical composition and particle type among size-fractionated street dust. Street dust samples were collected from road medians and street gutters. Chemical compositions of about 13,000 individual street dust particles were characterized by FESEM-EDS. They were classified into seven types by cluster analysis, and their possible sources were estimated. The particle type distributions showed some relations with the chemical composition distributions. This study showed that the chemical composition distributions among the street dust were typical for each element in relation to the particle type distributions.

Street dust contamination caused by ilmenite. This study shows a street dust contamination caused by mineral substances (ilmenite) derived from non-natural sources. The chemical composition of street dust collected in Kobe, Japan, was determined by energy dispersive X-ray fluorescence analysis and the distributions of Ti, Mn, and Fe compositions showed some contributions. FESEM-EDS and X-ray powder diffraction analysis detected many ilmenite particles ($(Fe, Mn)TiO_3$) in the street dusts. The chemical composition and morphological features of this ilmenite were different from those of ilmenite collected from natural sources (river sediments) in the same area. These results suggest that the presence of ilmenite derived from non-natural sources results in contaminations in the street dust.

Atmospheric deposition as a source of metal in the urban environment This study characterized metal particles from atmospheric depositions and estimate their contributions to metal composition in urban environment. Metal loadings from atmospheric deposition are one of source of metal in the urban environment. Therefore, many studies and investigations evaluate and monitor the metal loadings from atmospheric deposition. The analytical methods used in previous studies were mainly bulk analysis, which can detect accurate value of chemical composition and deposition mass. On the other hand, the method used in this study was single particle analysis, which can estimate individual sources from very small amount of sample. This study could evaluate metal loading from atmospheric deposition and characterize the individual

metal particles.

Characterization of metal particles in atmospheric deposition by single particle analysis during wintertime. The diameter and chemical composition of individual metal particles collected from atmospheric depositions were measured by single particle analysis and their sources of origin were estimated. Metal loading from atmospheric depositions is a significant metal source for the surface of natural environment or artificial buildings. The study area, Kobe (Japan), has long-range pollutant transportation problem of atmospheric particulate matters from northeastern Asian continent during winter and spring because of the strong seasonal wind and pollutant emission from the up-wind area. Thus, during the winter of 2003, metal particles collected from atmospheric depositions were characterised using a FESEM-EDS. Information on the chemical composition and particle size of individual metal particles revealed their emission sources and reaction history during transportation. Investigation of atmospheric deposition particles revealed the actual deposition loadings from the atmosphere to the surface of the environment. In this analysis, approximately 3000 metal particles were detected and classified into 14 types and were further reclassified into four groups of distribution patterns. The source area of the classified metal particles was estimated by the trajectory analysis: one group revealed long-range transportation (from the northeast of the Asian continent): Fe-Ba-Sb-Cu-S-Ti-O, Fe-Zn-O, Mn-Fe-O, Zn-O, Ni-O and Fe-O. The other group revealed local transportation: Cu-Zn-O and Cu-Sn-O. The other metal groups that were detected, such as Pb-O, Ag-O, Sn-Sb-O, Pb-Zn-Cl-Si-S-O and Bi-Cl-O, exhibited a different distribution pattern. Earlier studies, determining the source of atmospheric particulate matter by bulk composition analysis in the neighboring areas, showed similar metal source estimations. In addition to estimating their sources, by single particle analysis, this study could identify the several particles that contribute to the metal pollution.

Through the analysis, the flow of metal particles could be evaluated. The metal particles describe above were interact and related closely. For example, a brake dust

particle abraded away from an automobile will suspend for a while in the atmosphere near the road. Then they fall down to road surface and may be taken in a tire dust. The tire dust move to road side and to be street dust. Some of the street dust may be flowed to river by a rain event. Other street dust may be resuspended by a traffic wind and suspend in atmosphere and then they may deposit on soil. During the transportations, the brake dust contaminants various environment in urban. The all over the flow of metal is shown in the section *Genaral Conclusion*.

Contents

List of Figures

List of Tables

1 Introduction

This doctoral thesis describes the effect of particulate matter with metal compositions in the various urban environments such as soils, street dust, and atmosphere.

1.1 Background of study

In the urban environment, there are so many environmental problems such as atmospheric pollution, water pollution, soil pollution, acid rain, and so on. In order to improve the environment, many studies have been carried out. Particulate matters are the one of largest factors for such environmental problems. They are mainly discharged from the mechanism of friction or combustion process like automobile, plant, incinerator, and road materials. The suspended particulate matter, which has small particulate diameter mostly under 10 μm, affects human health, visibility, global climate, chemical pollution, or acid rain. The larger particulate matter with the diameter more than 10 μm will adversely impact to chemical contamination in soil, street dust, river sediments, and atmosphere. The leaching of chemical substances from the larger particulate matter also causes contaminations in water system. Especially, the particulate matters with metal composition yield serious concern for the environment.

Many earlier studies have investigated the chemical composition of environment matters such as soil, water, atmospheric particulate matters, or sediments, and characterized their leaching activity or chemical species. Studies also have estimated their sources or distributions. However, their analytical objects were mainly bulk samples, which show multiple effects from several sources all together, and it was difficult to determine the influence from individual sources. To estimate the contributions from individual sources in the environmental materials is essential to treat and evaluate the environmental impacts from each pollutant source. For the purpose, single particle analysis, which deals with individual particulate matters by micro analytical method such as scanning electron microscope, electron probe micro analyzer, is useful.

This study mainly dealt with metal particulate matter in urban environment, especially in Kobe city. The diameter of metal particles ranged from 0.2 μm to several

mm. The smaller particles will adversely affect the human health with absorbing them into the depth of alveo. Besides, the larger particles will cause chemical contamination in the environment. This study aimed to investigate the both grain size in order to know the whole influence from the particulate matter.

In the large part of this study, street dust and tire dust were investigated as the source of metal. The importance of the both materials will be mentioned in detail on the related sections. Generally, the tire dust is the largest composition of street dust, and the street dust is the one of largest pollutant from automobile especially in chemical contaminations. Addition to their abundance in volume and weight, they also contain toxic metal in their compositions. Beside, this study revealed that the tire dust also contains other smaller metal particulate inside their body. As the results, this study could identify the interaction of metal particles relating to traffic pollution.

This study also revealed the metal particles from atmosphere. Atmospheric particulate matters including metal components are also one of metal source in urban environment. Atmospheric particulate matter derives from various transport mechanism. For the long-range transport, they come from Asian continent far from several thousands kilometers. For the middle range transport, they originated from neighboring city apart from several hundreds kilometers, and for short range like several kilometers or meters, they derived from local sources with resuspention of street dust or soils. Emissions from manufacturing facility such as steel plant is also possible sources. To investigate these transportation mechanisms is one of important factor for the treatment of urban environment.

This study treats adversely affect from metal particles from various sources in urban environment. Main pathway of metal particles is direct inhalation into deep lung or alveolar region through atmosphere with fine particulate matter (less than 2.5 μ in diameter). Other way is to drink dissoluble metal for the water or to eat them with food. If the concentration of metals is especially high, the chronic or acute toxicity for human health are well known (e.g. renal dysfunction for Pb). There are many researches or reports about health impact or the loading estimate

of metal particles through the inhalation (e.g. Voutsa and Samara, 2002, Aust et al., 2002, US EPA, 2003). However because the concentration of ambient metal particles were not high enough to be appeared chronic or acute toxicity, it is difficult to evaluate the accurate effect from ambient metal particles without investigating the detailed characterization of the metal particles. Therefore the results of this study, which describes the morphological and chemical characterizations of the particles, will contribute to the risk estimation from the metal particles.

1.2 Relation among each section

Through all over the investigations, this study aims to show the metal particles flow in the urban environment. The pollutions caused by metal particles are not only the simple transportation from emission sources to environments but they contaminate one place and stay there for a while, and resuspend into atmosphere or are run off to gutters, and then they are transported to other place resulting in other pollutions. During the transportation, they interact with each other. In some case they take in other particulate matter, and in other case, they run together. Therefore, to estimate their flow is important if you evaluate the urban metal risk from metal particles (De Miguel et al., 1999). I propound the flow of metal in section 10 and discuss the relation between sections 3-9.

This doctoral thesis consists of seven chapters of scientific investigations. They are;

- Section 3: *Iron particles emitted from steel plant*
- Section 4: *Morphological characterization and chemical contribution of tire dust in street dust*
- Section 5: *Characterization of heavy metal particles embedded in tire dust*
- Section 6: *Single particle characterization of size-fractionated street dust*
- Section 7: *Street dust contamination caused by ilmenite*
- Section 8: *Atmospheric deposition as a source of metal in the urnab environment*

- Section 9: *Characterization of metal particles in atmospheric deposition by single particle analysis during wintertime*

Section 4 is the preliminary study of Section 5 and 6, and Section 8 is the preliminary study of Section 9. Section 7 is the focused study of a part of Section 6. The study of Section 3 and 5 have been published in reviewed journals. Section 6 and 9 are submitted and just peer-reviewed. Section 4, 7, and 8 are not considered for publishing in a reviewed journal now and they include non-published data and idea.

2 Analysis

2.1 Analysis equipment and statistical method

This study characterizes individual particle by using scanning electron microscopic analysis. This study also used X-ray fluorescence analysis for bulk chemical analysis of solid matter. Additionally, this study treats so many data sets (e.g. thouthands $\times$ dozen) determined by single particle analysis. Therefore, statistical method is essential to reduce the dimension of data matrix. For the purpose, cluster analysis and principal component analysis were used in this study. In this section, some characters of these analyses are mentioned.

Field Emission Scanning Electron Microscope equipped with Energy Dispersive X-ray detector (FESEM-EDS) was used to analyze the individual particles. The FESEM measurements were performed with a JSM-6330F cold field emission SEM (JEOL, Tokyo) with an energy dispersive X-ray spectroscopy (EDX) detector Link ISIS (Oxford-Instrument, Tokyo). This EDX detector is equipped with a super atmospheric thin window, which allows one to determine the low atomic number elements (from Be to U).

In FESEM, the electron gun of the SEM is equipped with a field emission cathode that emits probing beams narrower than the tungsten hairpin filament SEM. This results in an improved spatial resolution that facilitates analysis of metal particles with a diameter of more than 0.2 μm. Due to the electron gun system, FESEM exhibits instability in the probe current with time. In order to prevent this, the probe current was monitored constantly and 'flashing', which is a function to clean up the surface of the emitter with instantaneous high current, was carried out approximately every three hours to maintain a stable current. The analysis conditions used in this study were 15kv for accelerate voltage and 15mm for working distance.

Chemical composition analysis was carried out using an Energy dispersive X-ray Fluorescence (EDXRF), JSX-3220 (JEOL, Tokyo, Japan) spectrometer with an Rh target and Si (Li) detector. EDXRF is a simple and fast technique of elemental quantification of solid matter because it does not require that samples be prepared

as a solution. Several studies have proven the efficacy of the EDXRF method in analyzing the chemical composition of street dust or soil (Goldstein et al., 1996; Yeung et al., 2003).The quantity methods were determined by caliblation method and fundamental parameter(FP) method. The FP method allows the determination of the concentration ratios of measured elements without using standard samples.

Multivariate analyses such as hierarchical cluster analysis was used to reduce the dimension of the data matrix. The cluster analysis was based on Euclidean distances with Ward's error sum classification. The consistent Akaike's information criterion was used to determine the most effective number of the clusters. This semiquantitative analysis has been used in previous studies resulting in the successful classification of ambient particles (e.g. Jambers and Grieken, 1997; Sitzmann et al., 1999). We also used principal component analysis (PCA) of bulk chemical compositions to estimate the contributing factors, and compared them to the result of the single particle analysis. The detailed analysis method will be described in each section.

2.2 Sampling area

All the samples analyzed in this study were collected from southerneast part of Kobe city, Hyogo prefecture, middle part in Japan. The population of the city of Kobe was 1,510,000 in 2002. The northern part of the study area is a mountain, and the southern part is a harbor. Mount Rokko (931m), which consists primarily of granite, is located in the northern part of the study area (Huzita and Kasama, 1983).

In this study, some street dust samples were collected from Natinal Route 43 (R43). R43 has 6 lanes of traffic and there is also an elevated highway with 4 lanes of traffic above it. The mean traffic flow rate of R43 ranged from 64000 to 72000 vehicles per day, and the rate of heavy truck traffic ranged from 21.3 to 31.2% (Hyogo Prefecture, 1999). Sweeping maintenance on the road is carried out 3 times per month.

Descriptions of each sampling site will be mentioned in each section.

3 Iron particles emitted from steel plant

3.1 Introduiction

Steel plants have been known one of the largest source of metal pollutant for soil, water, and atmosphere (Nriagu et al., 1988). Especially, the steel plants are the largest source of Cr and Mn for the atmosphere and of Cr, Mo, Sb, and Zn in aquatic ecosystem from the cooling system (Nriagu et al., 1988).

The particulate matter emissions from steel plants are also one of problems near the plant facility. Prati et al. (2000) detected some elements that emitted from steel plant in the atmospheric particulate matter near the steel plant in Italy. However, few studies have been carried out about the detail morphology or distribution of the particulate matter by single particle analysis up to date except some studies. Machemer (2004) studied bulk chemical composition and individual particulate matter collected directory from steel manufacturing facilities, and the results indicated that various metal or graphite flakes (kish) particles were emitted from there.

Chemical composition of soils in this study area was investigated by the author and found that the Fe and Mn compositions in soils and street dusts were increase to the accompaniment of the steel plant situated southern part of the study area (Adachi and Tainosho, 2000). Therefore, this study aimed to investigate 1)the detailed morphology of particulate matter including Fe or Mn, 2)the distributions of the Fe or Mn particles in soil and street dust near the plant.

3.2 Sampling and analysis

The soils and street dust samples were collected from eastern part of Kobe City, Japan (Fig. 1). The dust samples were collected from the road along the seacoast close to the steel plant. The soil samples were collected from the park distributed with various distance from the plant. The soil samples less contained organic matter and consist of almost weathered granite. The soil and street dust samples were sampled by trowel and packed in plastic bag.

The samples were placed on brass sample holders coated by carbon paste (1.25

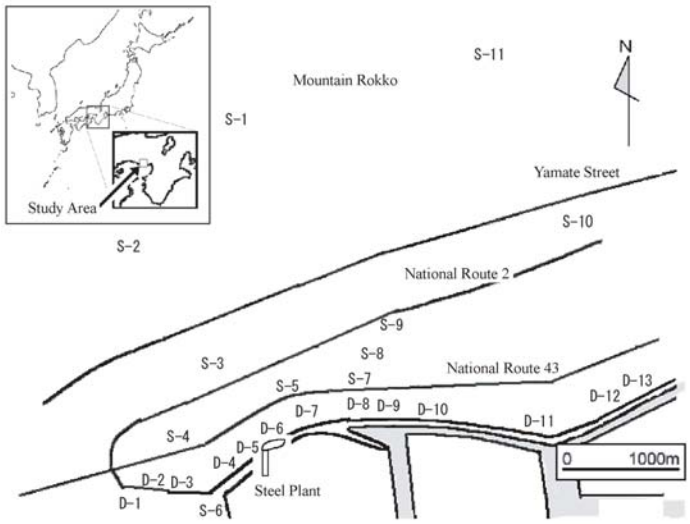

Figure 1: Location map of the sampling sites. S- means soil sample and D- means dust sample.

cm in diameter) and done a vacume evaporation by carbon. The total amounts of samples were determined by the difference of the weight before and after mounting samples.

FESEM-EDS was used to analyze the individual particles. The analysis conditions were 15kV for accelerate voltage and 15mm for working distance.

3.3 Results and discussion

3.3.1 Morphological features

For the observation analysis, natural and artificial particles were found in soil and street dust samples. The natural particles were almost mineral particles from geological source. For the artificial particles, especially focused on Fe or Mn including particles, so many flakes shaped and spherical shaped particles could be found (Fig.2). This study especially investigated the spherical particles (SP) because they could be estimated of their volume from their diameters and the source of them could be identified; the spherical shape means that they had experienced high-temperature

(Machemer, 2004, Piarna et al, 2000, Mogami et al., 1989). The dendrite structure found in their surface shows the same structure as seen in the particles caused by arc welding (Mogami et al., 1989). The maximum diameter of the SP was 140 μm and the average diameter with more than 4 μm was 9.3μm in soil samples and 16.7μm in dust samples.

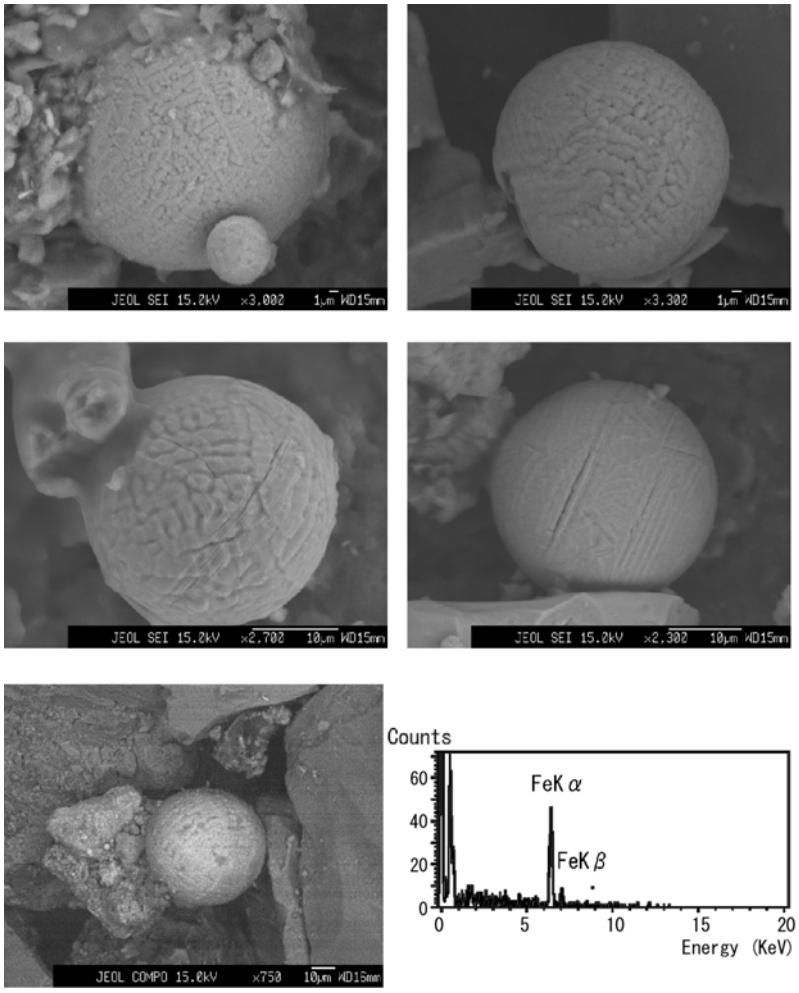

Figure 2: Secondry Electron Image of spherical iron particles

3.3.2 Distribution of iron spherical particles from the steel plant

The abundance of SP in the samples was determined from the total cross section area per the sample weight because the rate reflects the composition determined by surface analysis such as X-ray Fluorescence analysis (XRF). The diameters of all SP

with more than $4\mu m$ in each sample was detected at the magnification of 200. The cross section areas were calculated from the diameters.

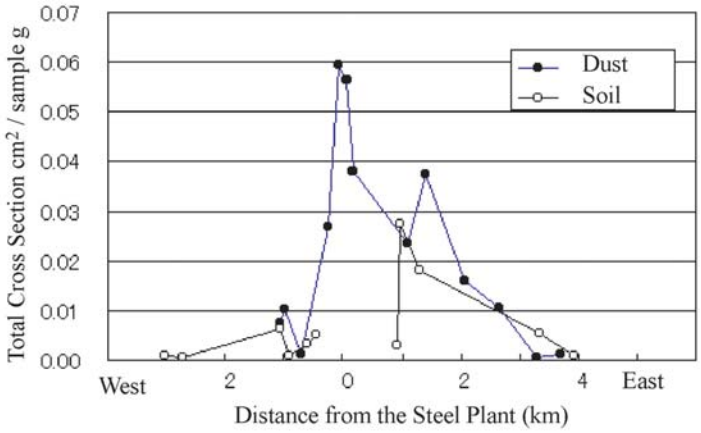

Figure 3: Distribution of spherical Iron particles from the steel plant

The results of distributions of SP are shown in Figure 3. The just point of steel plant is the place of blast furnace that had been until 1999. For the street dust samples, the distribution pattern indicates the decreasing of SP with the decreasing of distance from the steel plant. Additionally, some increasing at the points of 1-2 km from the steel plant could be found in the east and west directions. The similar distribution pattern could be seen in that of the soil samples. This pattern suggests the emission sources of SP. The distribution from the just point indicates the emission from the blast furnace. At the same time, the increasing at the 1-2 km points suggest the emission from the chimney with about 130m height. The bimodal distribution pattern was seen in other study (Haapala, 1998, Sugimae et al., 1974). The trend is attributed to the horizontal transportation by the wind and deposition speed with relation to the gravity and friction fource between air and the particles.

3.4 Conclusion

This study concluds that the spherical particles (SP) were derived from the steel plant judging from their morphological features and their bimodal distribution pattern. The results will contribute to the future study about the source estimation of

particulate matter in atmosphere, soil, and street dust. Additionally, this study also will contribute to the pollution study from steel plant. The SP will be a significant parameter of the emission from steel plant and we can estimate the contribution of steel plant from their abundance estimation of SP.

4 Morphological characterization and chemical contribution of tire dust in street dust

4.1 Introduction

Street dust contains many hazardous heavy metals such as Cu, Zn, and Pb (Hopke et al., 1980, Li et al., 2001, Miguel et al., 1997). Zn is the most frequent heavy metal in street dust. The primary source of Zn is tire dust (Hopke et al., 1980), which arises from friction between tire treads and asphalt pavement.

The weight of tire dust has been estimated to be 53×10^6 kg/year in 1996 in the UK (Environment Agency, 1998) and 16×10^8 kg/year in 1970 in the USA (Dannis, 1974). The tire dust affects human health as an allergen (Williams et al., 1995) and contributes to zinc contamination in the environment, particularly in atmosphere (Rogge et al., 1993, Cardina, 1973, Cardina, 1974, Pierson et al., 1974), sediment (Legret et al., 1999, Sutherland et al., 2000), water (Davis et al., 2001), and soil (Li et al., 2001, Cadle et al., 1980). Nevertheless, the tire dust itself has not been studied carefully beyond a few studies. Dannis (1974) investigated the morphology, size, and degradation of tire dust. Camatini et al. (2001) investigated the morphology of tire dust in laboratory and environmental samples using SEM and TEM, and analyzed the chemical composition by EDS.

In this study, we used FESEM-EDS to analyze individual tire dust particles and EDXRF to determine the chemical composition of street dust. To detect the content of the tire dust in the environment, many researchers have used gas chromatography (Cardina, 1973, Cadle et al., 1980), but by using EDXRF, which did not destroy the samples, we were able to estimate the contents from the ratio of darkness in the same samples analyzed with EDXRF.

The aim of this study is to analyze the generation mechanism of tire dust and to investigate the relation between the chemical composition of street dust and artificial materials.

4.2 Materials and Methods

4.2.1 Sample Collection and Preparation

The street dust samples were collected from Route 43 located in southeastern part of Kobe in Japan on 28 November 2000. Twenty-nine street dust samples were collected from the roadsides, crosswalks and road dividers. They were dried for a few hours at 105℃, and sieved through 100 mesh (under 150 μm).

4.2.2 Analysis

The morphology and X-ray mapping images of the tire dust were determined by using FESEM (JEOL JSM-6330F) with EDS (Oxford Link ISIS). The voltage for EDS analysis was 15kv, and the working distance was 15mm. Two kinds of samples were used for FESEM-EDS; a bulk sample of the street dust and an individual sample of the tire dust. The bulk samples were mounted on an aluminum sample holder coated with carbon paste. The individual sample was put on a slide glass and fixed with the carbon paste. Both samples were coated with carbon using vacuum deposition equipment (JEOL, JEE-400).

The chemical composition of the street dust was determined by EDXRF (JEOL JSX-3220). Analytical conditions were 30kv of the tube voltage, 500s of live times, and a fundamental parameters algorithm. The analytical elements were Na, Mg, Al, Si, S, K, Ca, Ti, Cr, Mn, Fe, Ni, Cu, Zn, and Pb. The major elements in soils (Na, Mg, Al, Si, K, Ca, Ti, Mn, and Fe) were shown as oxides. The street dust samples were placed in vinyl chloride tubes (13 mm in diameter and 4mm high), and pressed to make pellet samples at a pressure of $1200 kg/cm^2$. The pellet samples were used for EDXRF analysis and for determination of ratio of darkness.

We used the ratio of darkness for a simple method to identify the artifical impact. The image-processing method was useful because the street dust was mainly composed of natural materials(soils) and artifical material (asphalt and tire dust) whose color are almost black. The pellet samples were converted into digital data by using a scanner (EPSON, GT70005). The scanning conditions were 5161 pixels per inch and bitmap format. The ratio of the brightness level from 0 to 20 was detected using

image-processing software (Adobe Photoshop 5.5); here, the brightness level 0 is black and 255 is white.

4.3 Results and discussion

4.3.1 Morphology of tire dust

A back-scattered electron (BSE) image of the street dust is shown in Fig.4. The spindly, dark gray particles are tire dusts. White, bright, and sharp edges are mainly minerals. The lengths of the tire dust particles are mostly a few hundred μm.

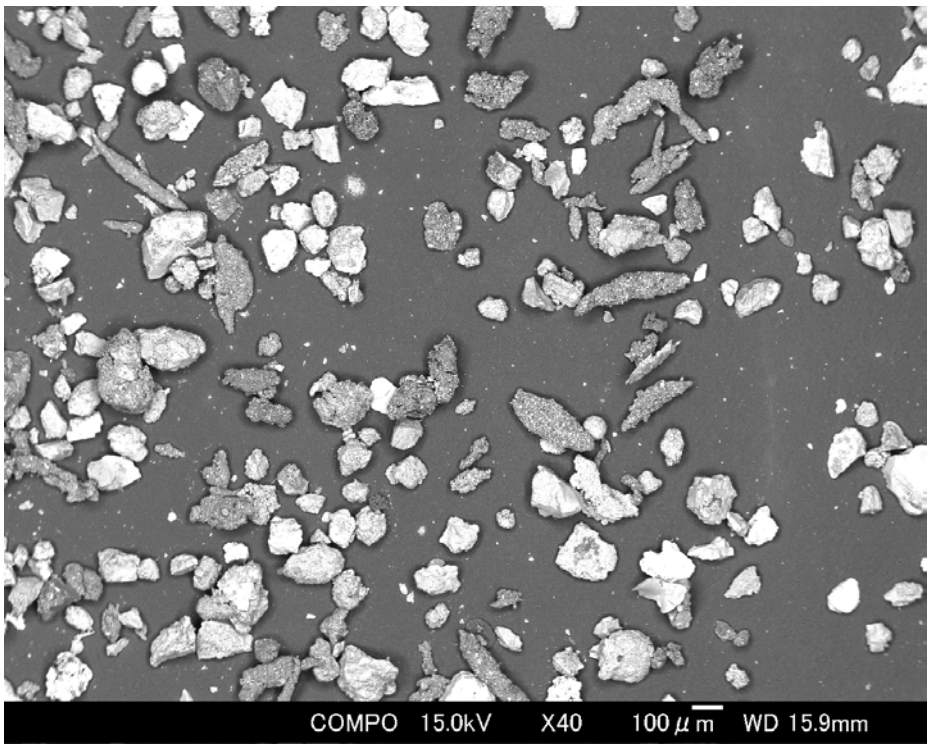

Figure 4: BSE image of a bulk street dust sample

The morphology of the tire dust observed in this study is different from that determined by other methods in earlier studies. Tire dust particles collected from a steel brush abrader (Camatini et al., 2001) or directly caught from tires (Dannis, 1974) were not spindly but instead were more irregular.

The lengths of the tire dust particles collected from the street dust were found to be larger in this study than by other methods. Dannis (1974) measured the lengths of

tire dust particles collected from sticky panels mounted under a car (from a few μm to 100μm) and from filter plates mounted under a car (20 μm). In the atmosphere, 25 to 40 % of tire dust particles ranged from 1.1 to 7.0 μm (Cardina, 1974).

These differences in length and morphology suggest that the tire dust particles in the street dust were generated by a rolling process again and again. The street dust particles were depositions on the road; therefore, they would have more opportunities to be rubbed between tires and a road. It is possible that the frequent rolling caused them to cohere and accumulate into larger particles. As a result, they became long and spindly in shape.

4.3.2 X-ray mapping on tire dust

BSE and X-ray mapping images of the tire dust are shown in Fig.5. The BSE image indicates that the tire dust has many particles attached to it that range from a few μm to 50 μm in size. These particles mainly consisted of Al, Si, S, Ca, and Fe. Zn was detected only slightly. Fig.6 shows a BSE image and an X-ray mapping image of the tire dust at high magnification (8000). S is distributed all over the surface and as a particle. Ca is distributed as many particulate matters with one or a few μm in size. Zn is distributed as a single particle.

Al and Si particles are probably minerals derived from soil or an aggregate of asphalt pavement. Fe particles may be from an anthropogenic source judging from their compositions. The distributions of S and Zn are consistent with the manufacturing process of a tire rubber. Tire rubber is composed of synthetic or natural rubber, carbon black, oil, zinc oxide, sulfur, and other chemicals (Environment Agency, 1998). In particular, sulfur is added to vulcanize the rubber, and zinc oxide is used to enhance and control the chemical reactions.

Particulate S and Ca may be derived from asphalt pavement. Camatini et al.(2001) indicated that the sources of S other than tire treads include sulfate, sulfide, and bitumen. As discussed above, the tire dust was rubbed on the asphalt pavement, and therefore can become attached to sulfate, sulfide, or bitumen. Additionally, Ca is contained in the asphalt pavement as a filler mixed with bitumen. The detailed

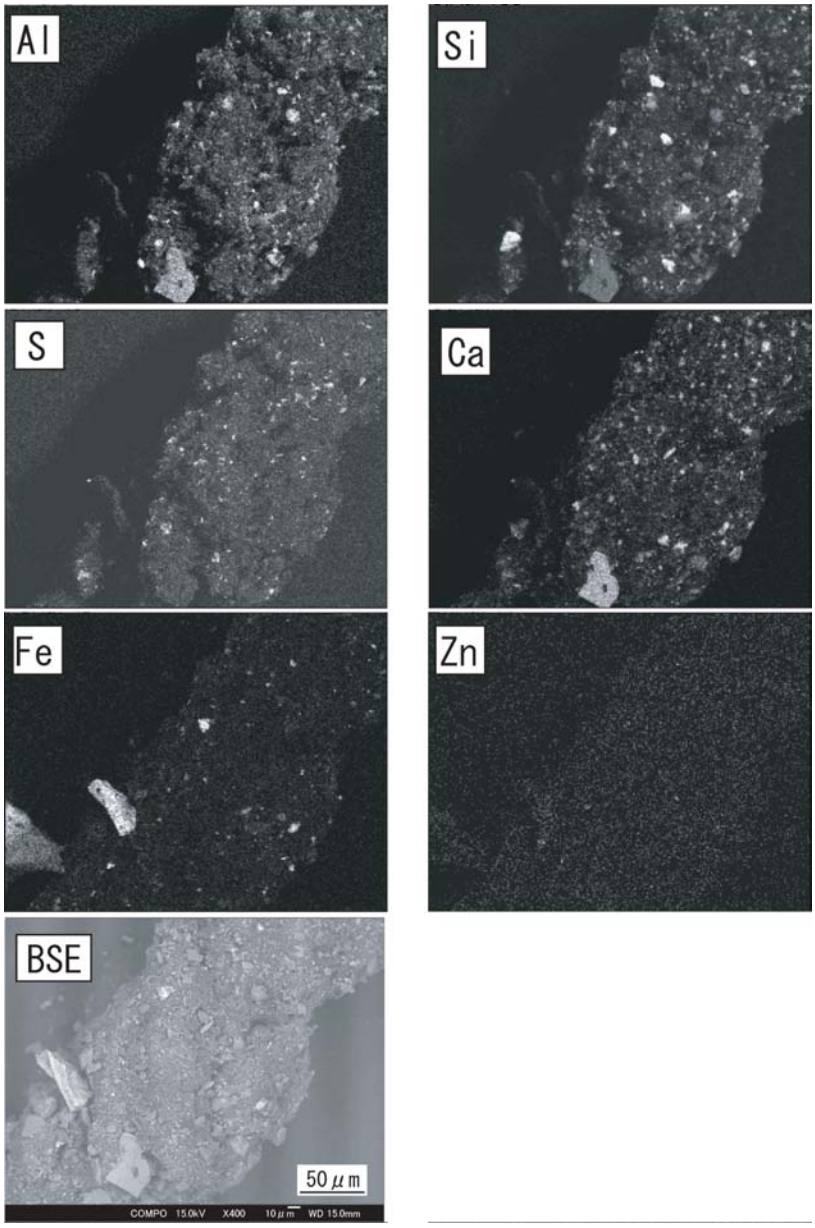

Figure 5: BSE and X-ray mapping image of a tire dust particle

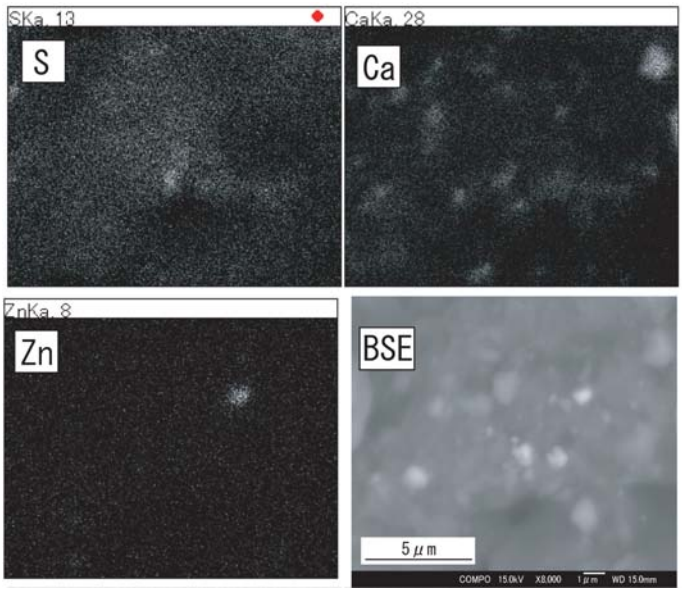

Figure 6: BSE and X-ray mapping image of a tire dust particle at high magnification (× 8000)

discussion between tire dust and metal particles will be described in the next section.

4.3.3 EDXRF analysis and estimation of the tire dust content in street dust

The chemical composition of the street dust is shown in Table 1. The major component of the street dust is soil, which mainly consists of Na, Si, Al, K, and Ca. Additionally, heavy metals and anthropogenic elements such as S, Ca, Ti, Cr, Fe, Ni, Cu, Zn, and Pb were present in high concentrations. The street dust is affected adversely by particles or gaseous pollutants from automobiles such as brake lining particles, oil leakage, and tires particles (Davis et al., 2001). Therefore, the street dust has high content of heavy metals and other anthropogenic elements.

The ratio of darkness in the street dust samples ranged from 5.0 to 61.5%. Correlation coefficients among Mg, S, Ca, Cu, Zn, and the ratio of darkness are listed in Table 2. These are closely related at a probability level of <0.01. The close relationship among S, Ca, Zn, and the ratio of darkness suggests that artifical materials such as tire dust and asphalt particles are the most dominant source for these elements, because the tire dust or asphalt particles included S, Ca, and Zn as indicated

Table 1: Concentration ratios of street dust. n=29

	Mean(Wt.%)	S.D.
Na_2O	2.59	0.43
MgO	1.51	0.22
Al_2O_3	11.28	0.85
SiO_2	53.28	5.59
S	2.04	0.76
K_2O	2.78	0.32
CaO	12.74	2.77
TiO_2	3.34	2.35
Cr	0.06	0.02
MnO	0.36	0.11
Fe_2O_3	9.47	1.83
Ni	0.02	0.00
Cu	0.03	0.01
Zn	0.46	0.17
Pb	0.03	0.02

in Figs.5 and 6. Additionally, Cu and Mg also have a close relationship. Cu is mainly derived from brake lining (Davis et al., 2001), and Mg is contained in asphalt pavement (Camatini et al., 2001), and cement (Miguel et al., 1997). These materials are so common in the street environment. Asphalt particles and tire dust themself were also black. On the other hand, natural materials, mainly soil, are almost soil and they are relatively white. Therefore, artificial materials are well indicated by the index of darkness in street dust.

The ratio of S/Zn was 4.4 in the street dust. This ratio is high compared to that in the rubber compound of tires, which is 0.64 (Environment Agency, 1998). This high ratio suggests that the main source of S was not tire treads, but bitumen, sulfate or sulfide.

Table 2: Correlation coefficients among MgO, S, CaO, Cu, Zn, and RD in street dust (n=29)

	MgO	S	CaO	Cu	Zn	RD[a]
MgO						
S	0.66**					
CaO	0.84**	0.88**				
Cu	0.52*	0.62**	0.66**			
Zn	0.71**	0.89**	0.79**	0.57**		
RD	0.67**	0.88**	0.81**	0.59**	0.94**	

[a] RD = ratio of darkness in street dust. *P<0.05, **P<0.01

4.4 Conclusion

This study characterized the morphology and chemical distribution of tire dust collected from the street dust and analyzed the chemical composition of the street dust and the ratio of darkness.

The tire dust particles collected from the street dust showed a long and spindly shape, and included many minerals or anthropogenic particles. The street dust was high in heavy metals (Cr, Ni, Cu, Zn, and Pb), and showed a close relationship between the rate of darkness and some elements (Mg, S, Ca, Cu, and Zn). These results suggest that the tire dust was generated by rolling and gathering, and in the course of these processes, they collected and incorporated particles from soils, asphalt pavement or brake linings. Asphalt or other black particles also contribute to the chemical composition. As the results of this study, it found that the darkness in street dust suggests their toxic compositions as an artifical materials. In the section 5 and 6, I studied the metal particles attached on a tire dust and relation between particlate matter and chemical composition in detail.

5 Characterization of heavy metal particles embedded in tire dust

5.1 Introduction

Tire wear debris (tire dust) is generated by the rolling shear of tire tread against road surfaces (Rogge et al. 1993). The mass of annual emission of tire dust was estimated to be 5.3×10^7 kg in 1996 in the UK (Environment Agency, 1998) and 2.1×10^8 kg in 2001 in Japan (Adachi and Tainosho, 2003), and tire abrasion on urban road in Germany was estimated from 55 to 657 kg/km/year on various roads (Muschack, 1990). This large amount of tire dust is a significant cause of pollution in the urban environment (Environment Agency, 1998). Zinc oxide is added as an activator during the vulcanizing process, comprising from 0.4% to 4.3% of the resulting tire tread (Smolders and Degryse, 2002), and zinc from tire dust is a significant pollutant in soil (Smolders and Degryse, 2002, Sadiq et al., 1989), air (Rogge et al. 1993), street dust (Fergusson and Kim, 1991), and urban runoff (Davis et al., 2001). Other heavy metal elements in tire tread also pollute the environment. Fukuzaki et al. (1986) showed that tire tread contains heavy metals such as Mn, Fe, Co, Ni, Cu, Zn, Cd, and Pb, and tire dust pollution contributes to some of these elements in the form of airborne dust. Sadiq et al. (1989) analyzed the metal concentrations in tires and showed that tire dust was a soil pollutant.

The road paving aggregates embedded in tire dust have been investigated (Camatini et al., 2001, Smith and Veith, 1982), but heavy metal particles derived from other sources have not yet been examined. Heavy metal particles are emitted on the road surface as part of brake dust, road paint, diesel exhaust particles (DEP), road construction materials, or car catalyst materials. When tire tread is abraded against the road surface, the tire tread debris will assimilate these particles. In this study, we examined brake dust, yellow paint, and tire tread materials as possible sources of metal particles in tire dust. Brake dust has been recognized as a significant pollutant for Cu, Sb, and Ba in the aerosols composition (Sternbeck et al., 2002), and it contributed 47% of the total loading for Cu in urban runoff (Davis et al., 2001). Yellow

paint contributed from 0.3% to 1.0% of airborne dust in Niigata, Japan (Fukuzaki et al., 1986). The bulk chemical composition and manufacturing process of brake dust, yellow paint, and tire tread are well known, but detailed morphologies and individual chemical compositions of the metal particles included have not been thoroughly investigated by the scanning electron microscopy (SEM) method. The aims of this study were to characterize the heavy metal particles embedded in tire dust and the traffic-related metal particles (brake dust, yellow road paint, and tire tread) as sources of embedded particles in tire dust.

5.2 Experimental Procedures

5.2.1 Sampling site

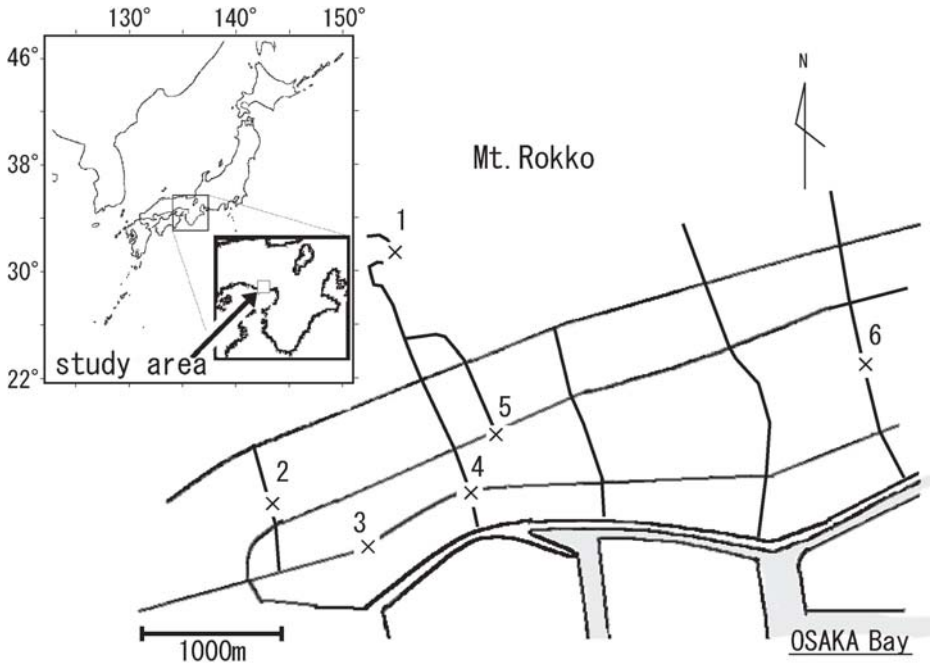

Figure 7: Sample location map

Street dust samples were collected from 6 sites in Kobe, Japan (Fig.7) during August of 2002.

The sampling sites selected were the same points at which a traffic census was carried out by the city of Kobe as a part of a national traffic census conducted in October of 1999 (Hyogo Prefecture, 1999). According to the data, the traffic volume

ranged from 4,944 to 50,366 vehicles per day, and the proportion of heavy truck traffic ranged from 4.7% to 22.3%. Sites 1, 2, and 6 are residential areas. Sites 3 and 4 are industrial areas, and Site 5 is a commercial area. Site 1 is located on a down slope, while the other roads are almost flat. Sites 2, 4, and 5 are crossroads. Sites 3 and 4 are different locations on the same road.

5.2.2 Sample collection

The tire dust samples investigated here were collected from street dust, which were the depositions from natural and human activities on the road (Brookman and Drehemel, 1981). The tire dust comprises a significant composition of the street dust. More than 100 g of street dust were gathered from roadsides with a nylon trowel at each sampling site. The collected samples were stored in plastic bags for subsequent sample preparation and analysis.

In addition to the tire dust samples, we collected 5 brake dust samples from the rim of front brake linings. The five selected cars were manufactured by three different Japanese automakers. We also picked up a yellow road paint sample from a fragment of line material painted on the road surface in the study area, and a tire tread sample was chipped off from the surface of a used tire (Bridgestone, 6.40R14, Japan).

5.2.3 Single particle analysis

The FESEM measurements were performed with a JSM-6330F cold field emission SEM (JEOL, Tokyo) with an energy dispersive X-ray spectroscopy (EDX) detector Link ISIS (Oxford-Instrument, Tokyo).

For the single particle analysis of the heavy metal particles embedded in tire dust, we used an acceleration voltage of 15 kV, a working distance of 15 mm, and an EDX collection time of 20 seconds. For the bulk analysis of traffic-related materials, we used 500 or 1000 seconds of EDX collection time.

The street dust samples were dried at room temperature and sieved through a 149-μm nylon screen. They were affixed to a carbon tape attached to aluminum studs. All samples were coated with carbon so they would have conducting properties.

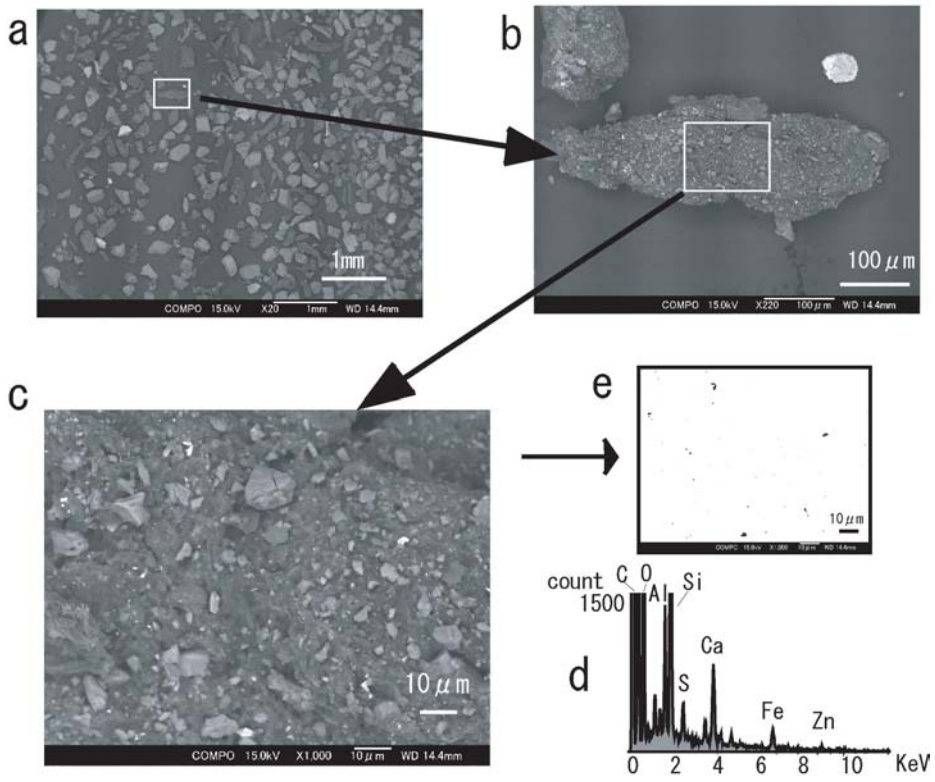

Figure 8: Detection method of heavy metal particles from tire dust surface. a: Selection of tire dust particle in street dust, b: Tire dust particle, c: Analytical area ($0.01mm^2$), d: EDX spectra in the analytical area, e: High contrast and negative image of the analytical area

Ten larger tire dusts whose shape had not been broken were selected from each street dust sample (Fig.8a, b). The length of the selected particles ranged from 220 to 1230 μm. Tire dust samples were distinguished from other types of debris by the following three features: (1) sausage-shaped particles (Dannis, 1974), (2) surface morphology resembling characteristic rough and ragged tire tread wear, (3) the presence of C, Al, Si, S, Ca, Fe, and Zn (Camatini et al., 2001, Kim et al., 2001). Backscattered electron images (BEIs) were taken in the range of $0.01mm^2$ at $\times$ 1000 (Fig.8c) from the middle part of each particle. Chemical compositions of the areas were also determined by EDX (Fig.8d), and they were defined as the bulk chemical compositions of tire dust.

Heavy metal particles were brighter than silicate mineral particles in the BEI; the brightness of the BEI reflects the atomic number of the object. The BEIs were converted to show high contrast with negative images to clearly distinguish heavy metal particles from the minerals (Fig.8e). All detected particles more than 0.2 μm in diameter were analyzed to determine their chemical composition and diameter.

The EDX quantification was determined using the standardlessZAF method, and recalculated to 100% for 24 elements (Mg, Al, Si, P, S, K, Ca, Ti, V, Cr, Mn, Fe, Ni, Cu, Zn, Sr, Y, Zr, Sn, Sb, Ba, La, Ce, and Pb). Because of the complex shape of the particles surface and their small diameters compared to the electron diffusion range, the quantification could lead to over- or underestimation. Therefore, we used a statistical method (a hierarchical cluster analysis program (HCA)) based on their major component elements to classify the particles. The HCA was based on Euclidean distances with Ward's error sum classification. The consistent Akaike's information criteria (AIC) were used to determine the most effective number of the cluster.

5.3 Results and discussion

Table 3: Chemical compositions of clusters and traffic related material (weight %)

	$B.D.^a$	$Y.P.^b$	$T.T^c$	$T.D.^d$	Cluster1	Cluster2	Cluster3	Cluster4
Mg	0.1±0.3	1.9±1.0	ND	1.9±0.5	0.9±1.2	1.3±0.9	1.2±1.5	0.6±0.9
Al	0.5±0.3	0.6±0.2	2.7	7.5±2.7	2.5±1.7	4.6±2.1	3.5±2.6	2.5±1.4
Si	1.6±0.7	6.1±4.1	2.8	21.2±2.4	5.8±3.3	12.9±4.2	8.3±5.8	5.8±3.2
P	0.0±0.1	ND	ND	0.6±0.3	0.2±0.6	0.4±1.2	0.6±2.0	0.1±0.3
S	0.9±0.4	0.3±0.5	25.6	2.6±0.9	0.9±0.8	2.6±1.7	4.5±5.6	1.1±0.8
K	0.2±0.4	ND	ND	1.9±0.4	0.4±0.5	0.8±0.7	0.7±1.1	0.3±0.5
Ca	0.3±0.3	50.9±7.2	1.4	10.1±3.5	2.1±1.7	5.8±4.1	4.0±5.2	2.6±2.8
Ti	1.3±2.1	ND	ND	1.2±0.6	0.5±1.2	0.6±1.2	3.4±7.6	0.3±0.6
V	ND	ND	ND	0.0±0.1	0.0±0.2	0.1±0.3	0.1±0.6	0.0±0.1
Cr	0.0±0.0	2.2±0.9	ND	0.0±0.1	0.2±1.0	6.1±3.7	1.7±8.4	0.0±0.2
Mn	0.7±0.1	ND	ND	0.1±0.1	0.5±1.1	0.1±0.3	0.8±4.0	0.1±0.3
Fe	58.0±6.7	ND	ND	5.5±1.5	48.8±10.0	2.8±2.3	13.1±10.3	1.2±1.9
Ni	ND	ND	ND	0.0±0.1	0.1±1.0	0.2±0.6	0.3±3.5	0.1±0.2
Cu	1.2±1.2	ND	ND	0.1±0.2	0.7±1.7	0.2±0.6	4.8±12.1	0.1±0.4
Zn	0.1±0.3	ND	17.4	1.6±0.8	0.7±1.5	0.8±2.4	1.8±4.4	57.9±10.4
Sr	0.1±0.1	ND	ND	0.9±0.3	0.1±0.4	0.4±0.9	1.8±9.7	0.1±0.5
Y	ND	ND	ND	0.0±0.1	0.0±0.1	0.0±0.1	0.2±1.8	0.0±0.1
Zr	0.7±0.8	ND	ND	0.1±0.2	0.1±0.4	0.1±0.5	1.6±5.7	0.0±0.4
Sn	ND	ND	ND	ND	0.1±0.5	0.1±0.5	0.7±3.8	0.1±0.3
Sb	0.9±1.0	ND	ND	0.0±0.2	0.3±0.8	0.1±0.6	1.3±5.5	0.1±0.4
Ba	1.5±1.9	ND	ND	0.1±0.2	0.5±1.5	0.2±0.9	7.2±12.0	0.1±0.4
La	ND	ND	ND	0.0±0.1	0.1±0.4	0.1±0.7	0.7±3.3	0.1±0.3
Ce	0.0±0.1	ND	ND	0.0±0.1	0.1±0.4	0.2±0.7	1.7±7.2	0.1±0.4
Pb	0.3±0.6	13.0±5.3	ND	0.1±0.2	0.1±0.4	26.3±10.2	0.5±1.2	0.1±0.3
O	31.0±0.6	30.5±3.3	50.1	44.9±1.2	34.3±2.4	33.7±4.5	36.0±6.2	27.2±3.4
n ^{e}	17	3	1	60	1246	162	344	536
d ^{f} (μm)					1.17	0.42	1.05	0.52

^{a}B.D.: Brake Dust, ^{b}Y.P.: Yellow Paint, ^{c}T.T.: Tire Tread, ^{d}T.D.: Tire dust, ^{e}n: number of particles, ^{f}d: averaged diameter

5.3.1 Brake dust

Three or four fragments from each brake dust sample were analyzed to determine their bulk chemical compositions and the particulate compositions by FESEM/EDX. The BEI and distribution of Cu, Sb, S, and Fe of brake dust are shown in Fig.9a and 9b, respectively. The diameter of particles in the brake dust was about 1 μm, which was within the range of average mass median diameters of brake dust measured under several condition tests (from 0.62 to 2.49μm) (Garg et al., 2000).

The brake dust consisted mainly of particulate Al, Si, S, Ti, Fe, Cu, and Sb (Fig.9b). Iron particles also contained slight amounts of S, Cu, Sb, and Ba. Some brake dust samples contained particulate $BaSO_4$ and Zr. When we averaged the bulk compositions of the brake dust fragments, we found that Fe was the most abundant heavy element, followed by Ba, Cu, Sb, and Zr (Table 3). Sternbeck et al. (2002) proposed diagnostic criteria for brake wear particles that included a ratio of 4.6 ±2.3 for Cu/Sb. The ratio in our analysis was 1.3. The low ratio compared to the criterion was because of the presence of Cu-free brake dust samples in this study. Cu is used to control heat transport, and Sb is used to enhance stability (ORNL, 2001). $BaSO_4$ is used to increase the density of the brake pad (ORNL, 2001).

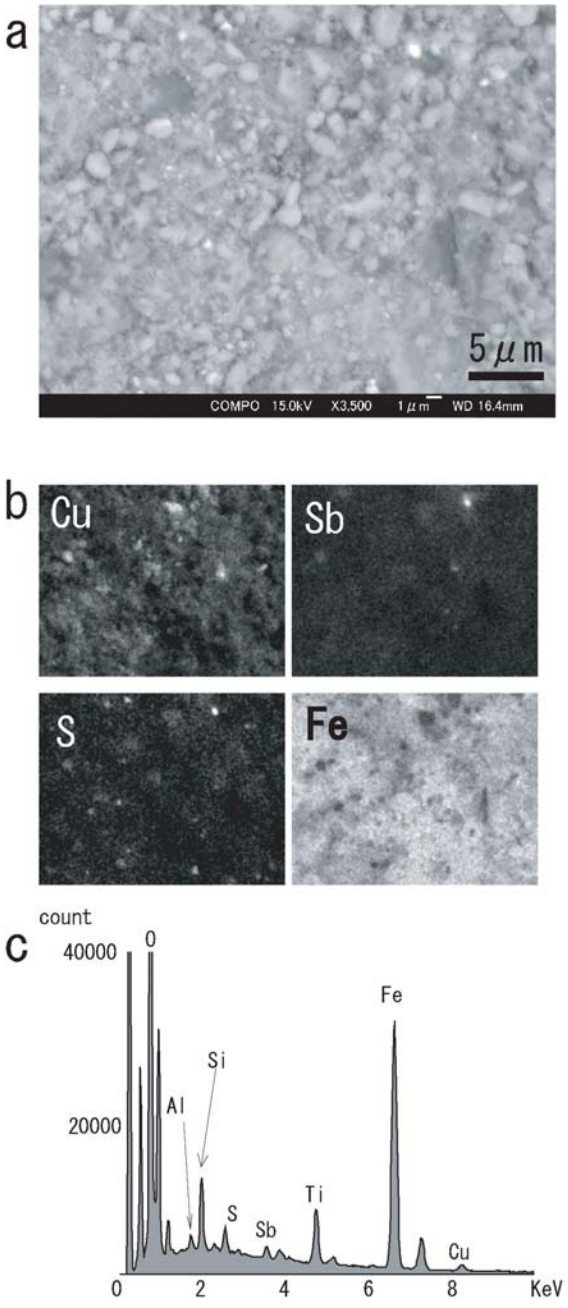

Figure 9: Brake dust. a: BEI of the brake dust, b: X-ray map of Cu, Sb, S, and Fe, c: EDX spectra of image a.

5.3.2 Yellow paint

The typical morphology and EDX spectra of yellow paint are shown in Fig.10. The bulk chemical composition is high in Si, Ca, Cr, and Pb (Table 3). The yellow paint consists of beads, Ca material, and $PbCrO_4$ particles. The $PbCrO_4$ is a particulate about 0.5 μm in diameter with an oval morphology (Fig.10a). The $PbCrO_4$ in yellow paint is one of the Pb contributors in street dust (Fukuzaki et al., 1986, Fergusson and Kim, 1991).

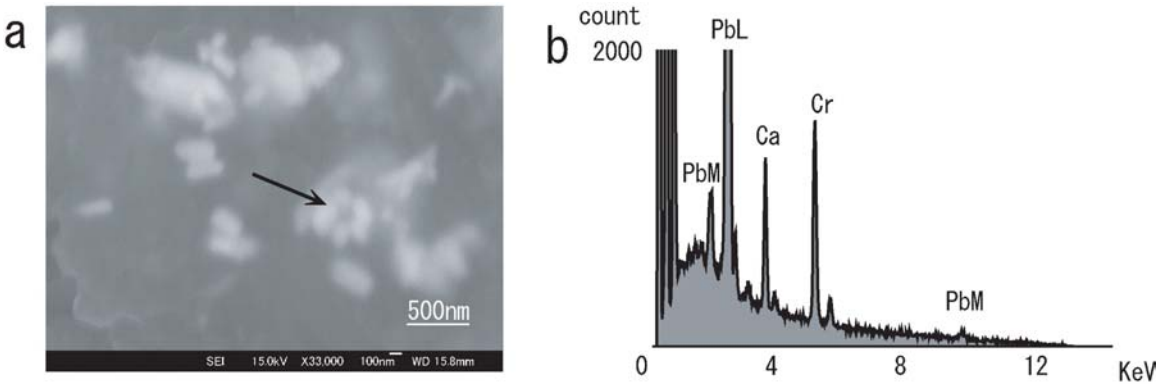

Figure 10: Yellow road paint material. a: SEI of a yellow paint fragment, b: EDX spectra of Cr/Pb rich particle

5.3.3 Tire tread

A cross section image of tire tread and EDX spectra are shown in Fig.11. Detected elements in tire tread were O, Al, Si, S, Ca, and Zn (Table 3). The diameter of particulate ZnO was about 1 μm or less, and the morphology was multi-angular (Fig.11a). Zinc oxide is added to activate vulcanization in the tire tread. Much of the Zn forms chelates with the accelerators, but the major part of the Zn in tire tread is excess ZnO and ZnS (Fauser et al., 1999).

5.3.4 Heavy metal particles embedded in tire dust

We detected 2288 heavy metal particles in 60 tire dust samples. The bulk chemical composition of the surface of tire dust debris was rich in mineral or asphalt pavement material characterized by Al, Si, K, and Ca, and smaller amounts of Fe, S, Mg, Zn,

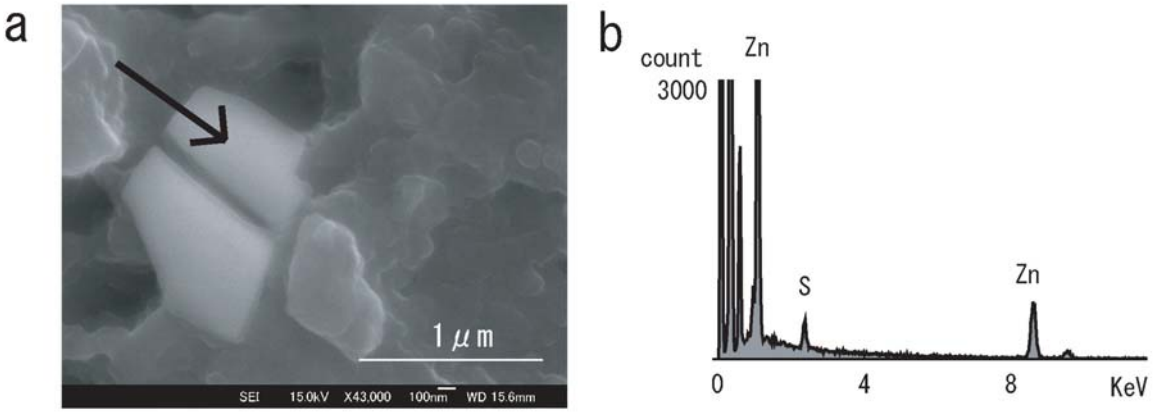

Figure 11: Cross section of tire tread. a: SEI of ZnO particle in tire tread. b: EDX spectra of ZnO particle

and Ti (Table 3). The chemical composition was quite different from that of tire tread. Mineral materials were found at high levels compared to the composition of tire tread, and some heavy metal elements were detected.

The embedded particles were divided into 4 clusters based on the consistent AIC and on particle compositions. Iron-, Cr/Pb-, and Zn-rich particles were classified into clusters 1, 2, and 4, respectively. The particles with multi-elemental composition were classified into cluster 3. Typical morphology and EDX spectra of the heavy metal particles are shown in Fig.12. In each EDX spectrum, Al, Si, and Ca may reflect neighboring material of the targeted heavy metal particles, such as asphalt pavement material, soil minerals, or tire tread itself.

Cluster 1

Cluster 1 is characterized by high Fe composition. Other heavy metal elements such as Mn, Cu, Zn, Sb, and Ba are contained in slight amounts in this cluster (Table 3). The average particle diameter is relatively large (1.17 μm). Iron is the most abundant heavy metal element in street dust (Hopke et al., 1980). The possible sources of Fe particles are brake lining material (brake dust) (Hopke et al., 1980, Hildemann et al., 1991, ORNL, 2001, Garg et al., 2000), automobile rust (Hopke et al., 1980), and motorcar exhaust (Weber et al., 2000).

In this study, the rich Fe content in the brake dust showed that it is an important

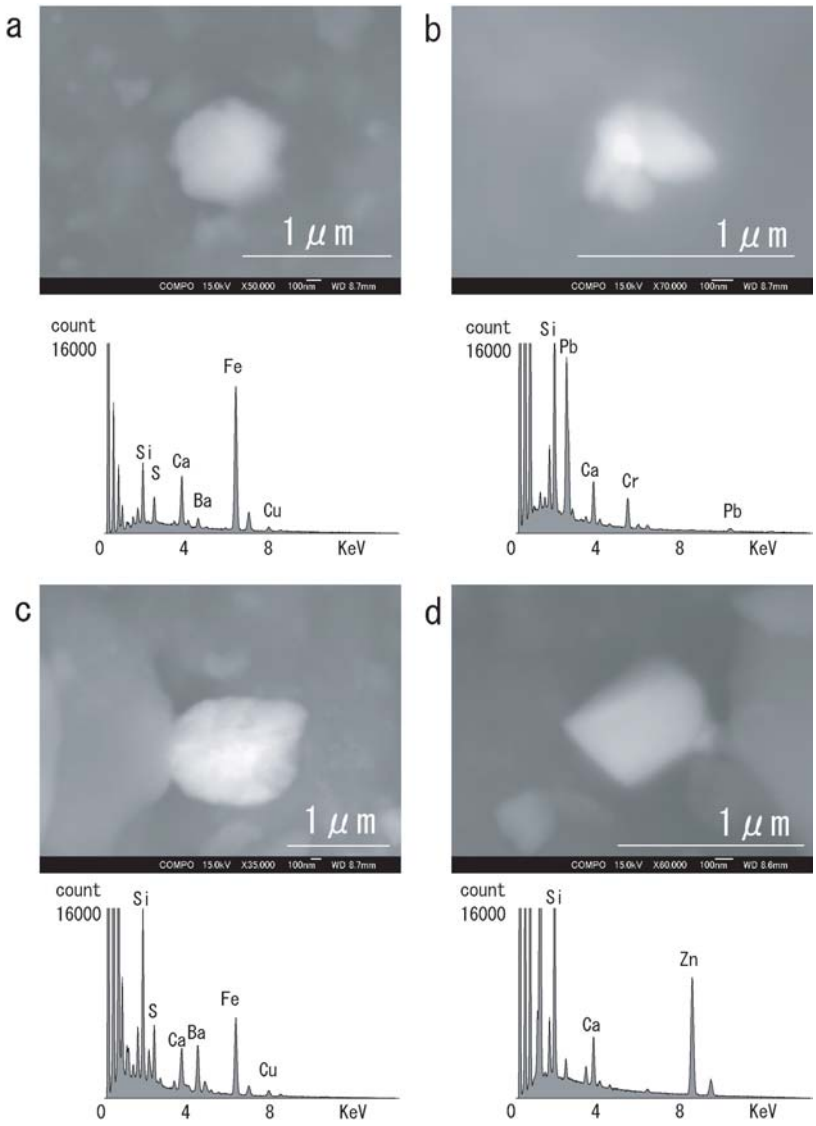

Figure 12: Typical image of metal particles embedded in tire dust. a: Cluster 1, b: Cluster 2, c: Cluster 3, d: Cluster 4

contributor of this cluster, as noted by the consistent particle diameter and chemical composition that was rich in Fe with a low level of Cu, Sb, and Ba. The ratio of Cu/Sb was 2.5 in this cluster, which was within the diagnostic criteria for brake wear particles (4.6±2.3) (Sternbeck et al. 2002).

A steel plant located in the southern part of the study area is also a source of Fe particles (Adachi and Tainosho, 2001). The chemical composition of most Fe particles derived from the steel plant was Fe and little Mn (several weight % or less) (Adachi and Tainosho, 2001).

Cluster 2

This cluster is rich in Cr/Pb. The average particle diameter is 0.42 μm. The morphology, shown in Fig.12b, is an aggregate of oval particles, which is similar to that of yellow paint shown in Fig.10a. Because the chemical composition, diameter, and morphology agree with that of $PbCrO_4$ in yellow paint material, we conclude that a large part of this cluster is abraded particles of yellow paint. The average molar ratio of Cr/Pb is 0.92, whereas the ideal ratio of $PbCrO_4$ should be one. This decrease means a minor presence of Pb-rich particles in this cluster. One of the possible sources of Pb particles is lead used in motor vehicle wheel balance weights (Root, 2000).

The abundance ratio of this cluster in each tire dust samples showed large variation among individual tire dusts (Average: 7%; SD: 7%; Max: 32%; Min: 0%) but not among sampling sites. This means that heavy metals embedded in tire dust need not indicate the sampling location. Additional investigation is needed to learn when tire dust assimilates metal particles and when tires abrade, and how far tire dusts are distributed in the environment.

Cluster 3

Cluster 3 is characterized by multiple elements (Ti, Cr, Fe, Cu, Zn, Sr, Y, Zr, Sn, Sb, Ba, La, Ce, and Pb) (Table 3). The average particle diameter in this cluster is 1.05 μm. The typical morphology and EDX spectra of this cluster are shown in Fig.12c. Because the brake dust has many Ti, Fe, Cu, Sb, Zr, and Ba particles, these particles are significant contributors to this cluster. The ratio of Cu/Sb (3.8) , which

was in good agreement with the diagnostic criteria for brake wear particles (4.6±2.3) (Sternbeck et al. 2002), also suggests the contribution of brake dust.

De Miguel (1997) has classified the elements in street dust (La, Sr, Y) as natural elements, and Sternbeck et al. (2002) showed that rare earth elements such as Ce, La, and Pr are hosted in a mineral phase in airborne particles. We found some heavy minerals such as allanit (Ca, Ce, Fe, Al, Si), zircon (Zr, Si), and monazite (P, Ce, La, Y, Th) by single particle analysis. This study area has a granite geological background, which includes these heavy minerals (Huzita and Kasama, 1983), so one of the possible sources of these elements is a natural source.

Classification into cluster 3 indicates multiple sources. Because the classification in this analysis was based on only major components of the particles, it is difficult to distinguish the particles with multi-elemental composition with exactness. Further division based on elementary ratios or detailed morphological analysis will help to classify them.

Cluster 4

Cluster 4 mainly consists of ZnO with an average particle diameter of 0.52 μm. The most typical morphology of the particles is square or multi-angular (Fig.11d). These characteristics agree with that of ZnO in tire tread (Fig.12a), so we conclude that most of the particles in this cluster come from ZnO in the tire tread. The abundance ratio of Cluster 4 was very different in each tire dust sample (Average: 22%; SD: 17%; Max: 56%; Min, 0%). Some tire dusts samples contained no particulate ZnO. The presence of particulate ZnO may depend on the manufacturing process of tire tread. Other possible sources of particulate Zn are metal plating, galvanized iron roofs(Fergusson and Kim, 1991), and brake dust (Davis et al., 2001, Fauser et al., 1999).

5.4 Conclusion

In this study we characterized the morphology and chemical composition of traffic-related material (brake dust, yellow paint, and tire tread) and heavy metal particles embedded in tire dust. Brake dust contains heavy metal particles such as Fe, Cu, Zr,

Sb, and Ba with a particle diameter of about 1 μm. Yellow paint contains Cr/Pb particles with an oval morphology and a diameter of about 0.5 μm. Tire tread has multi-angular ZnO particles 1 μm or less in diameter. A total of 2288 heavy metal particles were found embedded in tire dust and were classified into 4 groups by cluster analysis. Cluster 1 is rich in Fe, cluster 2 is rich in Cr/Pb, and cluster 3 is characterized by multiple elements. Cluster 4 consists mainly of ZnO. Judging from its chemical composition, particle diameter, and morphology, brake dust is a possible contributor of cluster 1 and 3, and yellow paint is a possible contributor of cluster 2. Zinc oxide in tire tread is a significant source for cluster 4.

These results suggest that tire dust assimilates traffic-related metal particles when the dust is rolled between surfaces and abraded. The interactions between tire wear debris and heavy metal particles may give the heavy metal risk to the tire dust. Further study that discusses the risk of heavy metal particles embedded in tire dust is needed.

6 Single particle characterization of size-fractionated street dust

6.1 Introduction

Particulate matters that are deposited on a road, usually called 'road sediments', 'road deposited sediments', 'street dusts' or 'road dusts', are significant pollutants in the urban environment because they contain high levels of toxic metals and organic contaminants such as polycyclic aromatic hydrocarbon (PAH) (Hopke et al., 1980; Fergusson and Kim, 1991; Hildemann et al., 1991; Rogge et al., 1993; De Miguel et al., 1997; Degirmenci et al., 2000; Li et al., 2001). Health hazards of street dust such as genotoxicity, estrogen-like cell growth activity (Degirmenci et al., 2000), dioxin-like activity (Matsui et al., 2002) and allergens (Miguel et al., 1999) have been reported. In addition to these risks, it is well known that street dust are sinks and sources of metals or other contaminants in an urban environment. Several studies have shown the environmental pollution caused by street dust in urban runoff (Legret and Pagotto, 1999; Sorme and Lagerkvist, 2002) and in the atmosphere (Manoli et al., 2002; Funasaka et al., 2003, Samara et al., 2003). For example, Funasaka et al. (2003) have showed that part of Zn and Pb in atmospheric particles is derived from road dust components in Osaka City, Japan.

Street dust consist of both natural and anthropogenic particles. Natural particles derive primarily from soil minerals, while anthropogenic particles derive from road construction materials (asphalt, concrete and road paint), automobiles (tire dust, brake dust, body rust and tail pipe exhaust), industrial inputs or atmospheric depositions. Regarding the sources of regional particles in Japan, Asian dust storm has brought metal and mineral particles in the spring (Var et al., 2000, Ma et al., 2001), and has been one of the sources of street dust in the fine fraction.

Most studies deal with relatively large particles of street dust (50-2,830 μm). The finer particles, less than 50 μm, can give helpful results regarding the relationship between atmospheric pollution and street dust. On the other hand, the coarser particles, greater than 50 μm, contribute mainly to elemental pollution of urban runoff or

soil. Some studies have indicated that the chemical composition of street dust varies with grain sizes between 20 μm and 1500 μm (Al-Rajhi et al., 1996) or between 63μm and 2000 μm (Sutherland, 2003). In several cases, toxic metals or metalloids are preferentially enriched in smaller grain sizes (Ellis and Revitt, 1982; Al-Rajhi et al., 1996; Sutherland, 2003). However, there have been no detailed studies to date focusing on the relationship between particle type distributions that characterized by single particle analysis and bulk chemical compositions in street dust. The aims of this study are 1) to investigate the particle size shift in a narrow area by the effect of rain or wind, 2) to classify the particles and to identify their sources and 3) to show the relationship between the distributions of the characterized particles and the bulk chemical compositions in the street dust. These results will facilitate the characterization of the compositions of street dust and the control of pollution, especially for urban runoff or soil, from road traffic.

6.2 Materials and Methods

6.2.1 Sampling sites

Fifty street dust samples were collected from a road median and two samples were also collected from a street gutter in Kobe, Japan during March of 2003 (Fig.13a). The road from which the samples were collected was R43. The mean traffic flow rate ranged from 64,000 to 72,000 vehicles per day, and the rate of heavy truck traffic ranged from 21.3% to 31.2% (Hyogo Prefecture, 1999). Sweeping maintenance of the road was carried out three times a month. The road median was at a height of 25 cm from the road surface.

6.2.2 Sample collection

For the samples collected from the road median, five transections (3 m in length) were established (Fig.13b) and 10 sampling locations were set up on each transection (Fig.13c). At each sampling location, rubber sampling frames (30 $\times$ 30 cm with an open area of 20 $\times$ 20 cm in the center) were emplaced (Fig.13d). The open area of the sampling frame (0.04 m^2) was swept using a brush and dust pan, and then

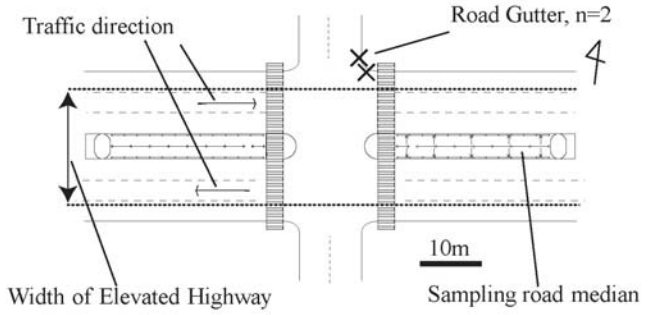

a: Sampling area

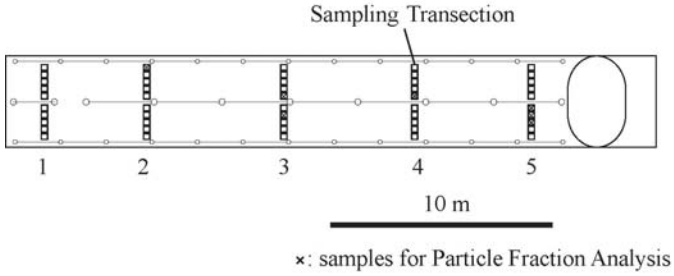

b: Road median

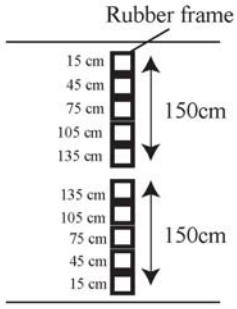

c: Sampling transection

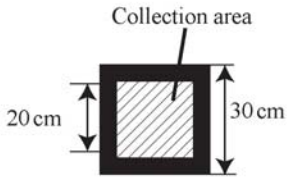

d: Rubber frame

Figure 13: Sampling map. a: Overview of the sampling site. b: Locations of sampling transections in the road median. c: Location of the sampling frames in the transection. d: Schema of the sampling frame.

vacuumed by a sweeper to collect the total load (Vaze and Chiew, 2002). Two bulk gutter samples were collected by the same method without using the sampling frame. The gutter was dry when the samples were collected. The collected samples were stored in plastic bags for subsequent preparation and analysis.

6.2.3 Sample preparation

The samples were dried for 48 hours at 105℃. They were then sieved using a nylon mesh screen into 10 fractions: >2830 μm, 1000-2830 μm, 840-1000 μm, 250-840 μm, 200-250 μm, 150-200 μm, 100-150 μm, 60-100 μm, 50-60 μm and <50 μm. All the fractions were weighed. Seven of the 50 road median samples with the greatest mass (shown in Fig.13b) and the two gutter samples were used for subsequent chemical composition and single particle analyses. Chemical composition analysis was conducted on all the fractions and single particle analysis was carried out on eight fractions (<1000 μm).

6.2.4 Analysis

Chemical composition analysis was carried out using an EDXRF. The analytical conditions were a tube voltage of 30 kV and a live time of 500 s. Each size-fractionated sample was homogenized under 50 μm by a tungsten carbide mill to reduce the particle size effect, and pressed into a pellet. The measured elements were Al, Si, K, Ti, Mn, Fe, Cu, Zn and Pb. The standard samples for EDXRF analysis should correspond to the physical state of the measured samples (diameter, density and state). Since the study area has weathered granite and granodiorite soil, we chose the Japanese geochemical reference samples JG1a, JG3 (granodiorite) and JG2 (granite) for the major part of the standard reference materials. We mixed size-controlled (<50 μm) metal powder (Ti, Mn, Fe, Cu, Zn and Pb) with these geochemical reference samples in order to analyze the metals. The precision and bias in this analysis were generally <10% except for Pb that had a low concentration (<0.015 wt.%).

Particle analyses were conducted by FESEM connected with a EDX detector. We used an acceleration voltage of 15 kV, a working distance of 15 mm and an EDX collection time of 20 s. The size-fractionated samples were decentralized to produce

an appropriate distance among the particles, and were affixed to carbon tape. All samples were coated with carbon. The beam was pointed at the center of each particle and the response area was within a distance of several micrometers. The EDX spectra did not reflect the compositions of all the particles; therefore, we used statistical analysis with a large number of particles to characterize their distributions in street dust.

Particle selection for single particle analysis was carried out as follows. Analysis areas were selected at the following magnitudes: $\times$ 20 (840-1000 μm, 250-840 μm, 200-250 μm, 150-200 μm), $\times$ 30 (100-150 μm), times 50 (60-100 μm), $\times$ 70 (50-60 μm) and $\times$100 ($<$50 μm). For the 840-1000 μm fraction, two areas were selected in order to collect a sufficient number of particles. In the other fractions, a single analysis area was selected. The EDX spectra of all particles in the area were collected (the maximum number of particles was 250). The results were presented as net X-rays that were calculated from the apparent concentration and were normalized to 100% in C, O, Na, Mg, Al, Si, P, S, Cl, K, Ca, Ti, Cr, Mn, Fe, Ni, Cu, Zn and Pb. Lead was used in the M-line to determine the net X-ray, and the other elements were used in the K-line. In order to avoid the overlap of neighboring elements in the EDX spectra, the elements with less than one sigma of the apparent concentration were deleted. Carbon X-rays were also detected due to the carbon coating; however, they were too weak to affect particle classification.

Multivariate analyses such as hierarchical cluster analysis was used to reduce the dimension of the data matrix. The cluster analysis was based on Euclidean distances with Ward's error sum classification. The consistent Akaike's information criterion was used to determine the most effective number of the clusters. This semiquantitative analysis has been used in previous studies resulting in the successful classification of ambient particles (e.g. Jambers and Grieken, 1997; Sitzmann et al., 1999). We also used principal component analysis (PCA) of bulk chemical compositions to estimate the contributing factors, and compared them to the result of the single particle analysis.

6.3 Results and discussion

6.3.1 Size distribution in street dust

Particle size distributions are shown in Figs.14 and 15. Figure 14 presents the particle size distributions averaged for each sampling transection and the gutter street dust. Figure 15 shows the particle size distributions of road median samples averaged for each distance from the road and the gutter samples. These transections and distances are shown in Figs.13b and 13c. The median grain diameter, D50, in the road median samples were 740-980 μm for each transection and 740-910 μm for each distance. The percentage of material <100 μm ranged from 8-10% in both the averaged samples, whereas it ranged from 17-22% in the gutter samples. The particle distributions among the road median samples were similar. Additionally, the particles concentrated to coarser fractions compared to those of the gutter samples (D50: 190 and 210 μm). This difference is possibly due to the effect of rain. The road median was covered by an elevated highway and was thus less affected by rain, while the gutter samples, which were residual, were carried by wash-off events and were therefore rich in small particle fractions (Vaze and Chiew, 2002). In addition, since vehicles cause reductions in particle size by abrasion, the gutter samples were possibly further reduced when they were displaced to the gutter.

6.3.2 Distribution of elements in street dust

The distributions of elemental concentrations in size-fractionated road median and gutter samples are shown in Fig.16. The concentrations were averaged for each size fraction. The distribution patterns between the road median and gutter samples are similar for Al, Si, K, Cu, Zn and Pb. For Mn, Ti and Fe, the concentrations in <200 μm fractions of the road median samples were higher than those of the gutter samples. Additionally, Ti in the road median samples exhibits a maximal value in the 60-100 μm fraction. Manganese, Fe, Cu and Pb show the highest concentrations in the finest fraction (<50 μm) and Zn shows the highest concentration in the 50-60 μm fraction. In other studies, concentrations of the metals (Cu, Zn and Pb) increased as the particle size decreased (Al-Rajhi et al., 1996). In this study, the decrease of Zn

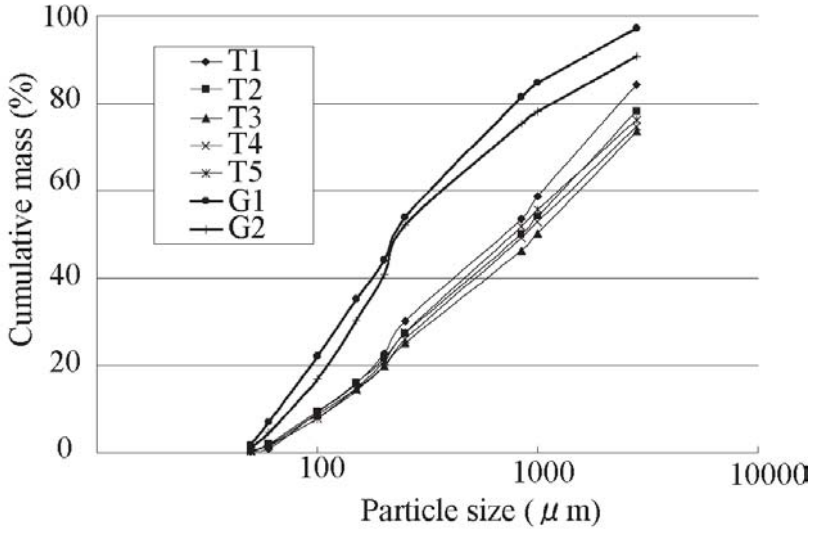

Figure 14: Particle size distribution in the sampling transections of the road median and the gutter samples. T: Transection. G: Gutter

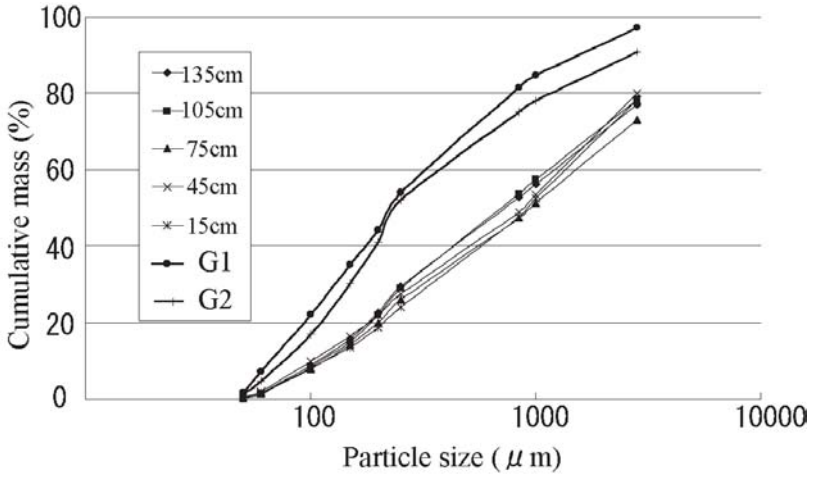

Figure 15: Particle size distribution in different distances from edge of the road median and the gutter samples. G: Gutter

composition in the finest fraction (<50 μm) is different from results of other studies, which may be due to the distribution of tire dust. The reasons for this are discussed in detail in a later section.

The mean concentrations of Cu, Zn and Pb in Hong Kong street dust with <2 mm fractions were 173 ppm, 1450 ppm and 181 ppm, respectively (Li et al., 2001), and that of Cu, Zn and Pb in Korea road gutter dust with <180 μm fractions were 64-124 ppm, 197-334 ppm and 58-534 ppm, respectively (Chon et al., 1998). The metal compositions in our study were generally high compared to those in other studies. This is probably due to the fact that the street dust in our study had less soil compositions because of the lack of bare ground around the road adjacent area.

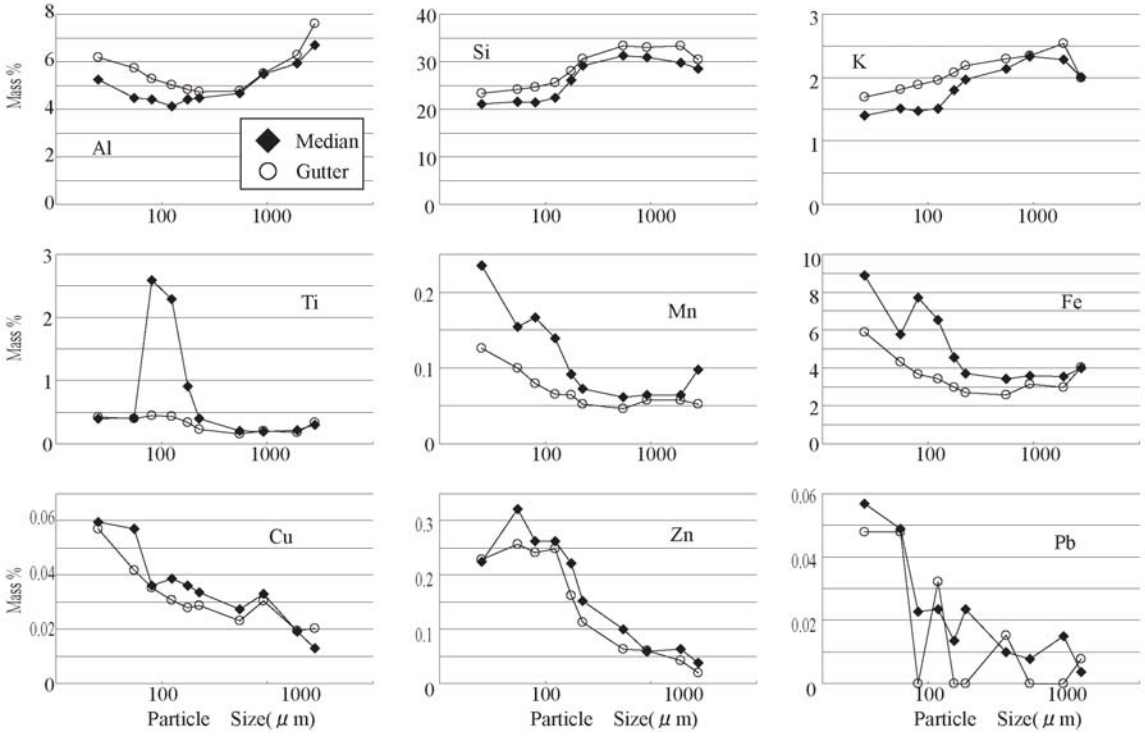

Figure 16: Distribution of elemental concentrations in the size-fractionated bulk street dust.

6.3.3 Particle classification and source apportionment

In the nine samples (seven road median samples and two gutter samples) with eight fractions, 13,099 particles were analyzed by FESEM, and 746 particles were

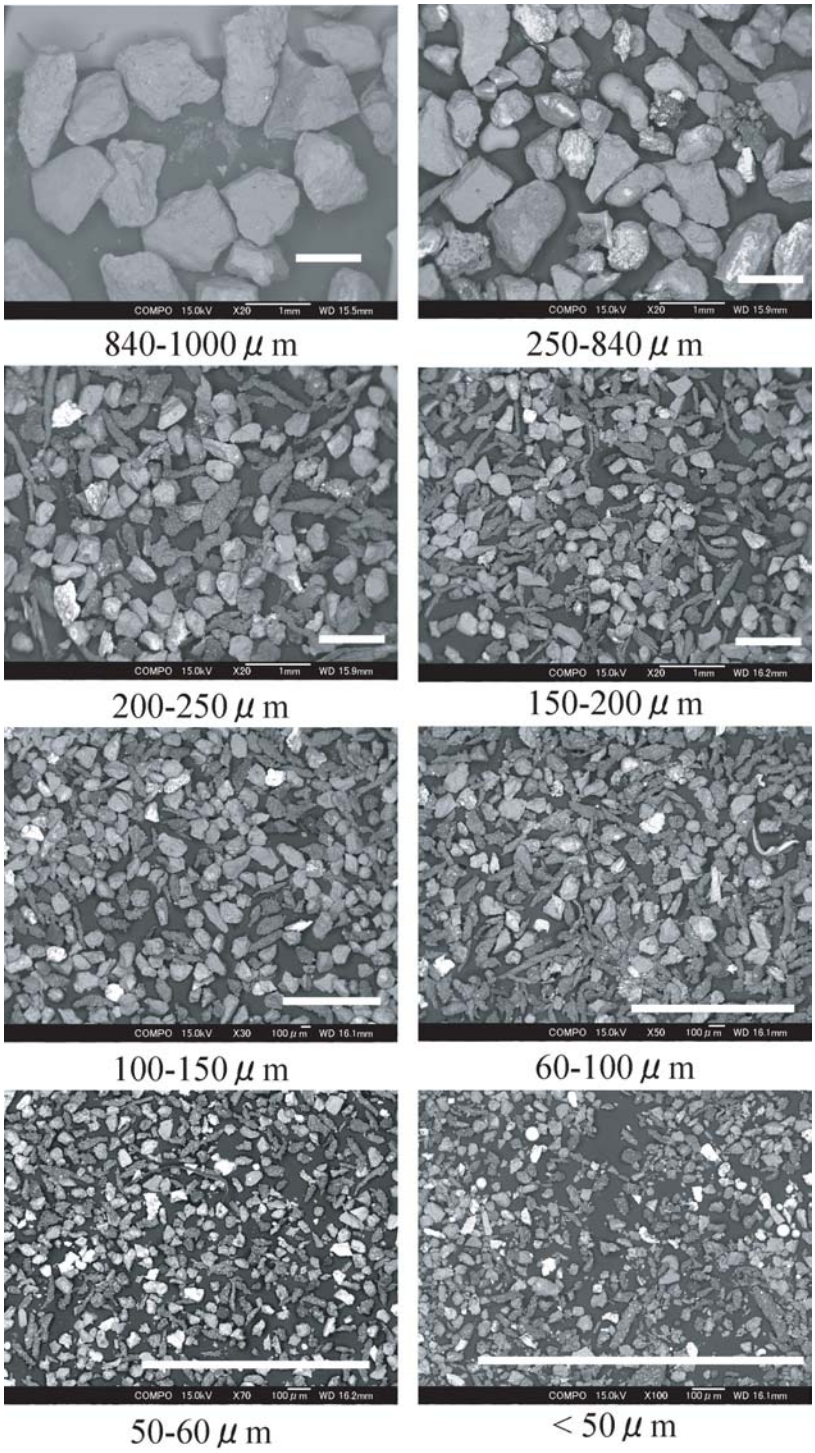

Figure 17: Typical images of each fraction in the road median sample (transection 5, 135 cm South); backscatter electron images (BEI). Scale bar indicates 1mm.

Table 4: Averaged net X-ray % of each particle type and reference materials

Type	1	2	3	4-1	4-2	5	6	AP^a	AP^b	FS^c	IL^d	QZ^e	TD^f
C	10.6	7.2	3.8	5.5	5	2.2	29.9	22.9	4.3	0.4	0.5	0.1	25.3
O	33.6	25.4	24.8	34.1	24.8	23.7	41	29.7	13.9	25.2	8.9	23.8	35.7
Na	0.3	0.1	2	0.1	<0.1	0.3	0.1	ND	ND	4	ND	ND	ND
Mg	1.3	1	1.1	0.7	0.2	0.2	0.4	0.7	0.7	ND	ND	ND	0.6
Al	10.1	6	14.5	2.3	2.9	3.5	4.3	4.9	2.3	15.8	2.3	0.6	8.2
Si	26.1	15.6	43	5.9	4.8	67.1	11.2	27.2	7.4	48.3	2.1	75.3	18.9
P	0.1	0.5	<0.1	<0.1	<0.1	<0.1	0.1	<0.1	ND	ND	ND	ND	ND
S	3.1	5.7	1.1	1.6	0.7	0.4	3	4.3	0.5	0.1	1.1	ND	1.8
Cl	1.4	2	0.6	1.6	0.4	0.2	1.5	0.3	ND	<0.1	0.2	ND	0.1
K	2	1.4	3.5	0.7	0.4	0.6	0.9	0.4	1	5.9	0.2	<0.1	1
Ca	7.7	31.6	3.6	4.5	1.8	1.1	5.4	8.4	68.5	0.2	0.8	<0.1	6.3
Ti	0.6	0.7	0.2	0.5	43.2	0.1	0.5	0.2	0.1	<0.1	61.7	0.1	0.6
Cr	0.1	0.1	<0.1	1.1	0.1	<0.1	<0.1	ND	<0.1	<0.1	ND	ND	<0.1
Mn	0.1	0.1	0.1	0.8	1.4	<0.1	0.1	<0.1	0.3	ND	0.2	ND	ND
Fe	2.8	2.2	1.5	40.1	14.1	0.5	1.4	0.8	0.9	ND	22.1	ND	1.4
Ni	<0.1	<0.1	<0.1	0.1	<0.1	<0.1	<0.1	0.1	0.1	ND	<0.1	ND	ND
Cu	<0.1	0.1	<0.1	0.2	0.1	<0.1	<0.1	ND	ND	<0.1	ND	ND	0.1
Zn	0.1	0.1	<0.1	0.2	<0.1	<0.1	0.1	<0.1	ND	<0.1	ND	ND	<0.1
Pb	0.1	0.1	<0.1	<0.1	<0.1	<0.1	0.1	0.1	ND	<0.1	ND	<0.1	0.1
n	2634	1425	3213	651	83	1579	2768	20	10	20	11	11	10

[a]AP(Asphalt): The EDX spectra were collected from asphalt surface without a Ca-bearing filler part. The asphalt sample was collected from the study area. [b]AP(Asphalt (Ca)): The EDX spectra were collected from a Ca-bearing filler part of asphalt. [c]FS(Feldspar): Feldspar contains both potassium feldspar (n=10) and sodium-calcium feldspar (n=10). The both feldspar were collected from granite rock in the study area. [d]IL(Ilmenite): Ilmenite samples were detected from road median samples based on their morphological and chemical features. [e]QZ(Quartz): Quartz samples were collected from granite rock in this area. [f]TD(Tire dust): Tire dust particles were detected from road median samples based on their morphological, chemical and constructional features.

excluded due to a low net X-ray (under 1,000 counts). In total, 12,353 particles were classified by the following treatment. Fractions over 1000 μm were mostly mineral or asphalt particles and were too large to analyze by FESEM; therefore, these fractions were excluded from the single particle analysis. The net X-ray of reference materials (asphalt, granite rock, tire dust and ilmenite) were also detected by FESEM-EDX. Asphalt was collected as an agglomerate sample from the same study area. A granite sample was collected from a base rock in the area. Tire dust and ilmenite samples that were identified from their morphological and compositional features in the street dust samples were also analyzed for reference materials. The features are mentioned later in this section (under 'particle type' 4-2 and 6).

Figure 17 shows typical backscatter electron images (BEIs). The images show the size fractions in the same sample collected from the road median (transection 5, 135 cm South). The brightness of the BEI reflects the atomic number of the elements. Particles in each fraction were classified by cluster analysis according to their net X-rays. They were classified into six or eight groups in each fraction, and a total of 53 groups were identified. All groups were then reclassified into six particle-type groups by cluster analysis. Additionally, high Ti-Fe-bearing particles were found in

abundance in particle type 4, which were confirmed to be ilmenite particles from their morphology, chemical composition and powder X-ray diffraction analysis. Ilmenite particles were found to play an important role in the compositions of Ti, Mn and Fe; therefore, ilmenite particles defined by high Ti (>30% net X-ray) in particle type 4 were reclassified as particle type 4-2, and the other particles in type 4 were defined as type 4-1. The average net X-rays of each particle-type group and reference materials are listed in Table 4.

Particle type 1 is rich in C, O, Al and Si. This group consists of particles combined with minerals and organic matter, and its most likely source is asphalt. An asphalt pavement consists of a mixture of aggregate and bitumen, which is a non-volatile residue from oil distillation (Fauser et al., 2000). The reference material asphalt without Ca-bearing parts also indicates its compositional features. The typical morphology of this group is rough particles exhibiting relatively dark brightness in BEI. Mineral-rich tire dust particles are also a possible source of this particle-type group. Given below is a detailed description of tire dust particles (particle type 6).

Particle type 2 is similar to type 1, except for the presence of a significant amount of Ca. The possible sources of the Ca-rich particles are soil, cement, gravel (Vega et al., 2001), building materials (Kim et al., 2001), road paint and the pavement (Fukuzaki et al., 1986). The Ca-bearing part of asphalt with high compositions of O, Si and Ca listed in Table 4 is regarded as one of the possible sources of this particle type.

Particle type 3 has the highest net X-ray percentage of Na, Al and K. Additionally, Si is an important element, with a moderate amount of Ca. The particles in this group are primarily rock-forming silicate mineral, especially feldspar, which contains three components, plagioclase ($NaAl_3SiO_8$), anorthite ($CaAl_2Si_2O_8$) and orthoclase ($KAlSi_3O_8$). Weathering material (e.g. clay) is also a possible source of this particle type, especially in fine fractions. The soil from the study area mainly consists of decomposed granite and granodiorite, which is rich in natural minerals such as feldspar and quartz. The reference material feldspar also indicates high compositions of Na, Al, Si and K.

Particle type 4-1 is rich in Fe. Iron is the most abundant metal element in street dust (Hopke et al., 1980). Particles exhibiting high brightness and sharp-edged or spherical particles found in finer fractions are mostly iron-bearing particles (Fig.17). Possible sources of Fe particles are automobile rust (Hopke et al., 1980), brake lining material (Hopke et al., 1980, Hildemann et al., 1991, Adachi and Tainosho, 2004) and automobile exhaust (Weber et al., 2000). The spherical Fe particles appeared to have originated primarily from a steel plant situated in the southern part of the study area (Adachi and Tainosho, 2001; Machemer, 2004). Metals such as Cr, Mn, Ni, Cu and Zn were also prominent in this cluster and most of them occurred as alloys with Fe. For example, stainless steel contains Fe, Cr and Ni in varying amounts. Manganese is the most frequent additive for steel, and Piña et al. (2000) showed a close relation between Mn and Fe in bulk urban aerosols. Cupper is used in brake lining materials with Fe (Adachi and Tainosho, 2004).

Particle type 4-2 is rich in Ti and Fe. The particles in this group are defined as ilmenite ($FeTiO_3$), which is present in granite as an accessory mineral. However, because the ilmenite particles in the collected street dust were too many to have been derived from a natural source, anthropogenic sources are possible. In the next section, the additional study about Ilmenite particles is carried out to determine their source or detailed characters. Particles in this group are rounded and exhibit high brightness (Fig.17). Compared to the composition of reference ilmenite, they had a low composition of Ti and Fe. However, the rates of net X-ray percentage of Fe/Ti were approximately 3.1 (type 4-2) and 2.8 (reference ilmenite).

Particle type 5 is rich in O and Si. This group is largely composed of quartz (SiO_2), which is a common mineral in a granitic area. Their compositions were very similar to that of the reference material quartz (Table 4).

Particle type 6 is rich in C, O, Si, S and Ca. This group was composed of mixed particles with high levels of organic matter and some minerals. The most likely contributor to this group is tire dust particles, which were commonly found in fractions $<250\ \mu m$ and exhibit a long and spindle-like shape, and low brightness (Fig.17). The reference tire dust particles identified from their morphological features also had high

compositions of C, O, Si and Ca, and a moderate composition of S. Tire dust particles are debris from tire treads; they consist primarily of organic matter (Rogge et al., 1993). Tire dust particles take in mineral or metal particles on a road when they abrade, and are therefore rich in Si, Ca and some metals (Smith and Veith, 1982; Camatini et al., 2001; Adachi and Tainosho, 2004). Some studies have suggested that tire dust particles typically have some S and Zn concentrations derived from their vulcanization process (Camatini et al., 2001; Kim et al., 2001; Smolders and Degryse, 2002; Adachi and Tainosho, 2004); however, the net X-ray in Zn was low in the present study. This is possibly because the X-ray collection time was too short to detect low-level components (a few percent). Organic materials such as bitumen-rich particles of asphalt are also a possible source of this particle group. It is difficult to distinguish organic-rich asphalt particles from mineral-rich tire dust particles with the methods used in the present analysis. Organic compound analysis is available for precise identification (Fauser et al., 2000).

6.3.4 Particle distribution in street dust

The distributions of the particle types are shown in Fig.18. In general, the abundance ratios of the road median samples are higher than those of the gutter samples in types 2, 4-1, 4-2 and 6. The distribution patterns of the road median and gutter samples were similar in all types except type 4-2. Type 4-2 showed a high composition in the 100-150 μm fraction in the road median samples compared to the gutter samples.

Type 1 particles show a bimodal distribution: 150-250 μm and 50-100 μm. Type 2 particles are high in the 50-60 μm fraction with large fluctuations. The distribution of type 3 is high in fractions over 1000 μm and under 50 μm. The abundance of type 4-1 increases with decreasing particle size; in contrast, type 5 increases with increasing particle size. Type 6 shows an abundance in the 60-100 μm fraction.

Machemer (2004) indicated that the diameters of Fe-bearing particles from an iron and steel manufacturing facility, which was one of the possible sources of particle type 4-1, were <1-10 μm. The authors have also investigated Fe-bearing spherical particles from steel plants in street dust in the study area and found that their average diameter was 16.7 μm (Adachi and Tainosho, 2001). These studies suggested that Fe-

bearing particles from steel plants were enriched in finer fractions. The mass median diameter of styrene butadiene rubber (SBR), which is an indicator of tire debris, was about 140 μm in roadway gutter material (Pierson et al., 1974); this was almost in agreement with the distributions of particle type 6.

6.3.5 Relation between bulk chemical compositions and particle distributions

Principal component analysis was carried out on the bulk chemical compositions of size-fractionated street dust to estimate the source apportionment addition to the cluster analysis. The results of PCs with eigenvalue >1 (PC1-3) are listed in Table 5. The first component with a high variance (63%) shows high loadings on metal elements (Ti, Mn, Fe, Cu, Zn and Pb) and negative loadings on mineral elements (Al, Si and K). This relation probably reflects the mixing rates of soil or asphalt indicated by particle types 1, 2, 3 and 5, which is in contrast to those of particle types 4-1 and 4-2 in the street dust. The second component indicates positive loadings on Al, Cu and Pb. The relationship between the elements was not shown clearly in the result of particle type distributions by cluster analysis. A possible explanation for relationship between these elements is that they are distributed as fine particles (<50 μm). Further analysis focusing on finer particles is required to identify the relation. The third component shows loadings on Al, Ti, Mn and Fe. The relationship between Ti, Mn and Fe suggests the presence of ilmenite particles (type 4-2). The presence of Al probably indicates the enrichment in the 150 μm fraction, which is the same as type 4-2 in type 2 and 3, which has a high Al content.

We found some relationships between the distributions of bulk chemical compositions and particle types. Particle type 3, which contain high Al content in their compositions, shows similar distributions to that of Al in bulk chemical compositions (Fig.16); i.e. their concentrations decrease in the middle particle diameter. The distributions of Zn and particle type 6 also show similar distributions. Zinc was hardly detectable in particle type 6, whose possible source was tire dust; however, the resemblance of these distributions indicated that the source of Zn was tire dust, as suggested by other studies (e.g. Smolders and Degryse, 2002). The distributions of

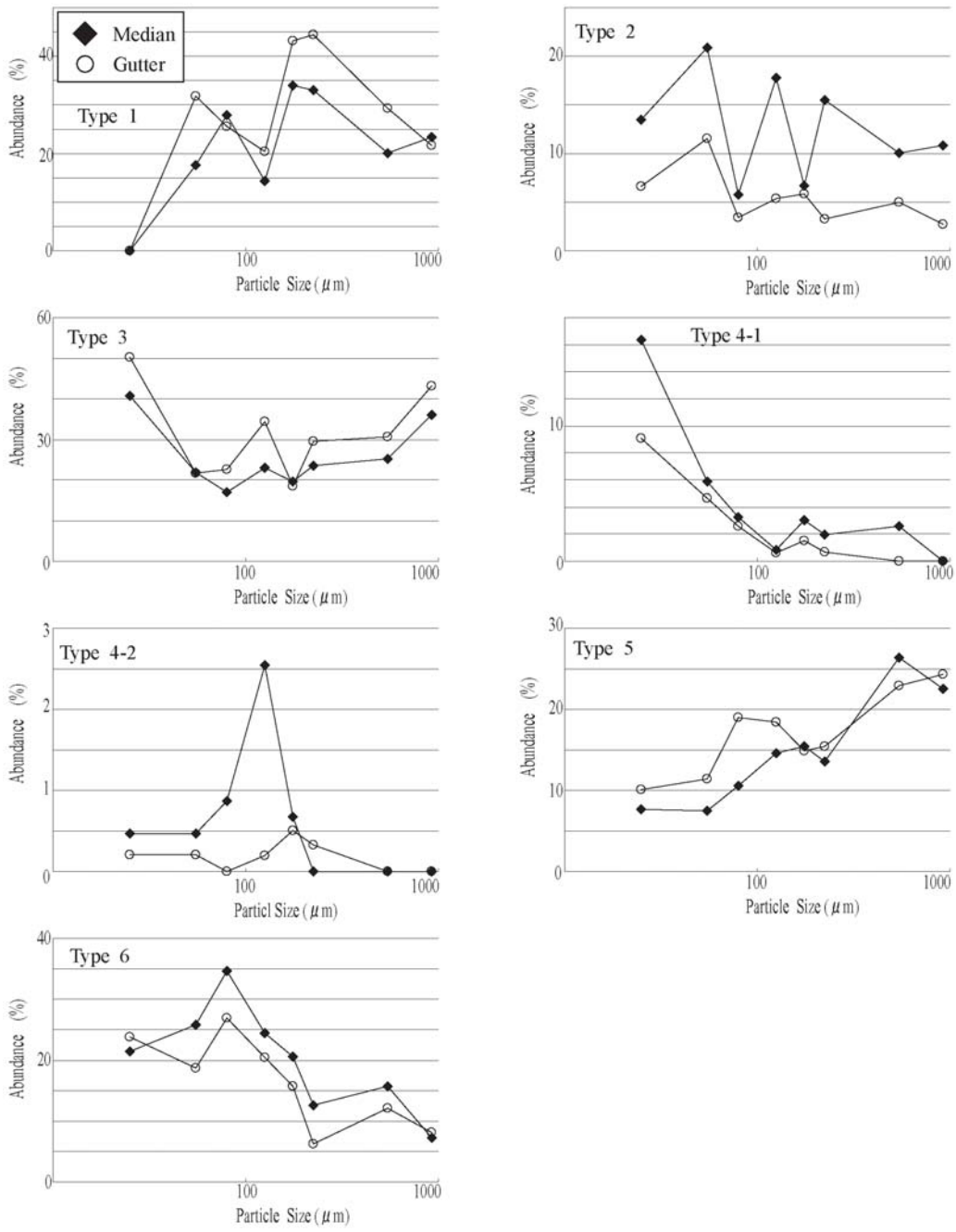

Figure 18: Distributions of abundance ratio of particle types in the road median and the gutter samples.

type 4-1 are similar to those of Mn and Fe in the bulk analysis. Additionally, the distributions of type 4-2 indicates the relation between Ti, Mn and Fe, especially in the 60-150 μm fraction of the road median samples. This is because type 4-2, which has high concentrations of Ti, Mn and Fe, shows biased distributions in the 60-200 μm fraction of the road median sample. However, the peaks of the distributions of particle type and bulk chemical composition exhibited a slight deviance; the distribution of the particle type had a strong peak in the 100-150 μm fraction, whereas that of bulk chemical composition had a strong peak in the 60-100 μm fraction. An analysis on a larger number of particles is required to conform to the bulk chemical composition.

Table 5: Variable loadings on the first three factors from a principal component analysis of bulk chemical composition among all size-fractionated street dust samples

	PC1	PC2	PC3
Al	-0.5	0.4	0.7
Si	-1.0	0.0	-0.1
K	-0.9	0.1	-0.1
Ti	0.6	-0.7	0.2
Mn	0.9	0.1	0.4
Fe	0.9	-0.1	0.4
Cu	0.7	0.4	-0.2
Zn	0.9	-0.1	-0.4
Pb	0.7	0.6	-0.1
eigenvalue	5.7	1.3	1.0
variance(%)	63.4	14.0	11.4
cumultatitive(%)	63.4	77.3	88.8

6.4 Conclusion

Street dust were collected from a road median and gutter in Kobe, Japan. The distributions of particles size, chemical composition and particle type of these samples were compared. The road median sediments showed a small variance between their particle distributions; whereas, there was a large variance between the road median and gutter samples. The particle types were classified into seven types by cluster analysis of about 13,000 particles, and their possible sources were estimated (asphalt, Ca-bearing materials, feldspar, Fe-bearing materials, ilmenite, quartz and tire dust). Some relationships between the distributions of chemical compositions and particle

types were founded. Street dust consist of multiple materials derived from both natural and anthropogenic sources. The dominant diameters of these compositions are varied, which influenced the bulk chemical compositions. As a result of varying particle size distributions due to the effect of wind, rain or traffic on the road environment, the bulk chemical composition of street dust was also altered. Therefore, single particle analysis used in this study is useful to analyze the metal contents in the street dust without being affected by their particle size distributions.

7 Street dust contamination caused by ilmenite

7.1 Introduction

Street dusts are a significant contributor to environmental pollution by heavy metals in the urban environment (Hopke et al., 1980; Fergusson and Kim, 1991; Rogge et al., 1993; De Miguel et al., 1997; Li et al., 2001). Street dust arises both from natural processes and from human activities; major contributors are motor vehicles (tire wear, exhaust, brake and clutch linings, mud and dirt carryout, truck spills, corrosion and abrasion of panels and undercoatings, and lubricants, coolants, hydraulic fluids and oil), sanding and salting, pavement wear, litter, biological debris, wind and water erosion from adjacent areas, and atmospheric pollution fallout (Brookman and Drehmel, 1981). In the case of elemental contamination, many artificial causes such as tire wear, exhaust, brake linings, oils, catalysts and pavement wear have been investigated for their influence in heavy metal loadings (Hopke et al., 1980; Fergusson and Kim, 1991; Hildemann et al., 1991; De Miguel et al., 1997; Adachi and Tainosho, 2003; Adachi and Tainosho, 2004); however, mineral substances have been less studied for their contribution to the pollutants. Mineral substances derived from both human activity and natural process. In terms of human activity, mineral substances are widely used as primary materials in many manufactories. When they spill in transportation or other processes, they may contaminate certain elements in the street dust.

The present study investigated street dust collected from Kobe, Japan, and analyzed ilmenite for its chemical contribution especially in Ti composition. The composition of ilmenite is $(Fe, Mn)TiO_3$. They are common accessory minerals in igneous rocks. On the other hand, ilmenite is a major source of Ti in the manufacturing process (Klein, 2001). The aims of this study are to confirm street dust contamination caused by ilmenite, and to determine whether the ilmenite were derived from natural or non-natural source.

7.2 Materials and methods

7.2.1 Sample collection

Sixty-four street dust samples were collected from 12 crossroads on Route 43 (R43) in Kobe, Japan during April of 2002 (Fig. 19).

More than 100g of street dust samples were collected from road dividers and gutters with a nylon trowel at each sampling point. Six samples of river sediments were collected from the Sumiyoshi River, which runs through the study area from north to south (Fig.19).

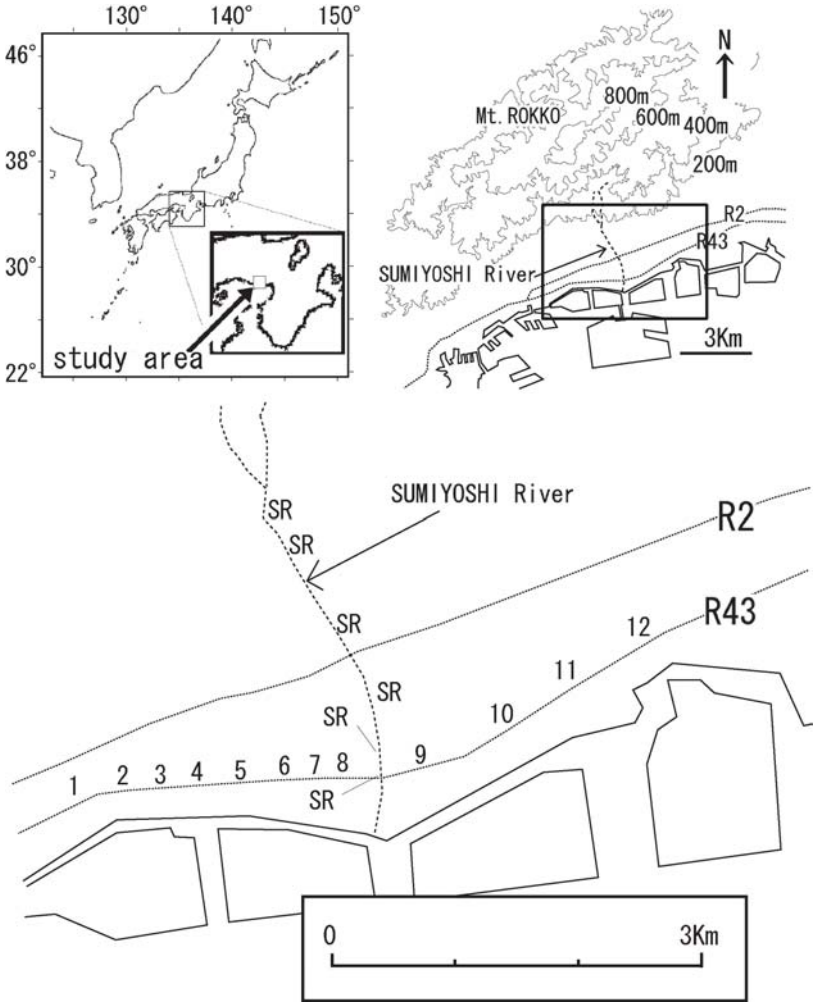

Figure 19: Location of study area and sampling points. The number indicates the sampling crossroad. SR: Sampling points of Sumiyoshi River sediments.

7.2.2 Analysis

Chemical composition analysis was conducted using an EDXRF with an Rh target and a Si(Li) detector. The analytical conditions were 30kv of tube voltage and 500s live time. The street dust samples were dried at room temperature and sieved through a 149-μm nylon screen, then pressed to make a pellet sample. The measured elements were Al, Si, K, Ti, Mn, Fe, Cu, Zn and Pb. X-ray powder diffraction (XRD) analysis was conducted by Cat2013 (Rigaku Corporation, Tokyo, Japan) with CuK X-ray source (40kV, 25mA). Street dust samples were ground well and placed on glass sample plates. For single particle analysis of the ilmenite particles by FESEM-EDS, we used an acceleration voltage of 15kV, a working distance of 15mm, and an EDS collection time of 100 seconds. The street dust and river sediments samples were affixed to a carbon tape and were coated with carbon for its conducting properties.

7.3 Results and discussion

7.3.1 Ilmenite contamination in street dust

The XRD pattern detected in the street dust (sampling point 7) is shown in Fig.20. The diffraction patterns are consistent with ilmenite patterns (32.7°, 35.3°, 40.5°, 49.0°, 53.3°). Reflections of quartz (36.5°, 39.4°, 42.4°, 45.7°, 51.9°) and calcite (43.1°, 47.5°) can also be seen in Fig.20. Quartz may reflect the soil and calcite may derive from asphalt filler.

The distribution of the averaged Ti composition in the street dust from each crossroad is shown in Fig.21. The distribution shows a higher Ti composition in the eastern part of the study area. The average Ti wt% was 1.3 and the maximum Ti wt% of the street dusts was 3.7 (sampling point 7). The Ti compositions in this analysis were high compared to that in other studies. The author has investigated the averaged Ti composition of 120 samples of park soils from the eastern part of Kobe, which was 0.25 wt% (Adachi and Tainosho, 2000). Yeung et al.(2003) conducted EDXRF analysis in street dust from Hong Kong and found a Ti contribution of 2370ppm; in other areas it was found to be 1100-7452ppm (Yeung et al.,2003), and Fergusson and Kim (1991) reviewed 800-3000ppm of Ti composition in urban street

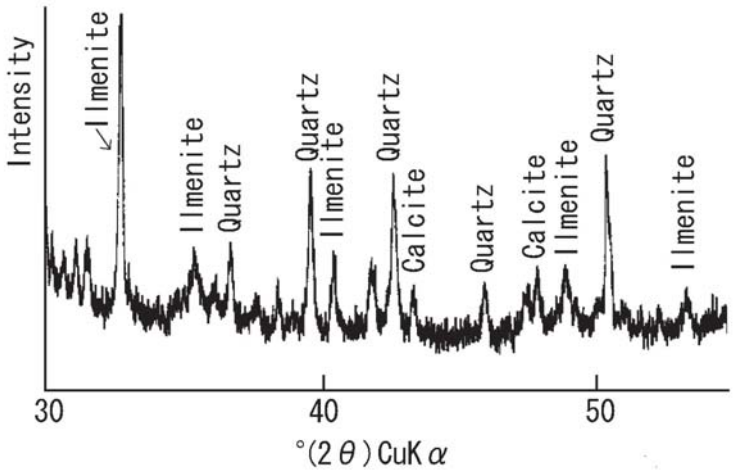

Figure 20: XRD pattern of high Ti street dust (sampling point 7).

dust.

Table 6: Variable loadings on the first four factors from a principal component analysis of chemical composition data in 64 street dust samples

	PC1	PC2	PC3	PC4
Al2O3	-0.9	-0.3	-0.3	-0.1
SiO2	-0.9	-0.3	-0.2	-0.1
K2O	-0.7	-0.6	-0.2	-0.2
TiO2	-0.7	0.6	0.1	0.0
MnO	-0.7	0.7	0.0	0.1
Fe2O3	-0.6	0.7	-0.2	0.0
Cu	0.5	0.1	-0.7	0.5
Zn	0.8	0.2	-0.1	-0.2
Pb	0.5	0.4	-0.3	-0.6
Eigenvalue	4.5	2.0	0.9	0.7
Variance(%)	50.2	22.6	9.8	7.9
Cumultatitive(%)	50.2	72.9	82.7	90.6

Multivariate analysis, principal component analysis (PCA), was conducted to estimate the component of contribution to the Ti concentration. Table 6 lists the loadings for the first four principal components (PCs) in the 64 street dust samples. PC1 shows 50.2% of variance relating to Cu, Zn and Pb, and shows a negative relation to Al, Si, K, Ti, Mn and Fe. This relation has also been found in other studies in roadside soils or street dust by PCA (De Miguel et al., 1997; Carlosena et al., 1998; Yeung et al., 2003). The loadings are attributed to anthropogenic sources, and especially to traffic sources such as tire dust, brake dust, and oil (De Miguel et al., 1997; Davis et al.,

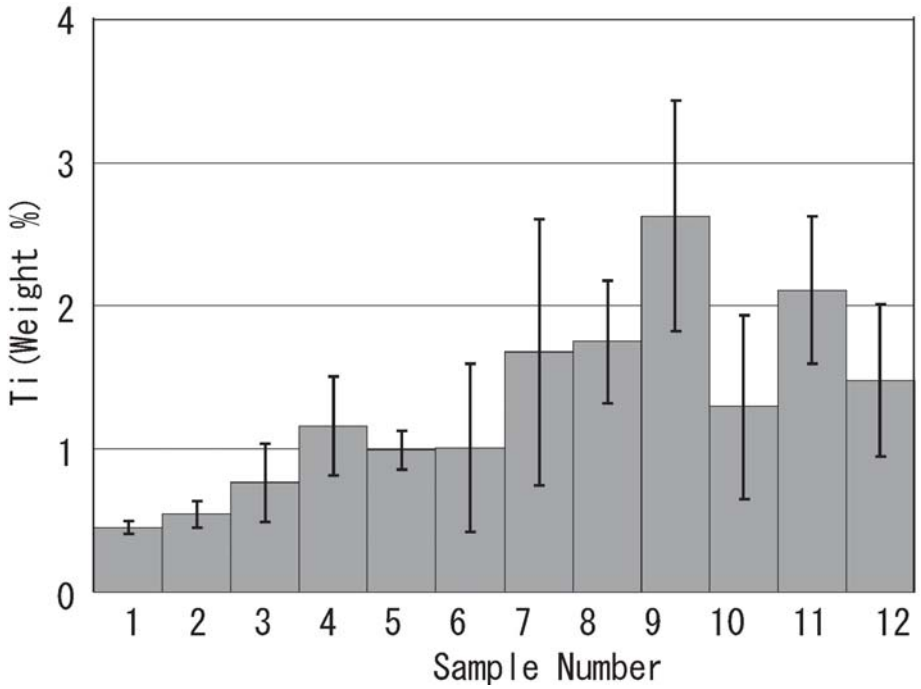

Figure 21: Distribution of Ti weight % in street dust samples. The data was averaged among the sampling points. Note that error bars represent standard deviation.

2001; Yeung et al., 2003). Titanium was also included in this anthropogenic group in some studies (De Miguel et al., 1997; Yeung et al., 2003). Titanium is found in traffic-related materials such as pavement, white paint (Fukuzaki et al., 1986), and brake dust (Hildemann et al., 1991); therefore, in a usual situation without identified special sources of Ti, it is assumed to arise from traffic elements.

PC2 shows 22.6% of variance relating to Ti, Mn and Fe distributions. The relationship between PC2 and Ti content is shown in Fig.22. They are related closely in higher Ti content (more than 2 wt.%). The study area includes a steel plant, which is one of the sources of Fe and Mn, but not of Ti (Adachi and Tainosho, 2000, Adachi and Tainosho, 2001). It is possible that PC2 reflects the contributions of both ilmenite and steel plants, and in higher Ti content, PC2 may be a good reflection of the ilmenite.

The morphology and EDS spectra of ilmenite particles in the street dust samples are shown in Fig.23. These particles show a rounded morphology. Fig.23D shows street dust with a high Ti content from the sampling point 7, and we could find

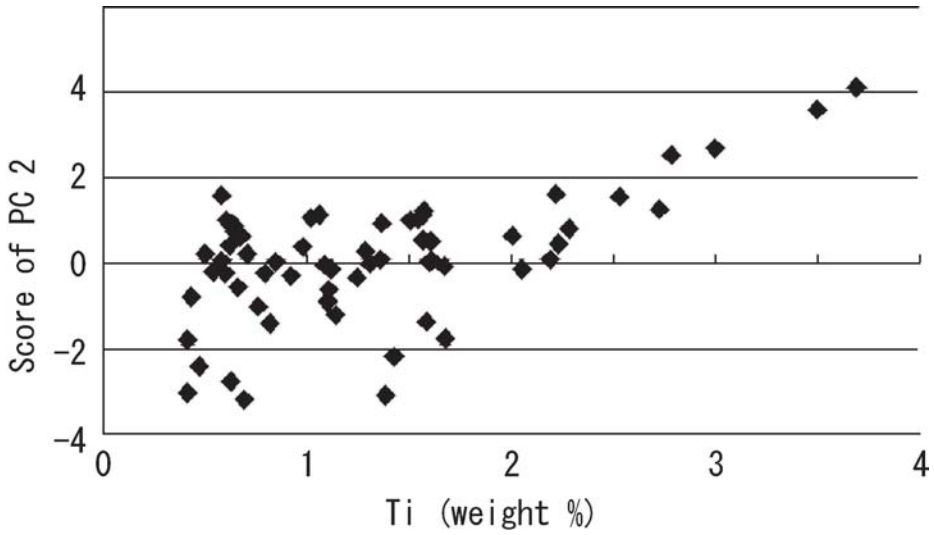

Figure 22: Relation between score of PC2 determined by PCA and Ti weight % in street dust samples.

so many bright rounded particles, which were ilmenite judging from their chemical compositions detected by EDS.

The average rate Ti/Mn in the street dust determined by EDXRF was 17.1 and in the median composition of the ilmenite the rate determined by FESEM-EDS was 18.4. If the ilmenite was the only source for Ti and Mn in the street dust, the both rate should be equal. The street dust contained other sources for Ti and Mn in practice, therefore the both rate was not equivalent exactly, but the both rate were close enough to explain the ilmenite contamination in the street dust.

From above results, we concluded the source of higher Ti compositions in the street dust was attributed to the ilmenite particles.

7.3.2 Chemical and morphological comparison of R43 ilmenite with river sediment ilmenite

In order to estimate the environmental impact of ilmenite particles, it is important to know whether they are derived from natural or non-natural sources. The study area contains granite as a background material and that has ilmenite as an accessory mineral. We characterized the morphologies and chemical compositions of the ilmenite particles in samples from geological sources, river sediments.

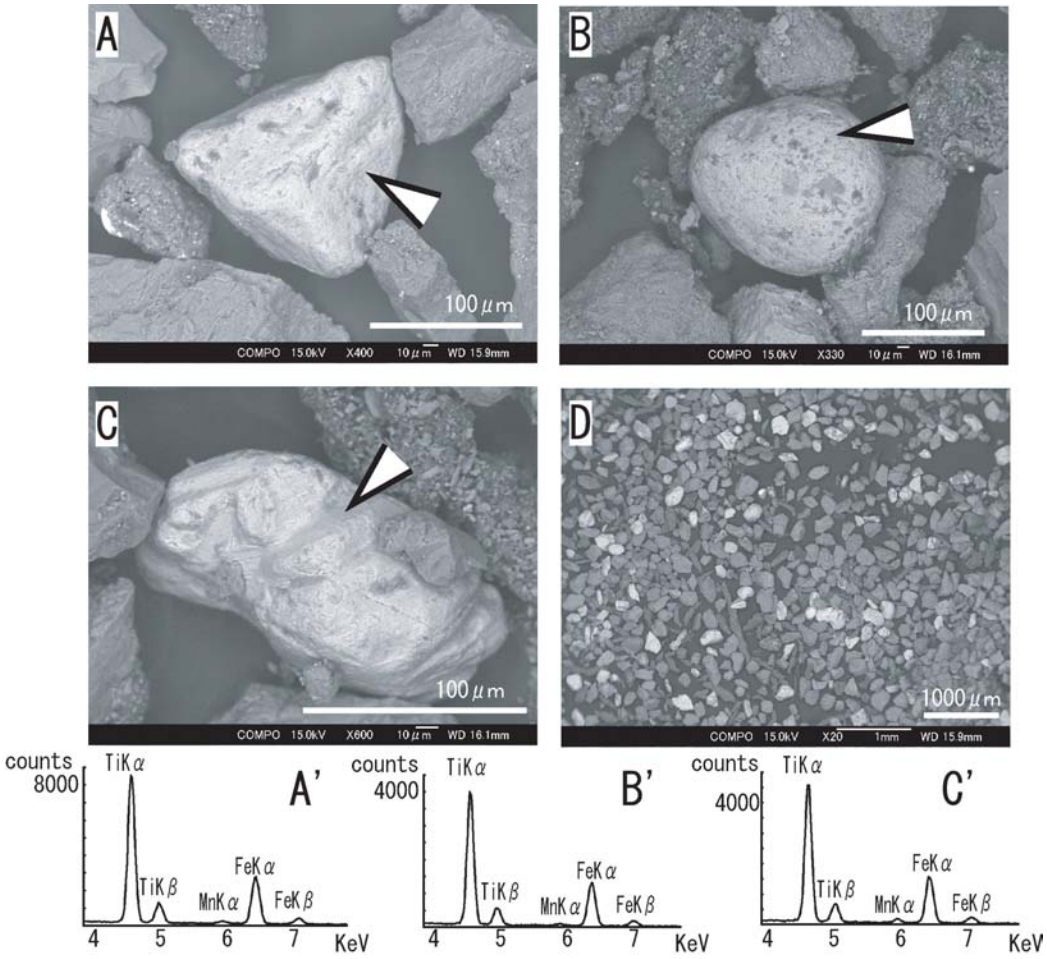

Figure 23: Back Scattering Electron (BSE) image of ilmenite corrected from street dust (a, b, and c) and the low magnitude of street dust (sampling point 7) (d), and their Energy Dispersive Spectrometer (EDS) spectra (a', b', and c').

Fig.24 shows the back-scattered electron (BSE) imaging and EDS spectra of ilmenite particles collected from river sediments. Ilmenite from river sediments showed both rounded (Fig.24A) and angular morphologies (Fig.24B). Because the sampling river has a short and steep flow path from the Rokko Mountain, some minerals are not well rounded.

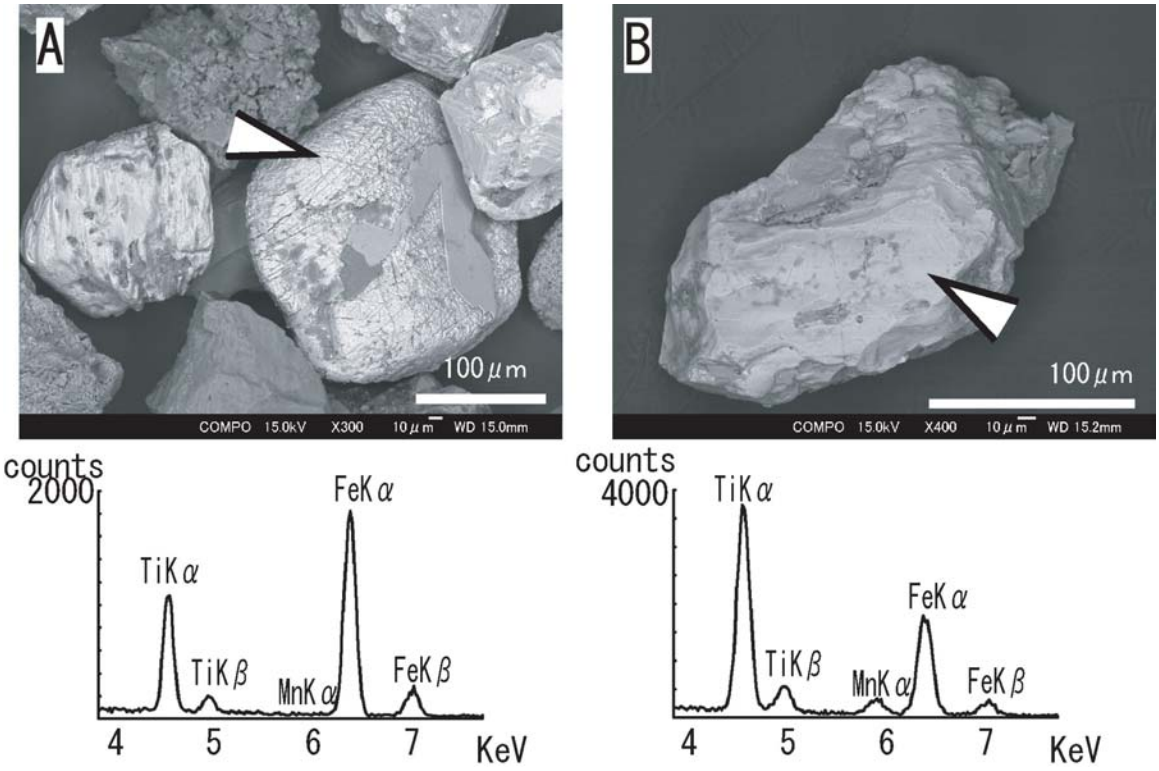

Figure 24: Back Scattering Electron (BSE) image of ilmenite corrected from river sediment (a and b) and their Energy Dispersive Spectrometer (EDS) spectra.

Fig.25 shows a triangular diagram for Fe, Ti and Mn in the ilmenite from the street dust (430 particles) and the river sediments (64 particles), in which Mn is decupled for emphasis. The distribution of the ilmenite from R43 is different from that from river sediments; the R43 ilmenite showed concentrations of Fe (30-40%), Ti (30-50%) and Mn× 10 (10-40%), while other the river sediments showed the following concentrations: Fe (20-40%), Ti (20-40%) and Mn× 10 (30-60%) in some samples, and Fe (20-80%), Ti (20-80%) and Mn× 10 (0-20%) in others.

Because the morphology and chemical compositions shown in Figs.24 and 25 indi-

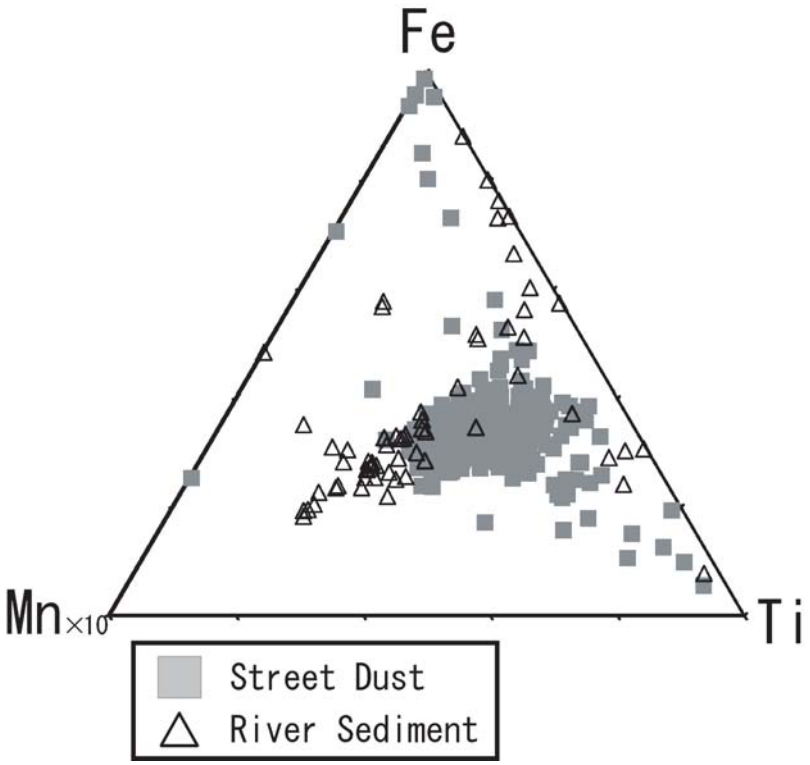

Figure 25: Diagrams showing the chemical characteristics of ilmenite corrected from street dust and from river sediment. Manganese content is decupled for emphasis.

cate differences between the ilmenite from R43 and that from the river sediments, it is possible that the ilmenite collected from R43 come from non-natural sources. The biased distribution of Ti composition in the street dusts (Fig.21) that showed the concentration in eastern part of the street dust, also suggests the non-natural source of the ilmenite. In this analysis, we could not confirm the exact source of the ilmenite. Further investigation about the plants that use ilmenite as primary materials in this area will be needed.

7.4 Conclusion

We confirmed the existence of contamination by mineral substances in street dust from Kobe, Japan. The findings of the present study are 1) Street dust in this area had a high Ti content as determined by EDXRF. The sources of this high Ti content were evaluated for ilmenite particles from the reasons of the XRD refraction, the distribution of Ti, Mn and Fe characterized by PCA, and the approximation of Ti/Mn ratio in the street dust and the ilmenite. 2) The source of the ilmenite particles found in the street dust samples is evaluated to be non-natural because of the differences in the morphology and chemical composition between R43 and river sediment samples.

8 Atmospheric deposition as a source of heavy metal in the urban environment

8.1 Introduction

This study has investigated heavy metal loadings from particulate atmospheric deposition by single particle analysis. Atmospheric deposition is a one of pathway of heavy metal loading in the urban environment. The atmospheric deposition loadings influence extensive area far away from a source of particles and result in "urban heavy metal risk". The study of atmospheric deposition is important to know the urban heavy metal background loadings.

Many studies have analyzed suspended particulate matters (SPM) which have less than 10 μm in diameter as a significant cause for atmospheric pollution. On the other hand, atmospheric deposition that included all large particles has been less interested except their amount. However, as concerned for the heavy metal ability, large particle depositions are more important than SPM.

To analyze the distribution of the amount or chemical composition of atmospheric deposition, it takes long time for a sampling period such as months, seasons, or even in years with a passive sampler. The long time sampling period enables an accurate deposition estimate, but it takes too long time to discuss an hourly or daily alteration of the deposition. The hourly and daily alteration is need to estimate sources of heavy metal deposition or harmful for the human health. Therefore, we used a single particle analysis to estimate the heavy metal loadings. Because this method analyzes individual particles by scanning electron microscope (SEM), it is possible to evaluate the heavy metal loadings from a few milli gram of deposition sample. Additionally, the single particle analysis gives morphological and grain size information of the deposition particles, therefore we can identify the source of the particles.

The object of this study is to estimate the heavy metal loadings in the urban environment from an atmospheric deposition by a single particle analysis. The heavy metal loading was determined by daily period, and the heavy metal contribution rates from several sources were also estimated.

8.2 Experimental Section

8.2.1 Sampling condition

Atmospheric deposition was collected at 24 hours during October 2003 in Kobe. The sample equipments were established on a roof of the building located in Kobe University at about 200-meter elevation. The sampling point is in residential area. The temperature in the sampling day was between 6.2 and 23.3℃. The average wind speed was 0.84 m/s (Max. 7.75 m/s) and the wind direction was mainly northwest.

8.3 Sampling equipments

We used two sampling equipments to trap an atmospheric deposition in order to measure mass deposition flux and heavy metal loading flux. The mass dry atmospheric deposition flux was measured using an aluminum foil coated with Apezion L grease on a flat plate (Fig. 26B). The total exposed surface was $1000cm^2$ (25cm × 40cm). The aluminum foil was weighted before and after the sampling, and the deposition flux ($mg/m^2/day$) was determined.

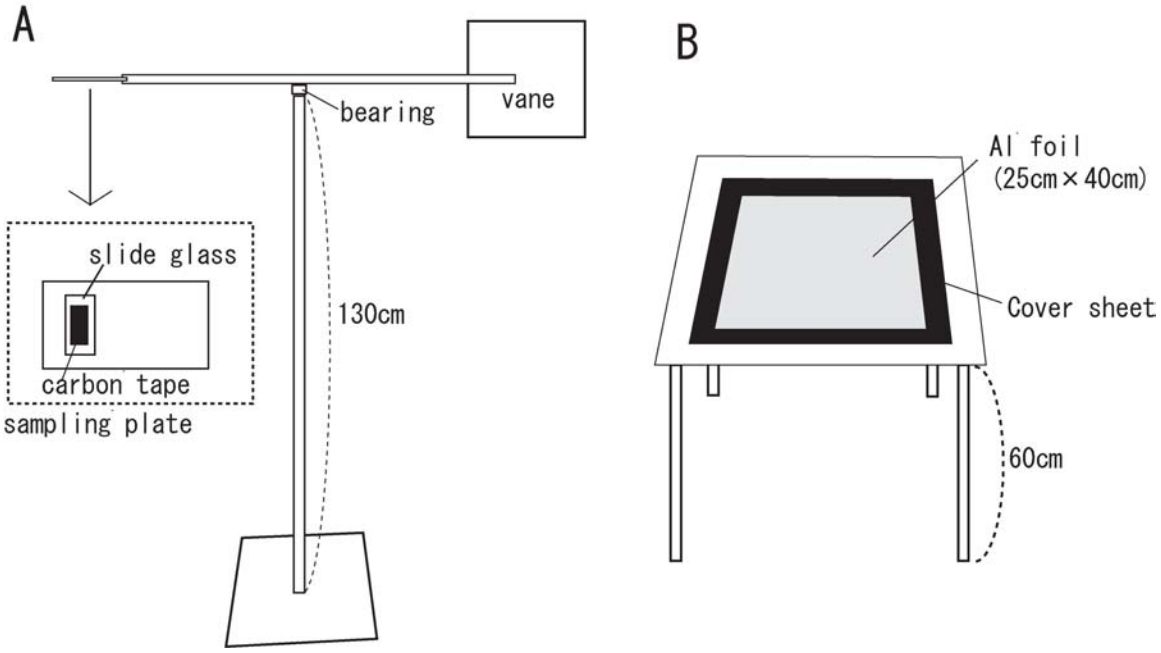

Figure 26: Schematic illustrations of sampling equipments. A: Atmospheric deposition sampler for SEM analysis. The direction of sampling plate is constantly toward the wind. B: Atmospheric deposition sampler for the mass loading measurement.

The atmospheric deposition for the SEM analysis was caught on a carbon tape (2cm × 3cm) adhered on a sharp leading edge, mounted on a wind vane (Fig. 26A)(Noll et al., 1988). These equipments reduce an edge effect that is caused by a local turbulence (Vawda et al., 1990). The collected deposited particles were analyzed their morphology, diameter, and chemical composition by FESEM-EDS. We used 15 kV of the acceleration voltage, 15 mm of the working distance, and 30 seconds of EDX collection time. Heavy metal particles were detected in backscattered electron images (BEIs). A BEI was taken at × 200 ($0.264mm^2$, 0.6mm × 0.44mm) and at totally 432 of BEIs were taken (114 mm^2). Heavy metal particles were brighter than silicate mineral particles in the BEI because the brightness of the BEI reflects an atomic number of the object. The detection limit of the particles in this method was about $0.5\mu m$ in diameters. We detected all heavy metal particles that derived from artificial sources. The EDX quantification was determined using the ZAF method, and recalculated to 100% for 26 elements (O, Na, Mg, Al, Si, P, S, Cl, K, Ca, Ti, V, Cr, Mn, Fe, Co, Ni, Cu, Zn, As, Sn, Sb, Ba, W, Pb, and Bi). Hierarchical cluster analysis program was used to divide the heavy metal particles. The cluster analysis was based on Euclidean distances with the Ward's error sum classification.

8.3.1 Heavy metal loadings flux

Each heavy metal loadings from atmospheric deposition was determined by a single particle analysis. Firstly, we determined the maximum diameters (d_{max}), minimum diameters (d_{min}) and chemical compositions (weight % (W)) of all heavy metal particles in the analysis area (A). The volumes of heavy metal particles (V) were calculated using the following equition (Zufall et al., 1998).

$$V = \pi/6 d_{max}^2 d_{min}$$

The loading fluxes in each heavy metal ($F_{metal}(mg/m^2/day)$) were determined as following equation.

$$F_{metal} = (\sum VW\rho)/A/day$$

where ρ means density of each element.

8.4 Results and discussion

8.4.1 Mass flux of atmospheric deposition

The mass flux of atmospheric deposition was $46mg/m^2$. The annual averaged atmospheric deposition flux in Kobe (Higashinada ward) was 2.5 $ton/km^2/30day$ (83 $mg/m^2/day$) using deposit gauge method at the period from April 2001 to March 2002 (Environmental Bureau, City of Kobe, 2002). The daily deposition loading data in this study is available because the difference between the two data was in a range of daily or monthly variation.

8.5 Single particle analysis

In the $114mm^2$ SEM analysis area, 204 of heavy metal particles were detected. Averaged d_{max} and d_{min} was $3.7\mu m$ and $2.5\mu m$, respectively. Particles other than the heavy metal particles were mainly salt, tire dust, fry ash (spherical mineral particles), or mineral particles. Heavy metal loadings evaluated from single particle analysis are shown in Fig.27. The most abundant heavy metal was Fe ($3488\mu g/m^2/day$) and followed by Sn. In deed, only two Sn-including particles were detected, and one large high Sn particle ($d_{max} = 20.1\mu m$ and $d_{min} = 17.3\mu m$) contributes to the high Sn loading. The detection sensibility of the heavy metal loading by the single particle analysis is extremely good but the reliability of the data rely on the total number of the data set.

The rate of heavy metal deposition per total deposition was 8.1%. Artificial heavy metal particles should be a small diameter compared to mineral dust and easy to suspend and transportation, therefore they were rich in the atmospheric deposition.

Table 7 shows the character of each cluster group. The heavy metal particles were divided into 10 groups based on the cluster analysis and the Euclidean distances. Iron rich particle groups were No.1, 2, and 4. They have relatively large particle diameter and contribute 73% abundance in heavy metal deposition particles. Iron has used many products and Fe particles have been a significant contributor in atmospheric aerosols (Weber et al., 2000). For example, Fe is used in automobile brake pad with Cu, Sb, and Ba. A steel plant is also significant Fe particles contributor. Spherical

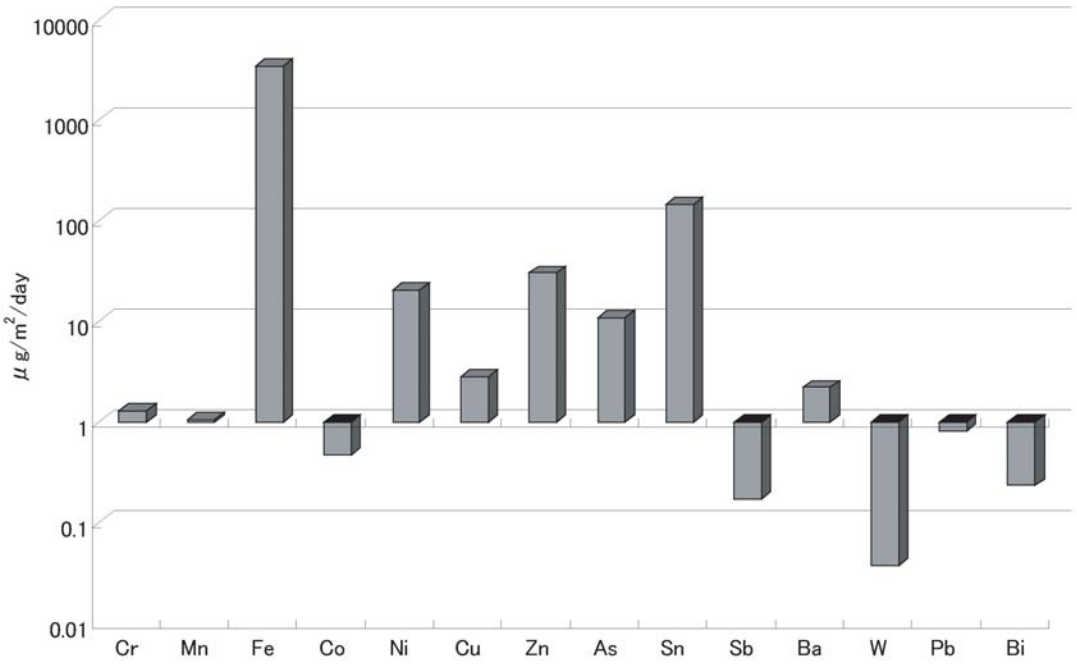

Figure 27: Heavy metal loading flux from atmospheric deposition

Fe particles with under 10 μm diameter were distributed in this area (Adachi and Tainosho, 2000), and they were also recognized in this analysis.

Cluster No.7 (Co-Ni-Zn-rich particles) was 10 % abundance. They were presence as several aggregate particles groups. Their sources are unidentified but Co and Ni has geochemical relationship. Cluster No. 3, 6, 8, 9, and 10 include very toxic heavy metal such as Pb, As, Sb, Cu, and Zn, and their particle size are quite small (from 0.9 to 2.8 μm). The small particles are easy to inhale in lung and affect human health. Additionally, if they fall down to a soil surface, they will cause a serious heavy metal pollution.

8.6 Conclusion

This study determined a mass loading and heavy metal loading from atmospheric deposition between a short collection times. The mass loading from atmospheric deposition was $46 mg/m^2/day$ and the heavy metal loadings were also determined

Table 7: Characteristic of calssified heavy metal particles

No.	Major elements*	Minor elements**	diameter $d_{max}(\mu m)$	abundance *** %
1	Fe	Cr, Mn, Zn, Sn, Sb, Ba	3.1	28
2	Fe		5.7	34
3	Pb	Cr, Fe, Co, Ni, Zn, As, Bi	1.7	3
4	Fe	Cu, Zn, As, Ba, W, Pb, Bi	4.3	11
5	Mn	Fe	2.5	1
6	As		1.4	2
7	Co, Ni, Zn	Ti	1.9	10
8	Ti, Sb	Cr	1.4	4
9	Cu, Zn	Ni	2.8	2
10	Zn	As	0.9	4

* Major elements >10Wt.%, ** Minor elements >0.1Wt.%, *** n=204

by single particle analysis method. The most abundance heavy metal was Fe and followed by Sn, Zn, Ni, As, and Cu. About 8% of atmospheric deposition was heavy metal particles. The heavy metal particles were divided into 10 groups based on their chemical composition by cluster analysis method. The cluster groups were large Fe-rich particle groups and small toxic heavy metal particle groups. Especially, the small toxic heavy metal particle groups were harmful for human.

This study clarified that atmospheric deposition contained many heavy metal particles even in one-day collection times. The atmospheric heavy metal particles will be a one of significant heavy metal pollutant for the urban soil, water, and sediments. The finding of this heavy metal loading mechanism will be helpful for a background heavy metal data to clean up a heavy metal pollution site or to evaluate the urban health risk.

In the next section, the analysis with more large number of metal particles and longer sampling period will be discssed to evaluate the source of metal particles and to characterize the metal particles in detail.

9 Characterization of metal particles in atmospheric deposition by single particle analysis during wintertime

9.1 Introduction

Atmospheric particulate matter plays an important role in the local and global environment. It affects human health, elemental loading, global climate and visibility. Atmospheric deposition is a process by which atmospheric particulate pollutants are transferred to the surface of the ground and the facades of artificial buildings. This process also plays an important role in the environmental impact. Metal loading from atmospheric deposition is one of the major sources of pollution in urban environments, soils or lake surfaces (Nriagu and Pacyna, 1988, Zufall et al., 1998, Holsen et al., 1993, Brewer and Belzer, 2001).

Metal loading by long-range atmospheric transportation from northeast Asia during the Asian dust storm period (spring) and during winter is a chief concern in Japan, which is compounded by the rapid industrial growth of China (Zhou et al., 1996, Choi et al., 2001, Ma et al., 2001, 2004a, 2004b, Ro et al., 2001, Funasaka et al., 2003, He et al., 2003, Kim et al., 2003, Mori et al., 2003, Guo et al., 2004). Using the data provided by the National Air Surveillance Network (NASN), the Japanese government has monitored bulk chemical composition including the metal elements in atmospheric particulate matter in 16 Japanese cities since 1965 (Var et al., 2000). These data indicated that the proportion of some artificial metals increased during the Asian dust period and during winter in spite of a decrease in the annual average concentrations of anthropogenic elements since 1974 (Var et al., 2000).

Classifying the pollutant sources as long-range or local is essential for the treatment of particulate matter. A scanning electron microscope attached with an energy dispersive X-ray spectrometer (SEM-EDS) was used to analyse the atmospheric depositions. Single particle analysis by SEM-EDS is a powerful tool for this purpose (Casuccio et al., 1983, Post and Buseck, 1984, Anderson et al., 1988, 1996, Saucy et al., 1991, Anderson et al., 1992, Katrinak et al., 1995, Malderen et al., 1996a, 1996b,

Piña et al., 2000, Mamane et al., 2001). The main advantages of this method over bulk chemical analysis are as follows: 1) it is more informative (chemical composition, morphology and particle diameter of each particle) and 2) it requires an extremely small amount of a sample (more than several hundred particles). Such a variety of information on the particles enabled us to evaluate the source of metal particles in greater detail while the small quantity of samples made it possible to for us estimate the variation in atmospheric deposition with a good time resolution.

The purpose of this study is to characterise the particle types of metal atmospheric depositions and estimate the metal particle groups, the flux of each deposited metal particle, and their sources. These results will be useful in estimating the actual point source of atmospheric particulate matter and in evaluating the health risks resulting from atmospheric metal particles.

9.2 Material and methods

9.2.1 Sampling

The sampling equipment was placed on the roof of a five-storey building belonging to the Faculty of Human Development in the Kobe University campus (34.44°N, 135.14°E). The university is located in the city of Kobe, which has a population of 1.5 million (Fig.28). The building is situated at an altitude of 200 m at the foot of Mount Rokko (elevation 931 m), with no significant local source of atmospheric pollutants or large roads within a radius of 500 m. A steel plant and coal-fired power plant are located near the seacoast, at a distance of 3 km to the southeast of the sampling area.

Samples of atmospheric deposition were collected during winter (9-18 December, 2003). During the sampling period, atmospheric depositions were collected every 24 hours starting at 14:00 (JST), except during one short rain event (11 December 10:00-24:00). In total, 10 sequential atmospheric deposition samples were collected (Table 7). During the sampling period, the average wind speed was 1.4 ms^{-1}, the temperature ranged from 0°Cto 18.2°C, and the average relative humidity was 63% (36-96%).

Samples of atmospheric deposition were collected with a double-sided carbon tape

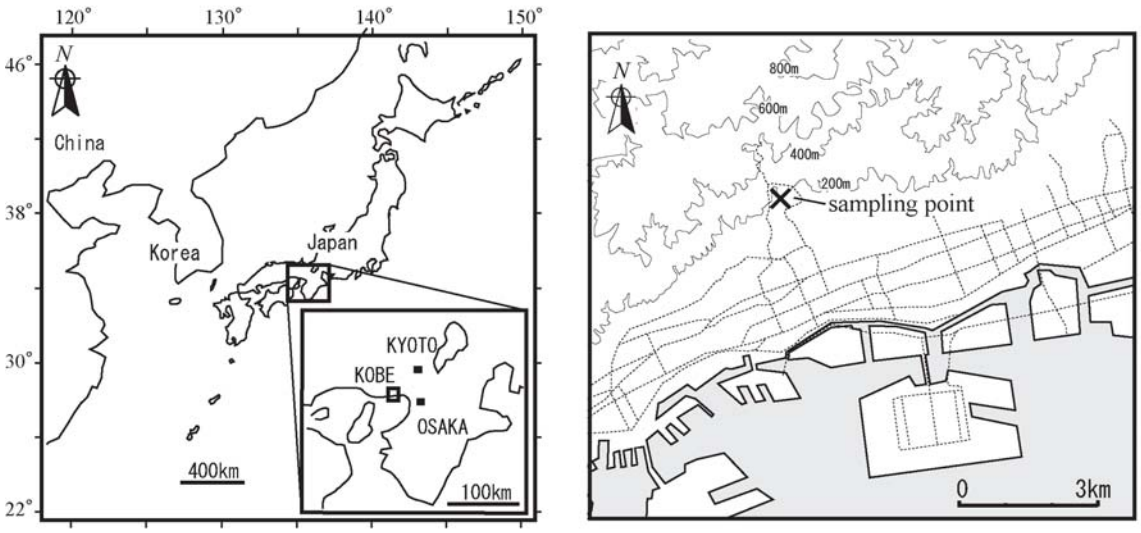

Figure 28: Sampling map of this study. Samples were collected at Kobe City, Japan.

(2 cm × 3 cm) adhered to a smooth glass plate that was attached to a clean stainless plate with a sharp leading edge (<10°). This arrangement was similar to that used in earlier studies (Noll et al., 1988, Kim et al., 2000, Yang et al., 2004). The sampling plate was mounted on a wind vane and pointed in the direction of the wind to reduce the edge effect caused by local turbulence (Vawda et al., 1990). Since the carbon tape is electrically conductive, the deposited samples could be directly observed without any additional treatment except for carbon coating. Thus, it was possible to count the actual number of deposition particles per surface area with lesser sampling loss.

9.2.2 Analysis

The carbon-coated atmospheric deposition samples were analysed by FESEM-EDS. The metal particles were detected by backscatter electron image (BEI), which reflects the atomic number of the materials with an appropriate contrast and brightness to distinguish the metal particles from the mineral or sea salt particles.

In this analysis, a large number of barium sulphate particles were detected and it is known to adversely affect the facades of buildings (Pérez-Rodríguez et al., 2004).

However, since it was difficult to separate the aggregated barium sulphate particles, they were excluded from the analysis.

The EDS spectra and diameter were recorded for all the metal particles detected with a diameter of more than 0.2 μm in the field of view (600 $\times$ 440 μm). The fields of views were continuously selected for every grids spacing of 1 mm in each sampling plate until the total number of metal particles exceeded 300. Mamane et al. (2001) showed that approximately 360 particles in the aerosol sample were needed for single particle analysis using a computer-controlled SEM to yield representative results. Although the number of particles in this study was slightly smaller, it is considered to be adequate because this study employed only selected metal particles.

The analysis conditions included an acceleration voltage of 15 kV, working distance of 15 mm and EDS collection time of 30 seconds. EDS quantification was determined by the standardless ZAF method and recalculated to 100% for 29 elements (O, Al, Si, P, S, Cl, K, Ca, Ti, V, Cr, Mn, Fe, Co, Ni, Cu, Zn, Sr, Zr, Mo, Ag, Sn, Sb, Ba, La, Ce, Nd, Pb and Bi). To eliminate overlapping and to avoid the detection of elements not listed above, only elements with an apparent concentration of more than one statistical sigma were used for the statistical analysis. Some particles containing the elements not listed above such as As, W and Pt were detected; however, the accurate value of these elements could not be assessed by multi-elemental quantification due to their too many characteristic radiation peaks which overlapped with those of the other elements. Hence, these elements could not be included in this analysis. Due to the complex shape of the surface of the particles and their small diameters compared to the electron diffusion range, this quantification method may lead to an over- or underestimation of the total count. However, the rate of amount was almost accurate and this facilitates classification of the particles by a statistical method such as the hierarchical cluster analysis program (HCA). The HCA was based on Euclidean distances with Ward's error sum classification. The consistent Akaike's information criteria (AIC) were used to determine the most appropriate number of the clusters.

9.3 Results and discussion

9.3.1 Classification of the metal particles

Table 8: Metal particle deposition flux and sampling times in each sampling day. The detections of metal particles were gone on until the number got to more than 300

	1	2	3	4	5	6	7	8	9	10
area (mm^2)	92.8	66.0	119.1	70.2	15.3	58.2	102.4	137.0	11.2	23.4
particle	301	301	300	300	304	303	301	300	307	306
hour	24	20	14	24	24	24	24	24	24	24
$particle/mm^2$/day	3.2	5.4	4.3	4.2	19.5	5.1	2.9	2.2	27.0	12.9

This analysis succeeded in detecting 3023 metal particles in an area of approximately 700 mm^2 within a total of 226 hours of sampling time. The maximum deposition flux of metal particles was 27.0 particles mm^{-2} day^{-1} on sampling day-9 (Table 8). All the metal particles available for statistical analysis (2886 particles) were classified into 14 groups by HCA and AIC (Table 9). The median grain diameter of each cluster group ranged from 0.4 to 1.2 μm. All the cluster groups except for clusters 4 and 5 mostly consisted of simple compositions containing only one or two metal elements and most of the particles were oxides. The most frequent cluster groups were of Fe oxide (clusters 13 and 14). They constituted 63% of all the metal particles. Their morphology was both spherical and irregular. Cluster 13 mostly consisted of Fe_2O_3; on the other hand, cluster 14 contained some other elements such as Si and Ca. Aerosol samples collected in Germany also included several Fe particles (0-17% in all particle groups) with similar chemical composition of Fe (65.55%) and O (33.8%) (Ebert et al., 2000). The second largest particle type was Cu-Zn-O (cluster 1). The mole ratio of Cu:Zn was 3:2; this was found in a certain type of brass. Cluster 2 was composed of Cu with Sn, and it was subdivided into particles of Cu-O and Cu-Sn-O (Cu: 60-70%, Sn: 2-8%). Cluster 5 consisted of Fe, Ba, Sb, Cu, S and Ti, which corresponded well with the compositions of brake wear dust (Sternbeck et al., 2002, Adachi and Tainosho, 2004). Other cluster types were mainly characterised by metal elements such as Pb, Bi, Fe-Zn, Mn, Ag, Zn, Ni and Sn-Sb.

By computer-controlled SEM, Conner et al. (2001) identified indoor, outdoor

and community site samples of individual particulate matter collected at Baltimore (USA). The most dominant metal particles in PM 2.5 were those containing Fe, followed by Pb, Cu and Zn particles. They also detected other particles characterised by metals such as Bi, Ti, Cr, Ni and/or V and Mn (Conner et al., 2001). A major part of the metal particle species and the rate of amount agreed well with this study.

Table 9: Chemical composition, particle diameter, number, and abundance percentage of classified metal particles

Cluster	Chemical Composition (weight %)	d	n	%
Cluster1	Cu(45), Zn(31), O(20)	1.1	499	17.3
Cluster2	Cu(65), Sn(4), O(24)	1.2	66	2.3
Cluster3	Pb(71), O(16)	0.5	74	2.6
Cluster4	Pb(33), Zn(6), Cl(5), Si(5), S(4), O(25)	0.5	45	1.6
Cluster5	Fe(16), Ba(6), Sb(5), Cu(5), S(4), Ti(4), O(33)	1.2	117	4.1
Cluster6	Bi(79), Cl(4), O(12)	0.4	7	0.2
Cluster7	Fe(40), Zn(22), O(29)	0.6	107	3.7
Cluster8	Mn(59), Fe(8), O(26)	1.0	25	0.9
Cluster9	Ag(84), O(11)	0.4	14	0.5
Cluster10	Zn(67), O(24)	0.8	43	1.5
Cluster11	Ni(73), O(24)	0.7	36	1.2
Cluster12	Sn(63), Sb(4), O(25)	0.4	46	1.6
Cluster13	Fe(68), O(31)	1.0	981	34.0
Cluster14	Fe(58), O(32)	1.0	826	28.6

d; particle diameter μm

9.3.2 Characterization of metal cluster groups

Principal component analysis (PCA) was used to characterise the distribution of cluster groups during the sampling period. PCA is a useful statistical technique to reduce the dimension of a large dataset. Figure 29 shows the plot of the first principle component (PC1, eigenvalue 6.7, variance 48%) compared with that of the second principle component (PC2, eigenvalue 3.0, variance 22%) (Fig.29a). Fig.29b shows the plot of PC1 compared with that of the third component (PC3, eigenvalue 1.9, variance 14%). In both the figures, four distribution groups could be determined based on the distribution patterns: Group A) clusters 5, 7, 8, 10, 11, 13 and 14 were located along the negative axis of PC1; Group B) clusters 1 and 2 were located along the positive axis of PC1 and PC3 and along the negative axis of PC2; Group C) clusters 3, 9 and 12 were located along the negative axis of PC1 and PC2; and Group

D) clusters 4 and 6 were located along the positive axis of PC1 and negative axis of PC2 and PC3.

The distributions of the particle diameters in the cluster groups are shown in Fig30. Groups A and B indicate that the most frequent particle diameter lies in the range of 0.5-1.0 μm; on the other hand, this is the range of the smallest diameter in groups C and D (0.2-0.5 μm). The distributions of particulate diameters between the cluster groups were consistent well among the distribution groups. Ma et al. (2004b) studied atmospheric particulate matter at Uji, which is located approximately 60 km to the northeast of this sampling area, during the winter of 2002. They investigated the element distributions in relation to particle size as a function of water solubility. The results indicated a bimodal distribution pattern in insoluble minor elements like Cu, Mn and Pb (the coarser particle diameter corresponded to approximately 3.45μm and the finer one corresponded to 0.67μm with a 50% cut-off diameter). This study also showed that a number of metal particles were concentrated at the diameter range of 0.5-1.0 μm or under 0.5 μm; however, less striking peaks were observed in the coarser fraction. This is probably because that this study used the particle number to indicate the amount of particles and this may introduce more emphasis to the fine particles compared to the indication by mass concentration.

Distribution patterns of the cluster groups are shown in Fig.31. The distribution of Group A in Fig.31a shows an increase on sampling days-5 and -9. Group B indicates an increase on sampling days-1 and -2 (Fig.31b). The distribution of Group C in Fig.31c indicates an increase on sampling day-9 and Group D exhibits an extremely poor deposition rate and shows no significant peaks (Fig.31c).

9.3.3 Source estimation of the metal cluster groups

In order to estimate the trajectories of air mass during the sampling period, this study used the HYbrid Single-Particle Lagrangian Integrated Trajectory (HYSPLIT) dispersion-trajectory model, which is primarily used as a diagnostic tool to evaluate the flow of the atmosphere. The trajectory results were produced using the website (www.arl.noaa.gov/ready) of the National Oceanic and Atmospheric Administration

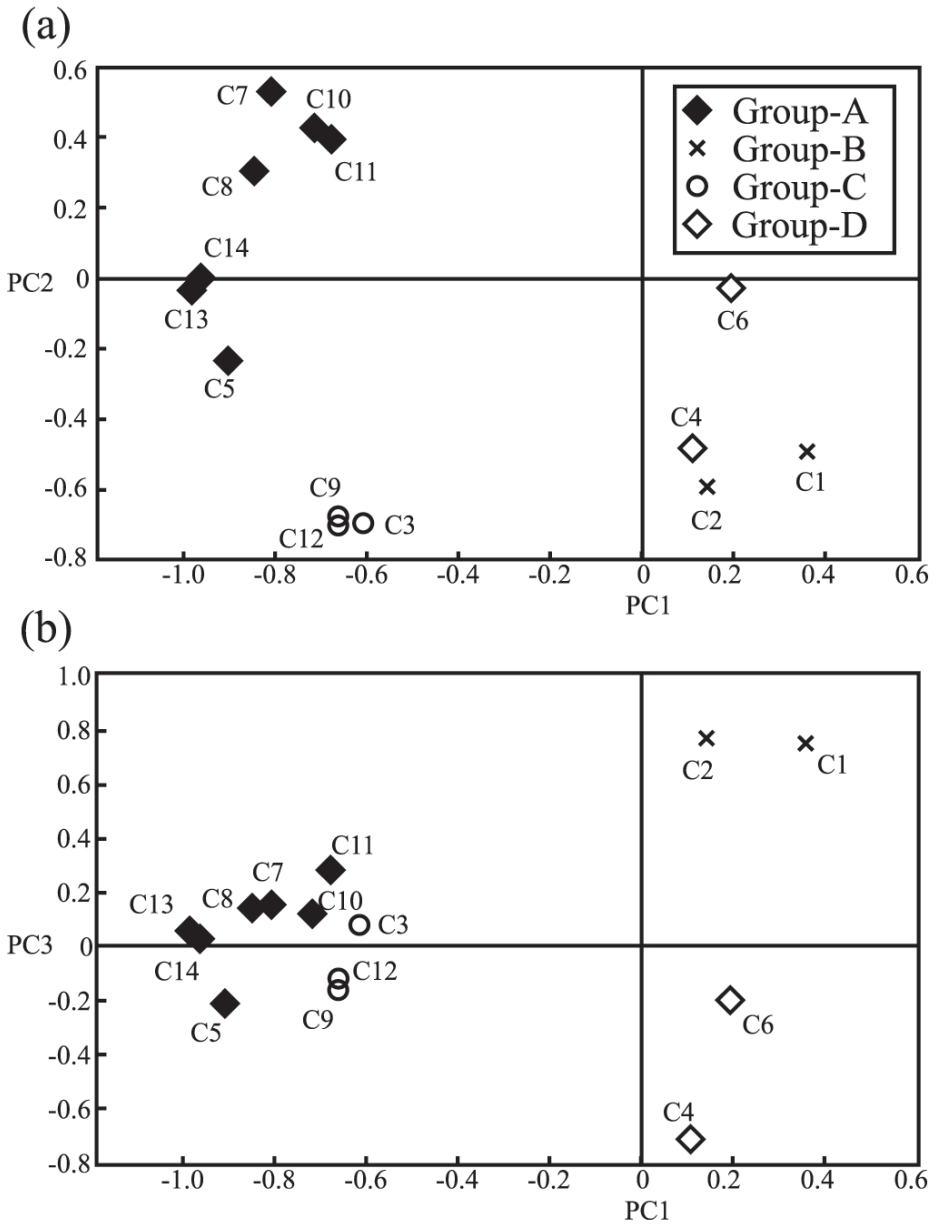

Figure 29: Classification of cluster types by Principal Component Analysis. (a) PC1 vs. PC2, (b) PC1 vs. PC3.

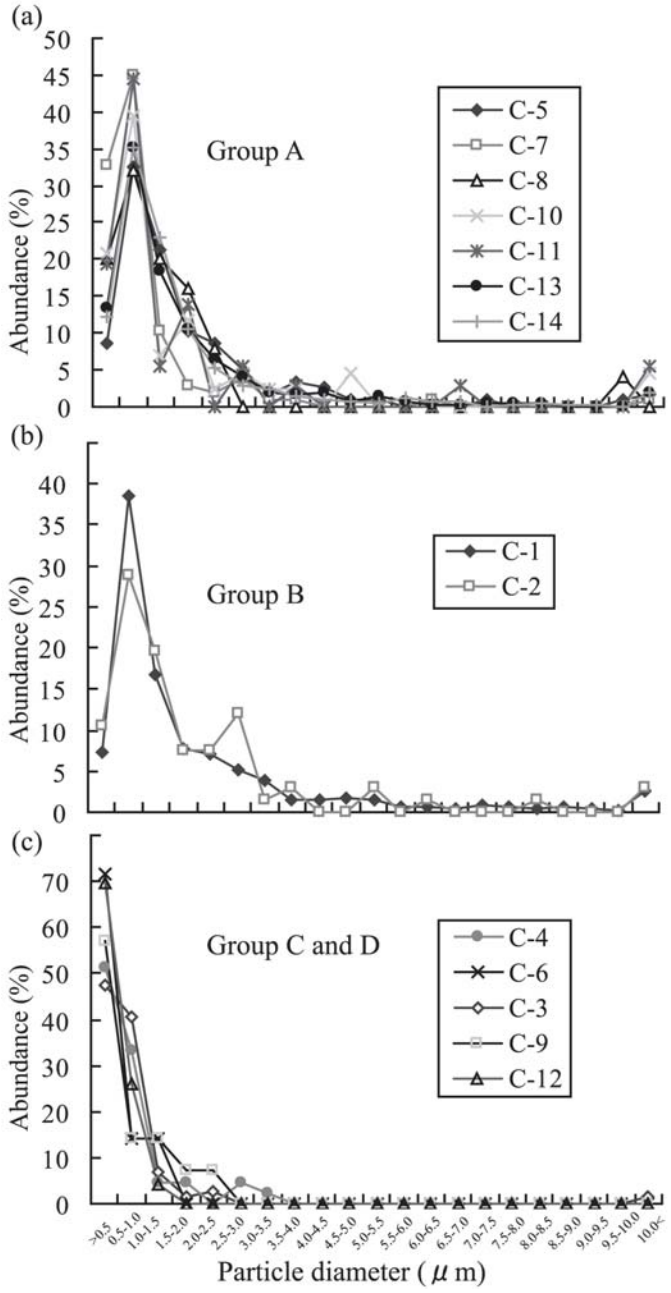

Figure 30: Distribution of particle diameter in each cluster type. (a) Group A, (b) Group B, (c) Group C (6C-3,9, and 12) and Group D (C-4 and 6)

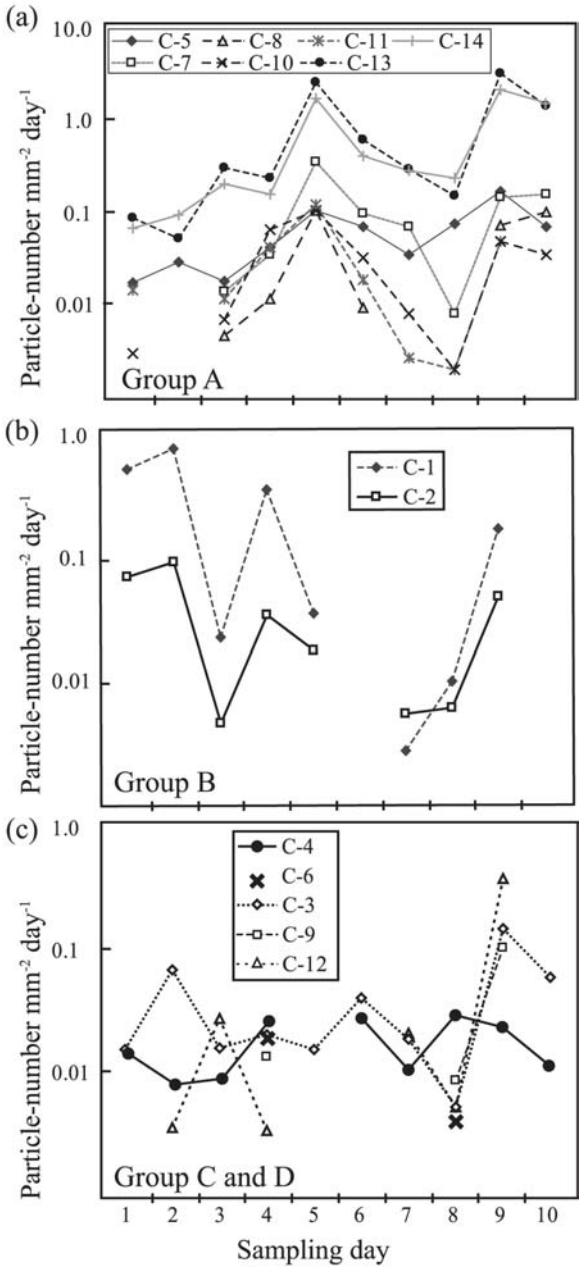

Figure 31: Distribution of deposition flux of each cluster type during the sampling period. (a) Group A, (b) Group B, (c) Group C (C-3,9, and 12) and Group D (C-4 and 6)

(NOAA) Air Resources Laboratory.

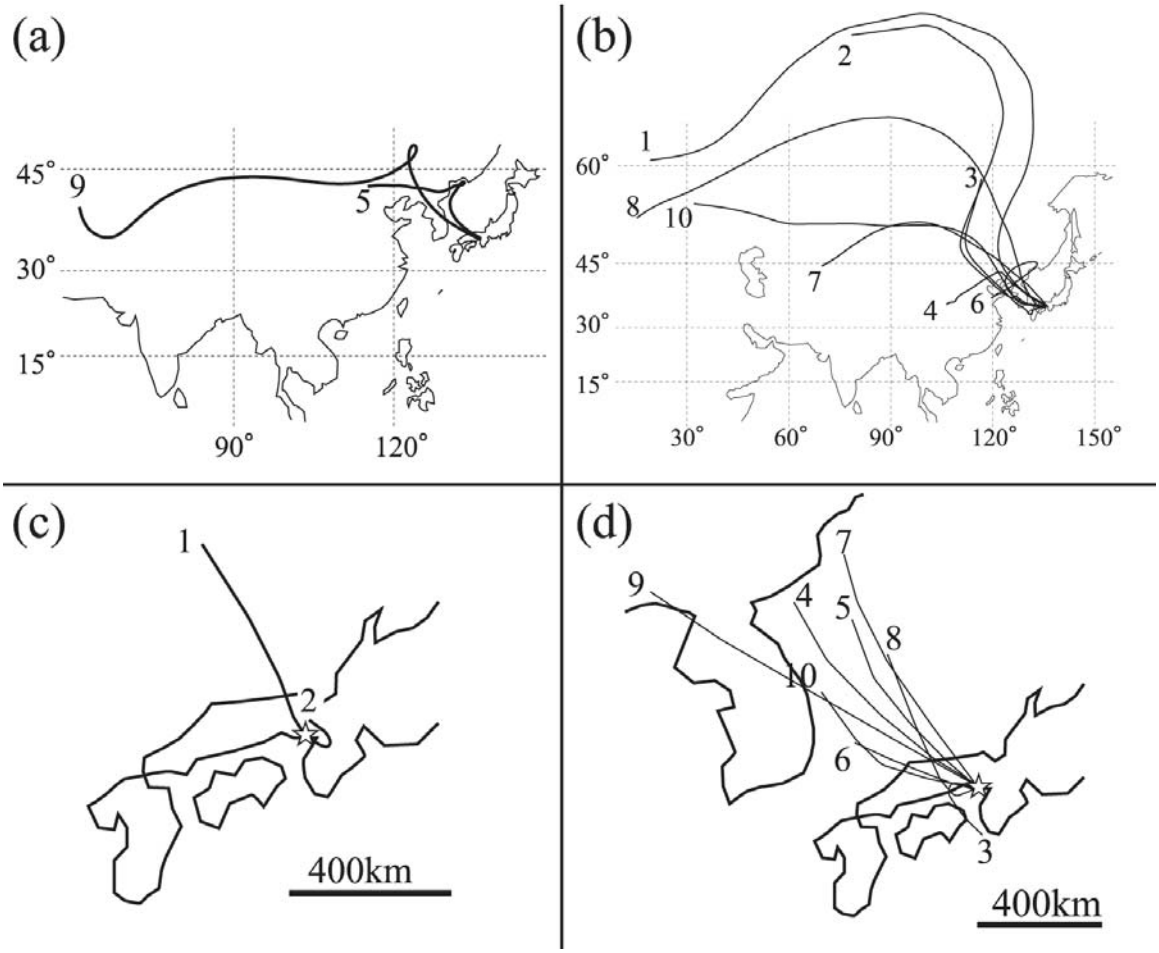

Figure 32: Backward trajectories in each sampling day arrived at Kobe (lat. 34.44 N, log. 135.14E). The trajectories were shown the results of 120 hours from the middle time of each sampling day period (2:00 a.m.). (a) Results of sampling day 1,2,3,4,6,7,8, and 10 (height 2000m), (b) Results of sampling day 5 and 9 (height 2000m), (c) Results of sampling day 3,4,5,6,7,8,9, and 10 (height 500m), (d) Results of sampling day 1 and 2 (height 500m).

Fig.32a indicates the trajectories recorded on sampling days-5 and -9 when Group A showed an increase in its deposition. In contrast, Fig.32b shows the trajectories recorded on other days. The trajectories in Fig.32a indicate that they had passed through the low-pressure systems occurring around the northeast of the Asian continent. This could imply that the metal particles belonging to Group A were updrafted from the area and eventually transported to the study area. Fig.32c shows the back trajectories recorded on sampling days-1 and -2 when Group B registered an increase.

The trajectories showed that the flows of atmosphere were derived from the eastern direction at a low altitude (500 m) on the first two sampling days. The neighboring cities to the west of the study area are high-developed urban area such as Osaka and Kyoto with populations of approximately 2.6 million and 1.5 million, respectively (Fig.28a). These cities could have contributed to a large amount of the metal particles listed under Group B.

Group C was mainly consisted of Pb, Ag and Sb-Sn particles that showed an increase on sampling day-9, which could indicate their long-range loading. Malderen et al. (1996b) also detected pure Pb particles with a small diameter (0.4-0.5 μm) above the North Sea and estimated the different sources such as automobile exhaust or production facilities. The sources of Ag, obtained from atmospheric depositions, found in snow and ice were estimated to be both natural (rock, soil dust and volcanoes) and anthropogenic (mining and smelting activities, industry or municipal waste incinerator) (Van de Velde et al., 2000).

Group D consisted of Pb or Bi, which did not show a significant increase on any day, and their total number was low. The two features of Group D are the inclusion of Cl and a smaller particle diameter (0.4-0.5 μm). Malderen et al. (1996b) detected small Pb particles (0.3-1.0 μm in diameter) associated with Cl and Zn in the aerosol particles collected above the North Sea and estimated their main source to be refuse incineration. Vaporized $PbCl_2$ from the incineration process is also one of the sources of these pollutants in Japan (Jung et al., 2004). Some residue of the previously used leaded petrol, characterised by Pb-Cl (Post and Buseck, 1984, Borm et al., 1990, Malderen et al., 1996b), may have remained. The sources of Bi, emitted by recent human activity, include refuse burning, ferromanganese alloys, aluminium metallurgy, silver and lead mining and smelting, and combustion of fossil fuels (Ferrari et al., 2000).

Although single particle analysis has some advantages over the bulk composition analysis, it also has the possibility to display a highly local irregular event due to the small amount of the sample required. As this study aims to estimate the source of global or area transportation, it should be compared with other studies that inves-

tigate metal element loadings from long-range or local area transportation by bulk chemical analysis in neighboring cities or areas.

Var et al. (2000) reported that some elements (e.g. Fe, As, Pb and Zn) enriched in winter compared to summer in various cities of Japan during 1989-1996. In contrast, Cu, Cr, Ni and V did not show the distribution. This suggested that the first set of elements was derived from the Asian continent while the latter set was mainly derived from some other source. Funasaka et al. (2003) investigated the chemical composition of particulate matters in two sites of Osaka for a period of three years from April 1999 to March 2002 in order to estimate the site-specific sources. They estimated that the concentration of Fe and Mn of coarse particle fractions (more than 2.1 μm) was enriched during the Asian dust period although there was no difference in other metal elements such as Cu, Zn and Pb during this period. Kim et al. (2003) investigated the elemental composition ratios during the Asian dust period (AD) and the non-Asian dust period (NAD) in Seoul in 2001. The ratio (AD/NAD), which referred to the contribution from long-range transportation, for Fe (3.0), Ni (2.6), Mn (2.2), Zn (1.2), Pb (1.2) and Cu (1.0) were fine fractions (PM 2.5). The source estimations of the metallic elements in the above studies are almost consistent with those of this study. Thus, the highest detected metal particle in this study could represent the metal particles contributed by global or local transportation. It must be noted that not all metal contributions are from metal particles, some mineral particles (e.g. Fe or Mn) also serve as sources of metal particles. However, this study could clearly estimate the contribution and sources of metal particles from atmospheric depositions by single particle analysis.

9.4 Conclusion

Atmospheric depositions were sampled in Kobe, Japan during the winter of 2003. The diameter and chemical composition of every individual metal particle were analysed by FESEM-EDS. During the sampling period (10 days), approximately 3000 metal particles were detected in an area of about 700 mm^2 and were classified into 14 cluster groups on the basis of chemical compositions. The cluster groups were reclassified

into four distribution groups according to the daily loading variation: Group A: Fe-Ba-Sb-Cu-S-Ti-O, Fe-Zn-O, Mn-Fe-O, Zn-O, Ni-O and Fe-O; Group B: Cu-Zn-O and Cu-Sn-O; Group C: Pb-O, Ag-O and Sn-Sb-O; Group D: Pb-Zn-Cl-Si-S-O and Bi-Cl-O. The relation between the daily variation in the particle loading of the distribution groups and the backward trajectory modeling of the air mass suggests that the particles of Group A originated from the northeast of the Asian continent and those in Group B originated from local transportation. This study analysed metal particles by single particle analysis and identified whether the properties (chemical compositions and diameters) of metal particles were contributed by global or local transportation. These results could be helpful in identifying the direct sources of metal particles or to estimate the risks of metal particles from atmospheric deposition.

10 General Conclusion

This study shows the urban pollutions especially caused by particulate matter including metal elements in Kobe, Japan. The results indicated in this study are related closely between the contaminant particulate matters. The detailed interactions were stated in each section. In this chapter, I show the overall relation between the particulate matters and urban environment.

Fig.33 shows the flow of particulate matters in the urban environment determined and estimated in this study. The solid line means the interaction of particulate matters determined in this study and the dashed line indicates the flow that can be estimated from this study.

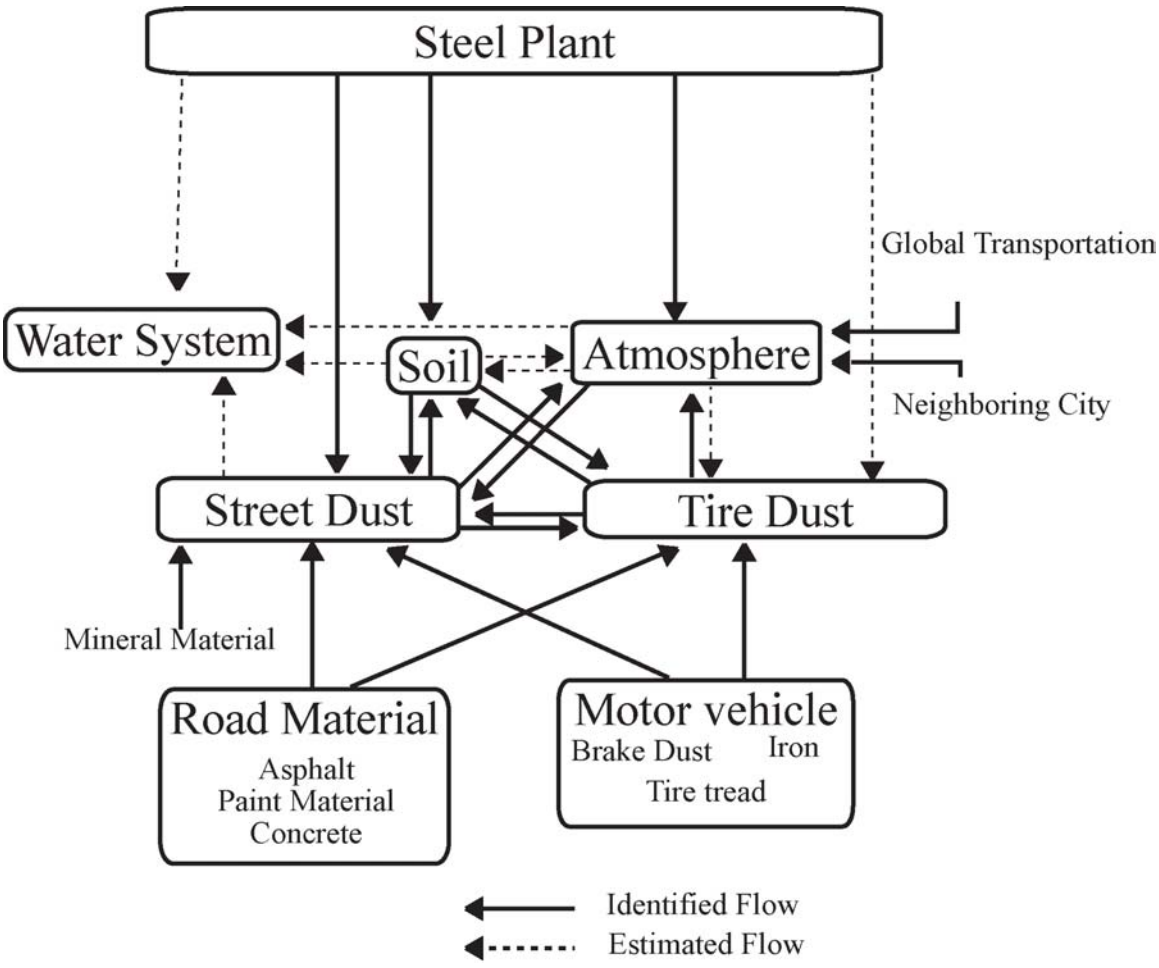

Figure 33: schematic model of metal particles flow in the Urban Environment

The spherical iron particles derived from the steel plant contaminate street dust and soils (in Chapter 3). The particles also indicated that they were deposited through the atmosphere. Additionally, they were expected to fall out into water system directory and be attached to the surface of tire dust. Road materials such as asphalt, concrete, and paint materials were present in street dust and the surface of tire dust (Chapter 5 and 6). Materials of motor vehicles such as brake dust, car body, and tire tread were also included in street dust and tire dust (Chapter 5 and 6). In some cases, mineral materials such as ilmenite contaminate street dust (Chapter 7).

Tire dust particles are major component of street dust (Chapter 5) and some of them are resuspended into the atmosphere (Chapter 8 and 9). Atmospheric deposition may be one component of the metal particles taken in tire dust particles. Street dust includes mineral particles from neighboring soil for their major component (Chapter 6). Street dust also may contain metal particles deposited on roads from the atmosphere. On the other hand, they are the one of largest pollutant for urban soil, atmosphere, and water system.

All over the flow, water system and soil could be final sink of metal particles in the urban environment. Finally, the metal particles carried into the water system will leach out and be taken in sea lives. During the transportation in the urban environment, they contaminate various materials. In order to know the pollutant mechanism, it is important to investigate the multi environment and particulate matter. Through the analysis, we can reveal the mechanism of metal pollution caused by particulate matter in the urban environment. This study could show the most part of metal pollution by particulate matter as the model case in Kobe city. The most part of the results in this study will apply to other urban environment although some regional sources should be considered. Therefore, I conclude that this study could indicate the significant the flow of metal particles and pollution mechanism.

11 Acknowledgments

Firstly, I would like to show my greatly acknowledgement for Professor Yoshiaki Tainosho for his support as my supervisor. Also, I wish to acknowledge my colleagues in our laboratory during my six years study for their suggestion, discussion, helps, knowledge, idea, and so on. Discussion with Professor Kazushige Tomeoka and the members of Planetary Material Science Laboratory in Kobe University was very valuable for me. I would like to thank Dr. Yasutaka Terakado for his support in use of XRD. For Professor T. Miyata and Professor S. Ueji, I wish to acknowledge their suggestions for this thesis.

I wish to thank Japan Student Services Organization and IUE memorial foundation for their financial support through three years of my doctoral course. I also would like to thank Kobe University and the group leaders of COE program (Origin and Evolution of Planetary Systems) for giving me a chance to work as a Research Assistant in their programs.

References

[1] Adachi, K., Tainosho, Y. 2000. Heavy metal pollution of surface soil in eastern part of Kobe city. Bulletin of the faculty of human development. 8, 89-102. (in Japanese)

[2] Adachi, K., Tainosho, Y., 2001. The behavior of spherical iron particles in soils and street dusts: Pollution analysis using field emission scanning electron microscope. Man and Environ. 27, 52-58. (in Japanese).

[3] Adachi, K., Tainosho Y., 2003, Soil Environment Affected by Tire Dust. In: Tazaki, K.; eds. International Symposium of the Kanazawa University 21st-Century COE Program. Water and Soil Environments, 17-18 March 2003, Kanazawa, Japan, 344-347.

[4] Adachi, K., Tainosho, Y., 2004. Characterization of heavy metal particles embedded in tie dust. Environment International 30, 1009-1017.

[5] Al-Rajhi, M.A., Al-Shayeb, S.M., Seaward, M.R.D., Edwards, H.G.M., 1996. Particle size efect for metal pollution analysis of atmospherically deposited dust. Atmos. Environ. 30, 145-153.

[6] Anderson, J.R., Aggett, F.J., Buseck, P.B., Germani, M.S., Shattuck, T.W., 1988. Chemistry of individual aerosol particles from Chandler, Arizona, an arid urban environment. Environment Science and Technology 22, 811-818.

[7] Anderson, J.R., Buseck, P.R., Saucy, D.A., 1992. Characterization of individual fine-fraction particles from the arctic aerosol at Spitsbergen, May-June 1987. Atmospheric Environment 26A, 1747-1762.

[8] Anderson, J.R., Buseck, P.R., Patterson, T.L., 1996. Characterization of the Bermuda tropospheric aerosol by combined individual-particle and bulk-aerosol analysis. Atmospheric Environment 30, 319-338.

[9] Aust, A.E., Ball, J.C., Hu, A.A., Lighty, J.S., Smith, K.R., Straccia, A.M., Veranth, J.M., Young, W.C., 2002, Particule characteriistics responsible for effects on human lung epithelial cells. Health effects Institute.

[10] Borm, W.V., Wouters, L., Grieken, R.V., Adams, F., 1990. Lead particles in an urban atmosphere: An individual particle approach. The Science of the Total Environment 90, 55-66.

[11] Brewer, R., Belzer, W., 2001. Assessment of metal concentrations in atmospheric particles from Burnaby Lake, British Columbia, Canada. Atmospheric Environment 35, 5223-5233.

[12] Brookman, E.T., Drehmel, D.C., 1981. Future areas of investigation regarding the problem of urban road dust. Environ Int. 6, 313-320.

[13] Cadle, S.H., Williams, R.L., 1980. Environmental Degradation of Tire-Wear Particles. Rubber Chem Technol. 53, 903-913.

[14] Camatini, M., Crosta, G.F., Dolukhanyan, T., Sung, C., Giuliani, G., Corbetta, G. M., Cencetti, S., Regazzoni, C., 2001. Microcharacterization and identification of tire debris in heterogeneous laboratory and environmental specimens. Materials Characterization. 46, 271-283.

[15] Cardina, J.A., 1973. The Determination of Rubber in Atmospheric Dusts. Rubber Chem Technol. 46, 232-241.

[16] Cardina, J.A., 1974, Particle Size Determination of Tire-Treads Rubber in Atmospheric Dusts. Rubber Chem Technol. 47, 1005-1010.

[17] Carlosena, A., Andrade, J.M., Prada, D., 1998. Searching for heavy metals grouping roadside soils as a function of motorized traffic influence. Talanta. 47, 753-767.

[18] Casuccio, G. S., Janocko, P.B., Lee, R.J., Kelly, J.F., Dattner, S.L., Mgebroff, J.S., 1983. The use of computer controlled scanning electron microscopy in environmental studies. Journal of the Air Pollution Control Association 33, 937-943.

[19] Choi, J.C., Lee, M., Chun, Y., Kim, J., Oh, S., 2001. Chemical composition and source signature of spring aerosol in Seoul, Korea. Journal of Geophysical Research 106, 18067-18074.

[20] Chon, H.T., Ahn, J.S., Jung, M.C., 1998. Seasonal variations and chemical forms of heavy metals in soils and dusts from the satellite cities of Seoul, Korea. Environ. Geochem. Health. 20, 77-86.

[21] Conner, T.L., Norris, G.A., Landis, M.S., Williams, R.W., 2001. Individual particle analysis of indoor, outdoor, and community samples from the 1998 Baltimore particulate matter study. Atmospheric Environment 35, 3935-3946.

[22] Dannis, M.L., 1974, Rubber Dust from the Normal Wear of Tires. Rubber Chem Technol. 47, 1011-1037.

[23] Davis, A.P., Shokouhian, M., Ni, S., 2001, Loading estimates of lead, copper, cadmium, and zinc in urban runoff from specific sources. Chemosphere. 44, 997-1009.

[24] De Miguel, E., Liams, J. F., Chacón, E., Mazadiego, l. F., 1999, Sources and pathways of trace elements in urban environments: a multi-elemental qualitative approach, The Science of Total Environment, 235, 355-357.

[25] De Miguel, E., Llamas, J.F., Chacón, E., Berg, T., Larssen, S., Røyset, O., Vadset, M., 1997. Origin and patterns of distribution of trace elements in street dust: unleaded petrol and urban lead. Atmos. Environ. 31, 2733-2740.

[26] Degirmenci, E., Ono, Y., Nagadome, H., Kanoh, S. Kawara, O., 2000. Genotoxicity and estrogen-like cell growth activity of samples extracted from street dusts. Environ. Toxicol., 15, 504-508.

[27] Ebert, M., Weinbruch, S., Hoffmann, P., Ortner, H.M., 2000. Chemical characterization of North Sea aerosol particles. Journal of Aerosol Science 31, 613-632.

[28] Ellis, J.B., Revitt, D.M., 1982. Incidence of heavy metals in street surface sediments: solubility and grain size studies. Water, Air, Soil Pollut. 17, 87-100

[29] Environment Agency (UK). 1998, Tyres in the environment. Bristol, Environment Agency.

[30] Environmental Protection agency (USA), 2003, Draft Report on the Environment 2003, USEPA.

[31] Environmental Bureau, City of Kobe, 2002.
Home page: http://www.city.kobe.jp/cityoffice/24/

[32] Fauser, P., Tjell, J.C., Mosbaek, H., Pilegaard, K., 2000. Quantification of bitumen particles in aerosol and soil samples using HP-GPC. Pet. Sci. Technol. 18, 989-1007.

[33] Fauser, P., Tjell, J.C., Mosbaek, H., Pilegaard, K., 1999, Quantification of Tire-Tread Particles Using Extractable Organic Zinc as Tracer. Rubber Chem Technol. 72, 969-977.

[34] Fergusson, J.E., Kim, N.D., 1991. Trace elements in street and house dusts: sources and speciation. Sci. Total Environ. 100, 125-150.

[35] Ferrari, C.P., Hong, S., Velde, K.V., Boutron, C.F., Rudniev, S.N., Bolshov, M., Chisholm, W., Rosman, K.J.R., 2000. Natural and anthropogenic bismuth in Central Greenland. Atmospheric Environment 34, 941-948.

[36] Fukuzaki, N., Yanaka, T., Urushiyama, Y., 1986. Effects of studded tires on roadside airborne dust pollution in Niigata, Japan. Atmos. Environ. 20, 377-386.

[37] Funasaka, K., Sakai, M., Shinya, M., Miyazaki, T., Kamiura, T., Kaneco, S., Ohta, K., Fujita, T., 2003. Size distributions and characteristics of atmospheric inorganic particles by regional comparative study in Urban Osaka, Japan. Atmospheric Environment 37, 4597-4605.

[38] Garg, B.D., Cadle, S.H., Mulawa, P.A., Groblicki, P.J., Laroo, C., Parr, G.A., 2000, Brake Wear Particulate Matter Emissions. Environ Sci Technol. 34, 4463-4469

[39] Goldstein, S.J., Slemmons, A.K., Canavan, H.E., 1996. Energy-dispersive X-ray fluorescence methods for environmental characterization of soils, Environ. Sci. Technol. 30, 2318-2321.

[40] Guo, Z.G., Feng, J.L., Fang, M., Chen, H.Y., Lau, K.H., 2004. The elemental and organic characteristics of PM2.5 in Asian dust episodes in Qingdao, China, 2002. Atmospheric Environment 38, 909-919.

[41] Haapala, H., 1998. The use of SEM/EDX for studying the distribution of air pollutants in the surrounding of the emission source. Environment Pollution 9, 361-363.

[42] He Z., Kim, Y.J., Ogunjobi, K.O., Hong, C.S., 2003. Characteristics of PM2.5 species and long-range transport of air masses at Taean background station, South Korea. Atmospheric Environment 37, 219-230.

[43] Hildemann, L.M., Markowski, G.R., Cass, G.R., 1991. Chemical composition of emissions from urban sources of fine organic aerosol. Environ. Sci. Technol. 25, 744-759.

[44] Holsen T.M., Noll, K.E., Fang, G.C., Lee, W.J., Lin, J.M., Keeler, G.J., 1993. Dry deposition and particle size distributions measured during the Lake Michigan urban air toxics study. Environmental Science and Technology 27, 1327-1333.

[45] Hopke, P.K., Lamb, R.E., Natusch, D.F.S., 1980. Multielemental characterization of urban roadway dust. Environ. Sci. Technol. 14, 164-172.

[46] Huzita, K., Kasama, T. 1983, Geology of the Kobe district. Quadrangle Series, scale 1:50000, Geol. Surv. Japan 115p.(in Japanese with English abstract, 8p)

[47] Hyogo Prefecture, 1999. Traffic census data in Hyogo Prefecture. [http://web.pref.hyogo.jp/douken/CensusHomepage(H13.10)/CensusKoutuuryou.htm] accessed January 28th, 2004.

[48] Jambers, W., Grieken, R.V., 1997. Single particle characterization of inorganic suspension in lake Baikal, Siberia. Environ. Sci. Technol. 31, 1525-1533.

[49] Jung, C.H., Matsuto, T., Tanaka, N., Okada, T., 2004. Metal distribution in incineration residues of municipal solid waste (MSW) in Japan. Waste Management 24, 381-391.

[50] Katrinak, K.A., Anderson, J.R., Buseck, P.R., 1995. Individual particle types in the aerosol of Phoenix, Arizona. Environment Science and Technology 29, 321-329.

[51] Kim, B.A., Tomiyasu, B., Owari, M., Nihei, Y., 2001. Individual particle analysis for source apportionment of suspended particulate matter using electron probe microanalysis. Surf. Interface Anal. 31, 106-113.

[52] Kim, E., Kalman, D., Larson, T., 2000. Dry deposition of large, airborne particles onto a surrogate surface. Atmospheric Environment 34, 2387-2397.

[53] Kim, K.H., Choi, G.H., Kang, C.H., Lee, J.H., Kim, J.Y., Youn, Y.H., Lee, S.R., 2003. The chemical composition of fine and coarse particles in relation with the Asian Dust events. Atmospheric Environment 34, 753-765.

[54] Klein, C. 2001, Mineral science: the 22nd edition of the manual of (after James D. Dana), 22nd edn. J. Wiley, New York

[55] Legret, M., Pagotto, C., 1999. Evaluation of pollutant loadings in the runoff waters from a major rural highway. Sci. Total Environ. 235, 143-150.

[56] Li, X.D., Poon, C.S., Liu, P.S., 2001. Heavy metal contamination of urban soils and street dusts in Hong Kong. Appl. Geochem. 16, 1361-1368.

[57] Ma, C.J., Kasahara, M., Höller, R., Kamiya, T., 2001. Characteristics of single particles sampled in Japan during the Asian dust-storm period. Atmospheric Environment 35, 2707-2714.

[58] Ma, C.J., Tohno, S., Kasahara, M., Hayakawa, S., 2004a. The nature of individual solid particles retained in size-resolved raindrops fallen in Asian dust storm event during ACE-Asia. Atmospheric Environment 38, 2951-2964.

[59] Ma C.J., Oki, Y., Tohno, S., Kasahara, M., 2004b. Assessment of wintertime atmospheric pollutants in an urban area of Kansai, Japan. Atmospheric Environment 38, 2939-2949.

[60] Machemer, S.D., 2004. Characterization of airborne and bulk particulate from iron and steel manufacturing facilities, Environ. Sci. Technol. 38, 381-389.

[61] Malderen, H.V., Grieken, R.V., Bufetov, N.V., Koutzenogii, K.P., 1996. Chemical characterization of individual aerosol particles in Central Siberia. Environment Science and Technology 30, 312-321.

[62] Malderen, H.V., Hoornaert, S., Grieken, R.V., 1996. Identification of individual aerosol particles containing Cr, Pb, and Zn above the North Sea. Environmental Science and Technology 30, 489-498.

[63] Mamane, Y., Willis, R., Conner, T., 2001. Evaluation of computer-controlled scanning electron microscopy applied to an ambient urban aerosol sample. Aerosol Science and Technology 34, 97-107.

[64] Manoli, E., Voutsa, D., Samara, C., 2002. Chemical characterization and source identification/ apportionment of fine and coarse air particles in Thessaloniki, Greece. Atmos. Environ. 36, 949-961.

[65] Matsui, S., Lee, B.C., Kawami, F., Shimizu, Y., Matsuda, T., 2002. High-performance liquid chromatography-bioassay profiles of endocrine disrupters discharged from point and non-point pollution sources in Lake Biwa basin. Lakes & Reservoirs: Research and Management. 7, 289-293.

[66] Miguel, A.G., Cass, G.R., Glovsky, M.M., Weiss, J., 1999. Allergens in paved road dust and airborne particles. Environ. Sci. Technol. 33,4159-4168.

[67] Mogami, K., Saitho, S., Makishita, H., 1989. Identification of spatters using a scanning electron microscope and an energy dispersive X-ray spectrometer. Reports of National Research Institute of Police Science. Research on forensic science. 42, 29-38.

[68] Mori, I., Nishikawa, M., Tanimura, T., Quan, H., 2003. Change in size distribution and chemical composition of kosa (Asian dust) aerosol during long-range transport. Atmospheric Environment 37, 4253-4263.

[69] Muschack, W. Pollution of street runoff by traffic and local conditions. Sci Total Environ. 93: 419-431, 1990

[70] Noll, K.E., Fang, K.Y.P., Watkins, L.A., 1988. Characterization of the deposition of particles from the atmosphere to a flat plate. Atmospheric Environment 22, 1461-1468.

[71] Nriagu, J.O., Pacyna, J.M., 1988. Quantitative assessment of worldwide contamination of air, water and soils by trace metals. Nature 333, 134-139.

[72] ORNL (Oak Ridge National Laboratory). 2001, Compositions, Functions, and Testing of Friction Brake Materials and Their Additives. Oak Ridge, TN: Metals and Ceramics Division.

[73] Pérez-Rodríguez, J.L., Haro, M.C.J., Maqueda, C., 2004. Isolation and characterization of barium sulphate and titanium oxides in monument crusts. Analytica Chemica Acta 524, 373-377.

[74] Pierson, W.R., Brachaczek, W.W., 1974. Airborne Particulate Debris From Rubber Tires. Rubber Chem. Thechnol. 47, 1275-1299.

[75] Piña, A. A., Villaseñor, G..T., Fernández, M.M., Kudra, A.L., Ramos, R.L., 2000. Scanning electron microscope and statistical analysis of suspended heavy metal particles in San Luis Potosi, Mexico. Atoms. Environ. 34, 4103-4112.

[76] Post, J.E., Buseck, P.R., 1984. Characterization of individual particles in the Phoenix urban aerosol using electron-beam instruments. Environmental Science and Technology 18, 35-42.

[77] Prati, P., Zucchiatti, a., Lucarelli, F., Mandò, P.A., 2000, Source apportionment near a steel plant in Genoa (Italy) by continuous aerosol sampling and PIXE analysis. Atmospheric Environment, 34, 3149-3157.

[78] Ro, C.U., Oh, K.Y., Kim, H.K., Chun, Y., Osán, J., Hoog, J.D., Grieken, R.V., 2001. Chemical speciation of individual atmospheric particles using low-Z electron probe X-ray microanalysis: characterizing gAsian Dusth deposited with rainwater in Seoul, Korea. Atmospheric Environment 35, 4995-5005.

[79] Rogge, W.F., Hildemann, L.M., Mazurek, M.A., Cass, G.R., Simoneit, B.R., 1993. Sources of Fine Organic Aerosol. 3. Road dust, tire debris, and organometallic brake lining dust: roads as sources and sinks. Environ. Sci. Technol. 27, 1892-1904.

[80] Root, R.A., 2000, Lead Loading of Urban Streets by Motor Vehicle Wheel Weights. Environ Health Perspect. 108, 937-940.

[81] Sadiq, M., Alam, I., El-Mubarek, A., Al-Mohdhar, H.M. 1989, Preliminary Evaluation of Metal Pollution from Wear of Auto Tires. Bull Environ Contam Toxicol. 42, 743-748.

[82] Samara, C., Kouimtzis, T., Tsitouridou, R., Kanias, G., Simeonov, V., 2003. Chemical mass balance source apportionment of PM10 in an industrialized urban area of northern Greece. Atmos. Environ. 37, 41-54

[83] Saucy, D.A., Anderson, J.R., Buseck, P.R., 1991. Aerosol particle characteristics determined by combined cluster and principal component analysis. Journal of Geophysical Research 96, 7407-7414.

[84] Sitzmann, B., Kendall, M., Watt, J., Williams, I., 1999. Characterisation of airborne particles in London by computer-controlled scanning electron microscopy. Sci. Total Environ. 241, 63-73.

[85] Smith, R.W., Veith, A.G., 1982. Electron microscopical examination of worn tire treads and tread debris. Rubber Chem. Technol. 55, 469-482.

[86] Smolders, E., Degryse, F., 2002. Fate and Effect of Zinc from Tire Debris in Soil. Environ. Sci. Technol. 36, 3706-3710

[87] Sörme, L., Lagerkvist, R., 2002. Source of heavy metals in urban wastewater in Stockholm. Sci. Total. Environ. 298, 131-145.

[88] Sternbeck, J., Sjödin, Å., Andréasson, k., 2002. Metal emissions from road traffic and the influence of resuspension- results from two tunnel studies. Atmospheric Environment 36, 4735-4744.

[89] Sugimae, A., Hasegawa, T., Matsuo, K., 1974. Trace metals in Airborne Particles. V. Survey of Iron in the Atmosphere. Journal of Japen Society of Air Pollution 9, 5-12.

[90] Sutherland, R.A., 2003. Lead in grain size fractions of road-deposited sediment. Environ. Pollut. 121, 229-237.

[91] Van de Velde, K., Barbante, C., Cozzi, G., Moret, I., Bellomi, T., Ferrari, C., Boutron, C., 2000. Changes in the occurrence of silver, gold, platinum, palladium and rhodium in Mont Blanc ice and snow since the 18th century. Atmospheric Environment 35, 3361-3366.

[92] Var, F., Narita, Y., Tanaka, S. 2000. The concentration, trend and seasonal variation of metals in the atmosphere in 16 Japanese cities shown by the results of National Air Surveillance Network (NASN) from 1974 to1996. Atmos. Environ. 34, 2755-2770.

[93] Vawda, Y., Harrison, R.M., Nicholson, K.W., Colbeck, I., 1990. Use of surrogate surfaces for dry deposition measurements. Journal of Aerosol Science 21, s201-s204.

[94] Vaze, J., Chiew, F.H.S., 2002. Experimental study of pollutant accumulation on an urban road surface. Urban Water 4, 379-389.

[95] Vega, E., Mugica, V., Reyes, E., Sánchez, G., Chow, J.C., Watson, J.G., 2001. Chemical composition of fugitive dust emitters in Mexico City. Atmos. Environ. 35, 4033-4039.

[96] Voutsa, D., Samara, C., 2002, Labile and bioaccessible fractions of heavy metals in the airborne particulate matter from urban and industrial areas. Atmospheric Environment. 36, 3583-3590.

[97] Weber, S., Hoffmann, P., Ensling, J., Dedik, A.N., Weinbruch, S., Miehe, G., Gütlich, P., Ortner, H.M., 2000. Characterization of iron compounds from urban and rural aerosol sources. J. Aerosol Sci. 31, 987-997.

[98] Williams, P.B., Buhr, M.P., Weber, R.W., Volz, M.A., Koepke, J.W., Selner, J.C., 1995, Latex allergen in respirable particulate air pollution. J Allergy Clin Immunol. 95, 88-95.

[99] Yang, H.H., Hsieh, L.T., Lin, M.C., Mi, H.H., Chen, P.C., 2004. Dry deposition of sulfate-containing particulate at the highway intersection, coastal and suburban area. Chemosphere 54, 369-378.

[100] Yeung ZLL, Kwok RCW, Yu KN (2003) Determination of Multi-Element Profiles of Street Dust Using Energy Dispersive X-ray Fluorescence (EDXRF). Applied Radiation and Isotopes 58: 339-346

[101] Zhou, M., Okada, K., Qian, F., Wu, P.M., Su, L., Casareto, B.E., Shimohara, T., 1996. Characteristics of dust-storm particles and their long-range transport from China to Japan case studies in April 1993. Atmospheric Environment 40, 19-31.

[102] Zufall, M.J., Davidson, C.I., Caffrey, P.F., Ondov, J.M., 1998. Airborne concentrations and dry deposition fluxes of particulate species to surrogate surface deployed in Southern Lake Michigan. Environmental Science and Technology 32, 1623-1628.